A New Digital Realization of Two-Dimensional Product Separable Transfer Functions

Rajab B. Khoja

A Thesis

in

The Faculty

of

Engineering

Presented in partial fulfilment of the requirements
for the degree of Master of Engineering
at Concordia University,
Montréal, Québec, Canada

January 1983

ABSTRACT

A New Digital Realization of Two-Dimensional Product Separable Transfer Functions

Rajab B. Khoja

A different method of exact realization of product separable 2-D transfer function has been proposed in this thesis. This is based on the digital realization of 2-variable analog cascade-decomposable network which is connected in tandem with a 2-variable digital parallel realization. Further 2-port wave digital realization of lossy elements in series or in shunt arm has been found and these are required in the exact realization.

The suggested realization has been compared with other structures from the view point of sensitivity and quantization errors.

ACKNOWLEDGEMENTS

The author wishes to express his gratitude to Professor V. Ramachandran for suggesting the problem and for his guidance throughout the course of this investigation, and for his advice during the preparation of the manuscript.

Thanks are also due to Sharon Carey and Karen Stevenson for typing of the thesis.

TO MY PARENTS

AND

TO THE AGAKHAN FOUNDATION (GENEVA)

TABLE OF CONTENTS

LIST OF TABLES

LIST OF FIGURES

LIST OF ABBREVIATIONS AND SYMBOLS

2-D	Two-Dimensional
$z_i, i = 1,2$	Complex variable in the digital domain
$s_i, i = 1,2$	Complex variable in the analog domain
$H(z_1, z_2)$	2-D transfer function
$H(s_1, s_2)$	2-D transfer function
$\bar{N}$	Analog network
$\begin{bmatrix} a_1 \\ \\ b_i \end{bmatrix}, i = 1,2$	Digital inputs and outputs at portsl and 2
$\begin{bmatrix} \mu_i & \lambda_i \\ \\ \nu_i & K_i \end{bmatrix} = [F_i]$	Chain matrix of a digital 2-port
$\begin{bmatrix} A & B \\ \\ C & D \end{bmatrix}$	Chain matrix of an analog 2-port network
$R_i, i = 1,2$	Port resistance at portsl and 2
$G_i, i = 1,2$	Port Impedance at portsl and 2
Z_a	Impedance of a series element
Y_b	Admittance of a shunt element in a ladder network
R_s	Input source resistance
R_L	Output load Resistance

S^H_m	Sensitivity of the function H with respect to parameter m
ΔM	Deviation in magnitude
Q	Quantization step
$t_i, i=1,2$	Sampling period
W C I	Wave Cascade Canonic realization
C D I	Direct Cascade Canonic Realizawtion
R_{II}	Proposed realization
PSD	Power Spectral Density
RPSD	Relative Power Spectral Density
$S_o(w)$	Absolute RPSD of the Output Noise due to Produce Quantization
$S_m(w)$	PSD of the noise generated by the multiplier m
z	2-D z transform
Vs	Versus
R_I	Approximate PSTF Realization

CHAPTER 1

INTRODUCTION

1.1 General

Two dimensional (2-D) digital filtering finds applications in areas such as image processing, seismic data processing, 2-D pattern recognition systems, geophysical exploration, radar, sonar, radio astronomy, prefiltering for picture encoding etc. [1].

The important advantages of 2-D filtering are restoration and enhancement to improve image quality [1]. 2-D filtering removes unwanted background noise from the image so that the details contained in the higher spatial frequencies are easier to see [2,3]. Also processing 2-D signals with 1-D filters results in complicated and large algorithms. These large and relatively complicated algorithms require higher memory and more execution time to produce the final required result.

1.2 Two-Dimensional Linear Digital Filters:

Like 1-D filters, 2-D filters can be classified in two categories namely non-recursive and recursive filters.

(1) Non-recursive filters:

2-D non-recursive filter transfer functions can be described using 2- dimensional z transforms as follows:

$$H(z_1,z_2) = \sum_{m=0}^{M} \sum_{k=0}^{K} a_{mk} z_1^{-m} z_2^{-k} \qquad (1.1)$$

The implications of Eqn. (1.1) are that many of the one-dimensional filter design techniques can be directly extended to two

or more dimensions by appropriate modifications to the design procedures.

In two-dimensional non-recursive filters, problems of stability do not occur because the impulse response sequence is bounded and exists only for a finite time. Thus the stability of $H(z_1,z_2)$ is guaranteed, since

$$\sum_{m=0}^{M} \sum_{k=0}^{K} |h(z_1,z_2)| < \infty \qquad (1.2)$$

for all finite M and K.

However, the disadvantage of such filters is that high selectivity can be achieved only by higher order transfer functions.

(2) Recursive filters:

The transer function of 2-D recursive filters using 2-D z transform can be expressed as a ratio of 2-D polynomials as follows[1].

$$H(z_1,z_2) = \frac{N(z_1,z_2)}{D(z_1,z_2)} = \frac{\sum_{i=0}^{I} \sum_{j=0}^{J} a_{ij} z_1^{-i} z_2^{-j}}{\sum_{k=0}^{K} \sum_{l=0}^{L} b_{kl} z_1^{-k} z_2^{-l}} \qquad (1.3)$$

where $b_{oo} = 1$, a_{ij} and b_{kl} are real coefficients.

For an input signal $X(z_1,z_2)$, the output of the filter is given by,

$$Y(z_1,z_2) = H(z_1,z_2) \times X(z_1,z_2) \qquad (1.4)$$

One of the important problems to be considered in the design of such filters is its stability. The stability of the 2-D recursive

filter in the bounded-input bounded-output sense is guaranteed if there exist no values of z_1 and z_2 for which, $D(z_1, z_2) = 0$ for both $|z_1|$ and $|z_2| \geq 1$ simultaneously [1]. It is also interesting to note that not all two-variable analog functions with strictly Hurwitz polynomial denominator upon bilinear transformation yield stable 2-D digital transfer functions [4]. This difficulty can be avoided by making sure that the given analog transfer function has very strictly Hurwitz polynomial (VSHP) denominator [5]. The Polynomial $D(s_1, s_2)$ is said to be very strict Hurwitz polynomial (VSHP) if $1/D(s_1, s_2)$ does not posses any singularities in the region (s_1, s_2), $Re(s_1) \geq 0$ and $Re(s_2) \geq 0$

The design of a 2-D recursive digital filter consists in obtaining the a_{ij} and b_{ij} coefficients in (1.3) such that $H(e^{jw_1 t_1}, e^{jw_2 t_2})$ approximates a given response $G(jw_1, jw_2)$ where w_1 and w_2 are respectively the horizontal and vertical spatial frequencies. Once the coefficients in (1.3) are found, it is necessary to ensure the stability of the filter. Therefore the stability of the filter is first ensured and then the design is carried out. When we start with a passive analog transfer function whose denominator is very strictly hurwitz polynomial and then obtain a corrosponding digital transfer function by using the double bilinear z transformation, then the stability in the digital domain is guaranteed.

1.3 Symmetry Associated with 2-D Transfer Functions [6-8]:

In many applications, a 2-D digital filter is required to have certain symmetry in its magnitude response. Very often, these symmetries (e.g. circular symmetry) are presented in the desired response. Symmetry

properties can be used to reduce the number of the variables in optimization procedure also [7]. It is also reported in [7] that by taking into account the symmetry contraints, considerable reduction in multiplications can be achieved in implementation of these filters. In what follows, we briefly review symmetry contraints,

(a) Centro - symmetry

$H(z_1, z_2)$ is said to possess centro-symmetry in its magnitude response if,

$$H(z_1, z_2) \times H^*(z_1^{-1}, z_2^{-1}) = H(z_1^{-1}, z_2^{-1}) \times H^*(z_1, z_2) \qquad (1.5)$$

where $H^*(z_1, z_2)$ is the transfer function with complex conjugate coefficients of $H(z_1, z_2)$.

(b) Diagonal symmetry

$H(z_1, z_2)$ is said to possess symmetry about the diagonals in its magnitude response if,

$$H(z_1, z_2) \times H(z_1^{-1}, z_2^{-1}) = H(z_2, z_1) \times H(z_2^{-1}, z_1^{-1}) \qquad (1.6)$$

(c) Quadrantal symmetry

$H(z_1, z_2)$ is said to possess quadrantal symmetry in its magnitude response if,

$$H(z_1, z_2) \times H(z_1^{-1}, z_2^{-1}) = H(z_1^{-1}, z_2) \times H(z_1, z_2^{-1}) \qquad (1.7)$$

(d) Octagonal symmetry

$H(z_1, z_2)$ is said to possess octagonal symmetry in its magnitude response if it possess both quadrantal as well as diagonal symmetries simultaneously in its magnitude response i.e.

$$H(z_1, z_2) \times H(z_1^{-1}, z_2^{-1}) = H(z_1^{-1}, z_2) \times H(z_1, z_2^{-1})$$

$$= H(z_2^{-1}, z_1^{-1}) \times H(z_2, z_1) \qquad (1.8)$$

(e) Circular symmetry

It is clearly proved in [7], [8] that, it is not possible to obtain exact circular symmetric stable rational transfer function with denominator other than unity in the analog domain.

From the foregoing, it is seen that product separability is required to achieve certain types of symmetries. For a separable function,

$$H(s_1, s_2) = h_1(s_1) \cdot h_2(s_2) \qquad (1.9)$$

The following can be noted:

(1) Any separable function $H(s_1,s_2) = h_1(s_1) \times h_2(s_2)$ is quadrantal symmetric.

(2) When $h_1(.) = h_2(.)$, $H(s_1,s_2)$ is also octagonal symmetric, where $h_1(.)$ is a single variable function.

(3) If magnitude circular symmetry is the main criterion, $|h_1(jw_1)|^2$ should approximate $\lambda e^{-\alpha w_1^2}$ for suitable values of λ and α.

(4) When stable all-pole 2-dimensional transfer functions are constrained to possess quadrantal symmetry, they turn out to be separable.

1.4 Realization of 2-D Functions:

Realization step is the process of converting the transfer function into a filter network. Different realizations of the same transfer function can have widely diverse performance in terms of round-off errors, coefficient sensitivity, number of different components used and suitability from the view point of hardware implementation etc, [9 - 14].

The realization can be accomplished using the following important methods,

(1) Direct

(2) Parallel

(3) Cascade

(4) Wave

It is known that the 1-D transfer functions can be realized using any of the above methods. But, in the case of 2-D transfer function realization, each method has got its own limitations. In addition, a prescribed method may not realize a given 2-D transfer function. We briefly review these limitations.

(1) Direct realization:

All 2-D transfer function can be realized using this method. This realization follows from the algorithm given by Shanks [15]. It is shown that Eqn.(1.3) can be written as,

$$Y(z_1,z_2) = \left[\sum_{i=o}^{I}\sum_{j=o}^{J} a_{ij}\, z_1^{-i}\, z_2^{-j}\right] x(z_1,z_2) - \left[\sum_{k=o}^{K}\sum_{l=o}^{L} b_{kl}\, z_1^{-k-1} z_2^{-l}\right] Y(z_1,z_2) \qquad (1.10)$$

Eqn. (1.10) can be realized directly using different approaches shown in [16]. The main limitation of direct realization is that it results in higher roundoff errors.

(2) Parallel Realization:

In the case of parallel realization it is required to expand the given 2-D transfer function into partial fractions. Except in special cases, this is not possible.

(3) Cascade Realization:

For cascade realization, it is required that the given 2-D transfer function is expressed as a product of several lower-order 2-D transfer functions. This may not be possible as a 2-variable polynomial is not, in general, factorizable.

(4) Wave Realization:

The wave digital realization starts from a given analog network which is transformed into digital domain by the double bilinear transformations. As is evident, exact realizations of product separable transfer funtions are not possible. [17, 18].

1.5 Scope of Thesis

In this thesis we have suggested another method to realize product separable low-pass 2-D transfer functions (PSTF). This is based on the digital realization of 2-variable analog cascade-decomposable network which is connected in tandem with a 2-variable digital parallel realization (Each of these parallel blocks can be realized in a number of ways). This requires two-port wave-digital realizations of lossy elements in the corresponding analog ladder network. These are discussed in chapter 2 and it is shown how such realizations can be used to exactly realize PSTFs.

In chapter 3, the magnitude responses for different 2-D low-pass PSTF realized in chapter 2, will be studied. Also the magnitude responses of exact realization of PSTF with approximate realization of PSTF has been compared.

In chapter 4, the sensitivity and quantization error effects of

the three different network structures of 2-D transfer function realizations are compared. These structures considered are,

(1) cascade-direct canonic realization, where each transfer function is realized by a direct canonic structure.

(2) cascade-wave realization, where each transfer function is realized by wave-digital structures.

(3) suggested cascade-parallel wave realizations. Chapter V gives the summary and discussions of the thesis.

Chapter 2

REALIZATIONS OF 2-D PRODUCT SEPARABLE TRANSFER FUNCTION (PSTF)

2.1 Introduction

There has been relatively little effort being directed towards the realization of 2-D recursive PSTFs. Apart from direct realization, a continued fraction expansion approach [16] has been adopted to obtain different realizations for a 2-D recursive digital filter transfer function. Also, two-variable doubly-terminated lossless analog ladder networks can be used [14, 17, 18] to realize approximate PSTFs.

Here, we present an approach to realize a PSTF. As will be shown, in order to get exact PSTF, it is required to have a digital two-port network corresponding to an analog ladder network which shall have combination of a resistance and a reactive element in its series or shunt branch.

In section 2.2 a brief review of wave realization of two-port containing lossless elements in series or shunt branches is given [14]. Using similar method, two-port wave digital realization of combined reactive and resistive element in series or shunt arm is given in detail in section 2.3. This realization is later used in section 2.4 to get overall PSTFs.

2.2 Digital Realization Corresponding to Lossless Element in Series or Shunt Branch

Let the impedance of series element in network ($\tilde{N}$) of Fig. (2.1) be denoted by Z_a and admittance of the shunt element is denoted by Y_b with the bilinear transformation $s = (z - 1)/(z+1)$. Then for the series element Z_a, the two-port description is given as [14],

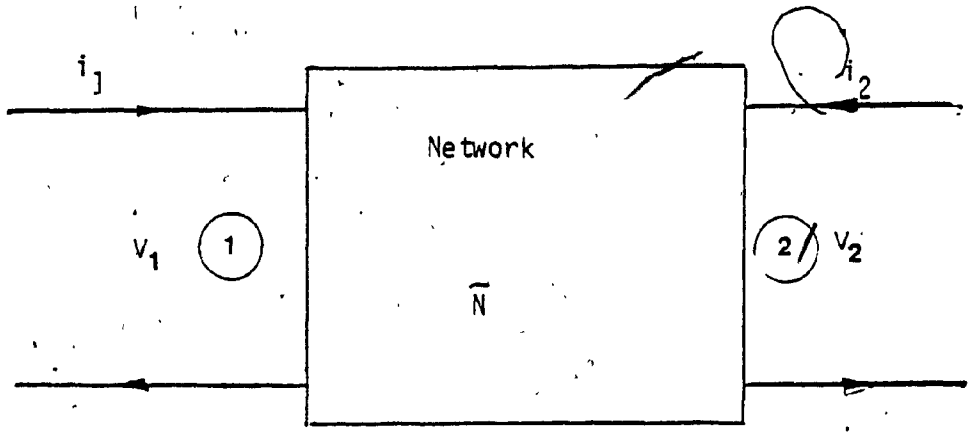

Fig. 2.1

General Two-Port Network

$$\begin{bmatrix} a_1 \\ b_1 \end{bmatrix} = \begin{bmatrix} \mu_1 & \lambda_1 \\ \nu_1 & K_1 \end{bmatrix} \begin{bmatrix} b_2 \\ a_2 \end{bmatrix} = [F_1] \begin{bmatrix} b_2 \\ a_2 \end{bmatrix} \tag{2.1}$$

where a_i and b_i $(i=1, 2)$ represent, respectively inputs and outputs at ports 1 and 2, and,

$$\begin{bmatrix} \mu_1 & \lambda_1 \\ \nu_1 & K_1 \end{bmatrix} = [F_1]$$

represents the chain matrix of the digital 2-port with

$$\left.\begin{aligned} \mu_1 &= \frac{Z_a + R_1 + R_2}{2R_2} \\ \nu_1 &= \frac{Z_a + R_2 - R_1}{2R_2} \\ \lambda_1 &= 1 - \mu_1 \\ K_1 &= 1 - \nu_1 \end{aligned}\right\} \tag{2.2}$$

where $R_i (i = 1, 2)$ represent port resistance at ports 1 and 2.

Similarly, for the shunt element Y_b we have,

$$\begin{bmatrix} a_1 \\ b_1 \end{bmatrix} = \begin{bmatrix} \mu_2 & \lambda_2 \\ \nu_2 & K_2 \end{bmatrix} \begin{bmatrix} b_2 \\ a_2 \end{bmatrix} = [F_2] \begin{bmatrix} b_2 \\ a_2 \end{bmatrix} \tag{2.3}$$

where

$$\left.\begin{aligned} \mu_2 &= (Y_b + G_1 + G_2)/2G_2 \\ \lambda_2 &= (Y_b + G_2 - G_1)/2G_2 \\ \nu_2 &= (1 - \mu_2) \\ K_2 &= (1 - \lambda_2) \end{aligned}\right\} \qquad (2.4)$$

and $G_i (i=1, 2)$ represent port admittance at ports 1 and 2

Now the realization can be described as in [14] :

For the series element:

$$\left.\begin{aligned} b_1 &= a_2 + (a_1 - a_2)\frac{\nu_1}{\mu_1} \\ b_2 &= a_2 + (a_1 - a_2)\frac{1}{\mu_1} \end{aligned}\right\} \qquad (2.5)$$

For the shunt element:

$$\left.\begin{aligned} b_1 &= a_2 + (a_1 + \sigma a_2)\frac{\nu_2}{\mu_2} \\ b_2 &= -a_2 + (a_1 + \sigma a_2)\frac{1}{\mu_2} \end{aligned}\right\} \qquad (2.6)$$

$$\sigma = G_2/G_1$$

Realizations for Eqns. (2.5) and (2.6) are shown in Figs. 2.2 and 2.3.

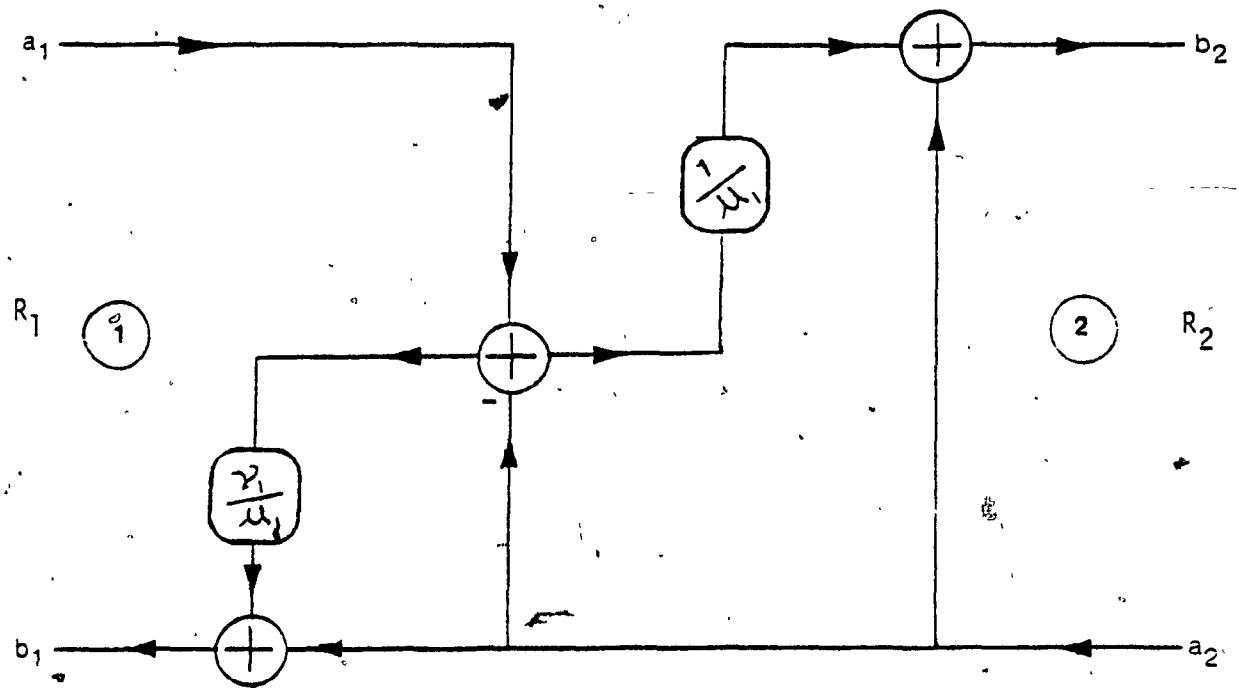

Fig. 2.2

Digital Two-Port Realization of Eqn. (2.5)

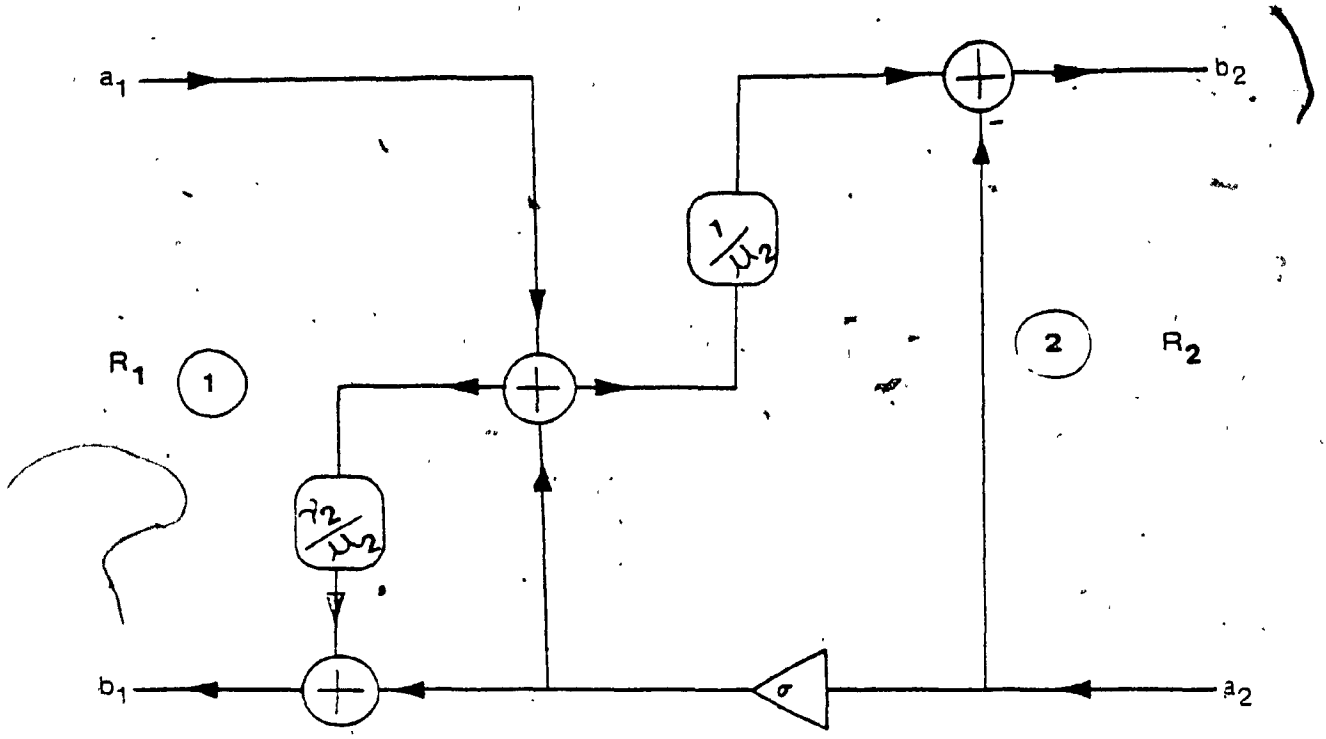

Fig. 2.3

Digital Two-Port Realization of Eqn. (2.6)

2.3 Realization of Combined Reactive and Resistive Element

To realize certain type of transfer function it is required to have two-port realization building blocks of combined reactive and resistive elements in series or in shunt arm.

In this section we will discuss detailed realization procedures for different combinations of a resistance and a reactive element in the series or in the shunt arm.

2.3.1 Realization of Different Combinations in Series:

(1) Series combination of inductor (L) and resistance (R) in series arm:

From Fig. 2.4,

$$Z_a = Ls + R \tag{2.7}$$

By bilinear z transformation $s = (z - 1)/(z + 1)$

we get,

$$Z_a = (L(z - 1) + R(z + 1))/(z + 1) \tag{2.8}$$

Now from section 2.2 we have,

$$\left.\begin{aligned} \mu_1 &= (Z_a + R_1 + R_2)/(2R_2) \\ \gamma_1 &= (Z_a + R_2 - R_1)/(2R_2) \end{aligned}\right\} \tag{2.9}$$

From Eqn. (2.8) substituting the value of Z_a in Eqn. (2.9) we have,

$$\mu_1 = \frac{z(R + L + R_1 + R_2) + (R_1 + R_2 + R - L)}{2R_2(z + 1)} \tag{2.10}$$

$$\gamma_1 = \frac{z(R + L + R_2 - R_1) + (R_2 - R_1 + R - L)}{2R_2(z + 1)} \tag{2.11}$$

$$\frac{\nu_1}{\mu_1} = \frac{z\,(L + R + R_2 - R_1) + (R_2 + R - R_1 - L)}{z\,(L + R + R_2 + R_1) + (R_2 + R + R_1 - L)} \qquad (2.12)$$

To avoid delay free loops in the digital realization the numerator of $\frac{\nu_1}{\mu_1}$ should be at least one degree less than that of the denominator. This condition can be ensured by putting,

$$L + R + R_2 - R_1 = 0 \qquad (2.13)$$

Hence, Eqn. (2.12) is reduced to,

$$\frac{\gamma_1}{\mu_1} = \frac{\frac{R_1}{R_2} z^{-1}}{1 + \frac{R_1}{R + R_2} z^{-1}} = \frac{\alpha_4 z^{-1}}{1 + \alpha_3 z^{-1}}$$

where, $\alpha_4 = \frac{R_1}{R_2}$ and $\alpha_3 = \frac{R_1}{R + R_2}$

$$\frac{1}{\nu_1} = \frac{\frac{R_2}{R_1}(1 + z^{-1})}{1 + \frac{R_1}{R + R_2} z^{-1}} = \frac{(1 + z^{-1})\alpha_2}{1 + \alpha_3 z^{-1}}$$

From Eqn. (2.6)

$$b_1 = a_2 + (a_1 - a_2)\frac{\gamma_1}{\mu_1} = a_2 + (a_1 - a_2)\frac{\alpha_4 z^{-1}}{1 + \alpha_3 z^{-1}} \qquad (2.14a)$$

$$b_2 = a_2 + (a_1 - a_2)\frac{1}{\mu_1} = a_2 + (a_1 - a_2)\left(\frac{(1 + z^{-1})\alpha_2}{1 + \alpha_3 z^{-1}}\right) \qquad (2.14b)$$

Fig. 2.5 shows realization of Eqns. (2.14a) and (2.14b) which is corresponding to the analog network shown in Fig. 2.4.

It should also be noted that the resistance is in series with the input resistance. Hence, wave-digital structure can be realized with the lossless inductor in the series arm with the condition that the input port resistance is changed.

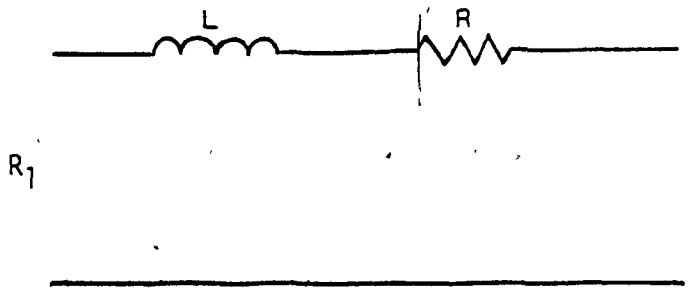

Fig. 2.4

Lossy Inductance in the Series Arm

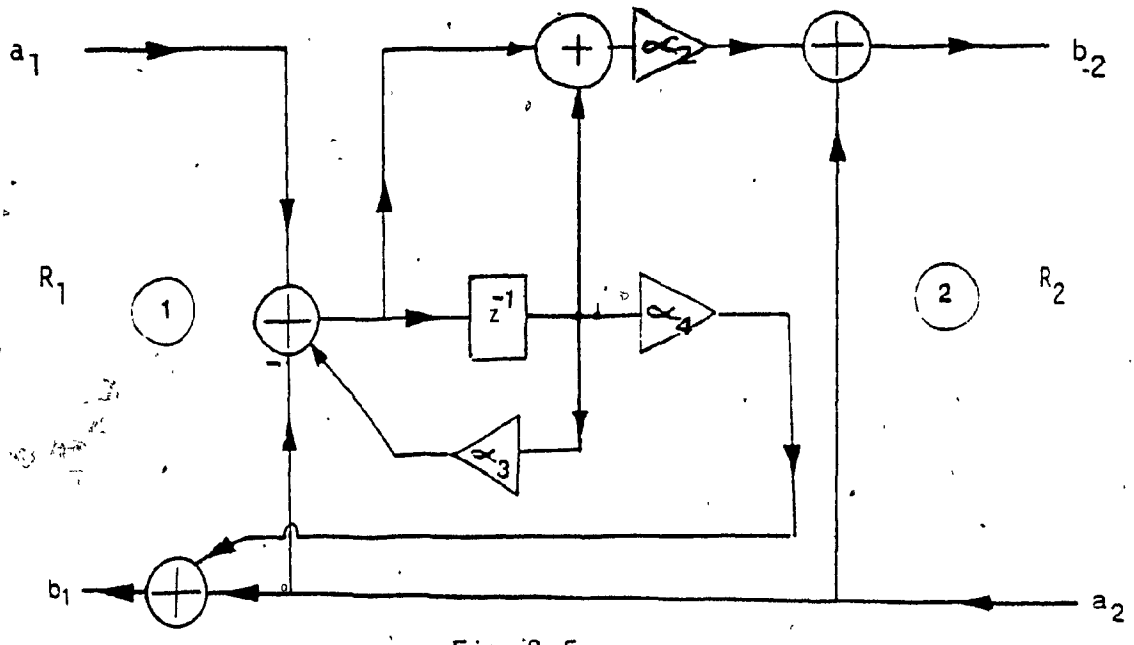

Fig. 2.5

Two-Port Wave Digital Realization of Fig. 2.4

(2) Series combination of capacitor (C) and resistance (R) in the series arm:

From Fig. 2.6,

$$Z_a = R + 1/Cs = \{R(z-1) + 1/C(z+1)\}/(z-1) \qquad (2.15)$$

making the transformation

$$C \to \frac{1}{L}, \quad z^{-1} \to -z^{-1},$$

$$Z_a = \frac{L(z-1) + R(z+1)}{z+1} \qquad (2.16)$$

This is the same as Eqn. (2.8).

Hence, realization is carried out using the same approach as shown earlier.

The realization is shown in Fig. 2.7. It is clear that the realization is the same as Fig. 2.5 with z^{-1} replaced by $-z^{-1}$ and L replaced by 1/C.

(3) Parallel combination of inductance (L) and Resistance(R) in series arm:

From Fig. 2.8 we have,

$$Z_a = RLs/(Ls+R) = RL(z-1)/((R+L)z+(R-L)) \qquad (2.17)$$

Also,

$$\mu_1 = \frac{Z_a - R_1 + R_2}{2R_2}, \quad \nu_1 = \frac{Z_a + R_2 - R_1}{2R_2}$$

Substituting the value of Z_a,

$$\mu_1 = \frac{RL + (R_1 + R_2)(R+L)z + (R_1 + R_2)(R-L) - RL}{2R_2\,((R+L)z + (R-L))} \qquad (2.18)$$

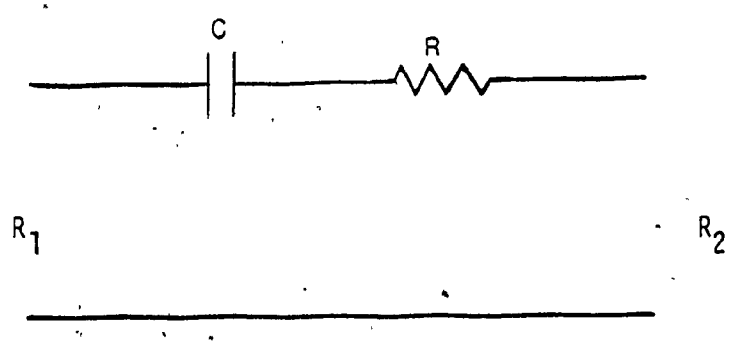

Fig. 2.6

Series Combination of a Capacitance and a Resistance in the Series Arm

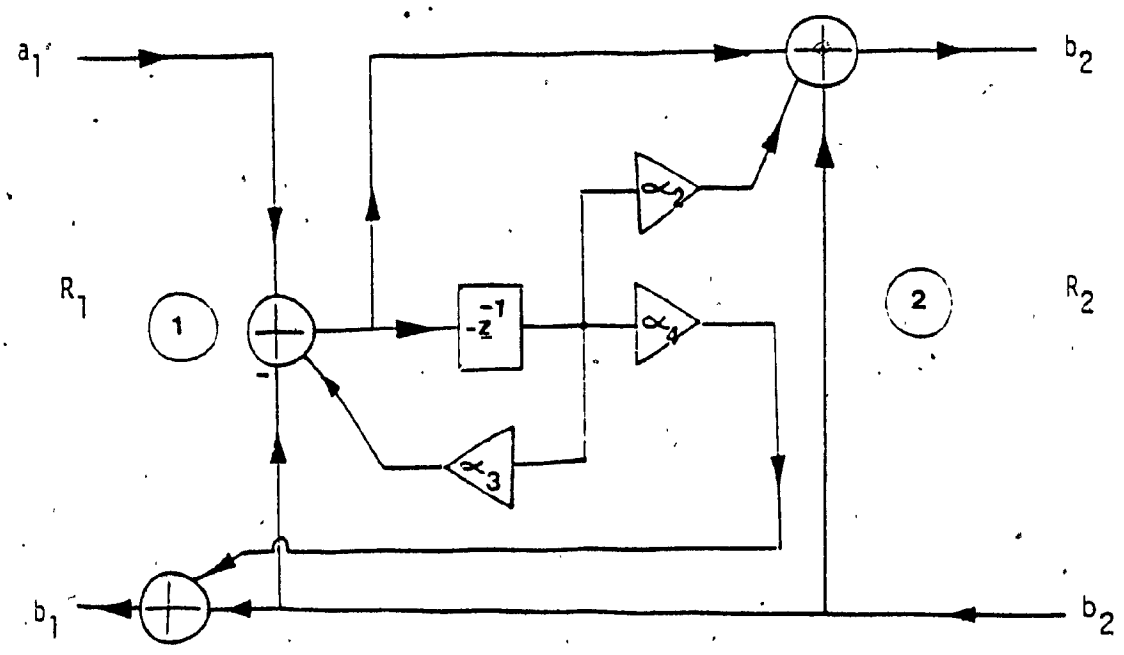

Fig. 2.7

Two-Port Digital Realization of Fig. 2.6

$$\gamma_1 = \frac{RL(z-1) + (R_2 - R_1)\left\{(R+L)z + (R-L)\right\}}{2R_2\left((R+L)z + (R-L)\right)} \qquad (2.19)$$

From Eqn (2.18) and Eqn (2.19) we get,

$$\frac{\gamma_1}{\mu_1} = \frac{\left\{RL + (R_2 - R_1)(R+L)\right\} z + (R_2 - R_1)(R-L) - RL}{\left\{RL + (R_1 + R_2)(R+L)\right\} z + (R_1 + R_2)(R-L) - RL} \qquad (2.20)$$

To avoid delay-free loops, we should ensure degree of numerator of $\frac{\gamma_1}{\mu_1}$ is less than that of the denominator.

$$\therefore \quad RL + (R_2 - R_1)(R+L) = 0 \qquad (2.21)$$

From Eqn. (2.21) we have,

$$\left.\begin{aligned} R_1 &= R_2 + \frac{RL}{R+L} \\ R_2 &= R_1 - \frac{RL}{R+L} \\ L &= \frac{(R_1 - R_2)R}{R + R_2 - R_1} \\ R &= \frac{(R_1 - R_2)L}{L + R_2 - R_1} \end{aligned}\right\} \qquad (2.22)$$

Substituting Eqn. (2.22) in Eqns. (2.20) and (2.18) we have,

$$\frac{\gamma_1}{\mu_1} = \frac{\frac{R_2}{R_1}\left\{R\,\frac{(R_2 - R_1)}{R_2}\right\} z^{-1}}{1 + \left\{\frac{R_1 L + R_2 R}{R_1 (R+L)}\right\} z^{-1}} \qquad (2.23)$$

$$\frac{1}{\mu_1} = \frac{\frac{R_2}{R_1}\left\{1 + \frac{R - L}{R + L} z^{-1}\right\}}{1 + \left\{\frac{R_1 L + R_2 R}{R_1 (R + L)}\right\} z^{-1}} \qquad (2.24)$$

Making the following designation,

$$\frac{R_2}{R_1} = \alpha_1$$

$$\frac{R - L}{R + L} = \alpha_2 \qquad (2.25)$$

$$\frac{R (R_2 - R_1)}{R_2} = \alpha_3$$

$$\frac{R_1 L + R_2 R}{R_2 (R + L)} = \alpha_4$$

Eqn. (2.23) and Eqn. (2.24) become,

$$\frac{\nu_1}{\mu_1} = \frac{\alpha_1 (\alpha_3) z^{-1}}{1 + \alpha_4 z^{-1}} \qquad (2.26)$$

$$\frac{1}{\mu_1} = \frac{\alpha_1 (1 + \alpha_2) z^{-1}}{1 + \alpha_4 z^{-1}} \qquad (2.27)$$

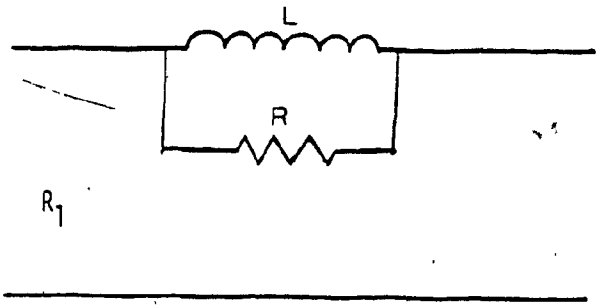

Fig. 2.8

Parallel Combination of an Inductance (L) and a Resistance (R) in the Series Arm

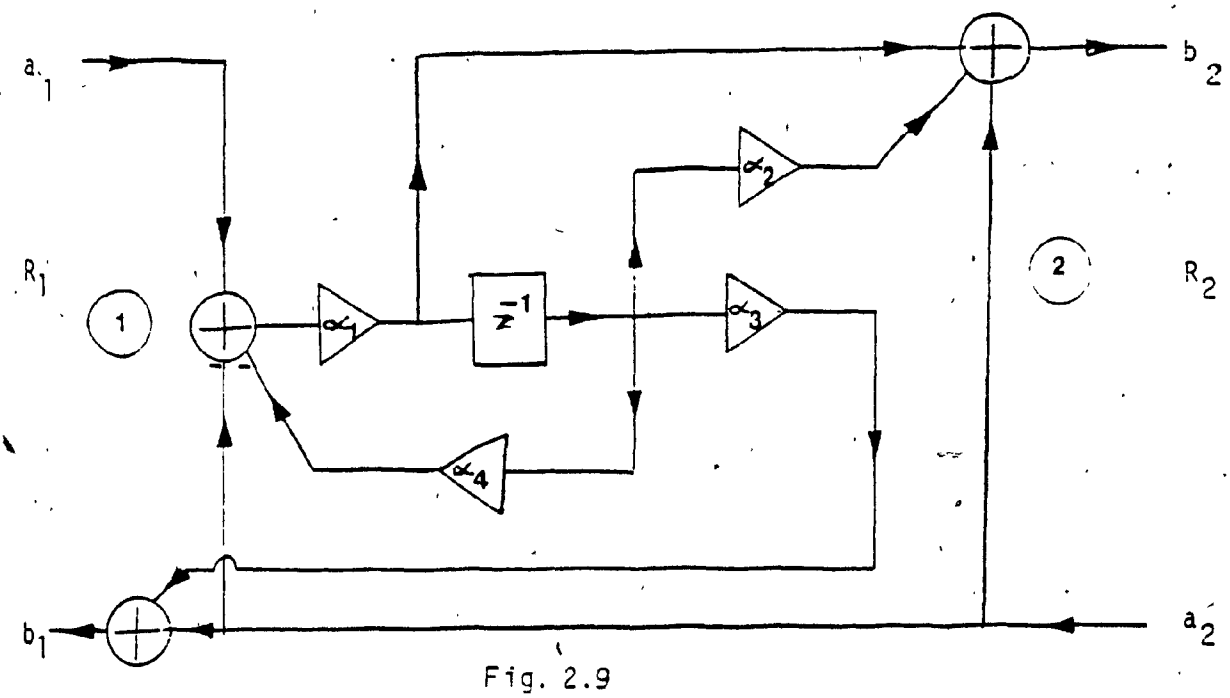

Fig. 2.9

Two-Port Wave-Digital Realization of Fig. 2.8

Substituting Eqns. (2.26) and (2.27) into Eqn. (2.5), we have,

$$b_1 = a_2 + \frac{\alpha_1 \quad \alpha_3 \quad z^{-1}}{1+\alpha_1\alpha_4 \; z^{-1}} \; (a_1 - a_2) \tag{2.28}$$

$$b_2 = a_2 + \frac{\alpha_1 \; (1+\alpha_2) \; z^{-1}}{1+\alpha_1\alpha_4 \; z^{-1}} \; (a_1 - a_2) \tag{2.29}$$

The corresponding realization is shown in Fig. 2.9

(4) Parallel combination of capacitance (C) and resistance(R)

From Fig. 2.10,

$$z_a = \frac{R}{RCs + 1} \tag{2.30}$$

making the transformation

$s \rightarrow \frac{1}{s}$ and $C \rightarrow \frac{1}{L}$ we get,

$$z_a = \frac{RLs}{Ls + R} \tag{2.31}$$

which is the same as Eqn. (2.17). The two-port digital realization is shown in Fig. 2.11, which is the same as that of Fig. 2.9 with z^{-1} replaced by $-z^{-1}$ and L replaced by $\frac{1}{C}$.

Table 2.1 shows different combinations of reactive and resistive elements in series arm of network ($\overline{N}$) and their two-port wave digital realizations.

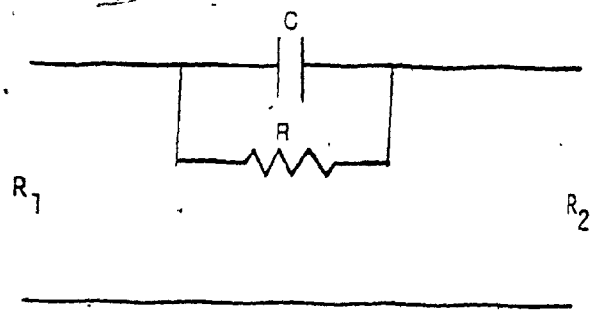

Fig. 2.10

Parallel Combination of a Capacitance (C)

and a Resistance (R) in the Series Arm

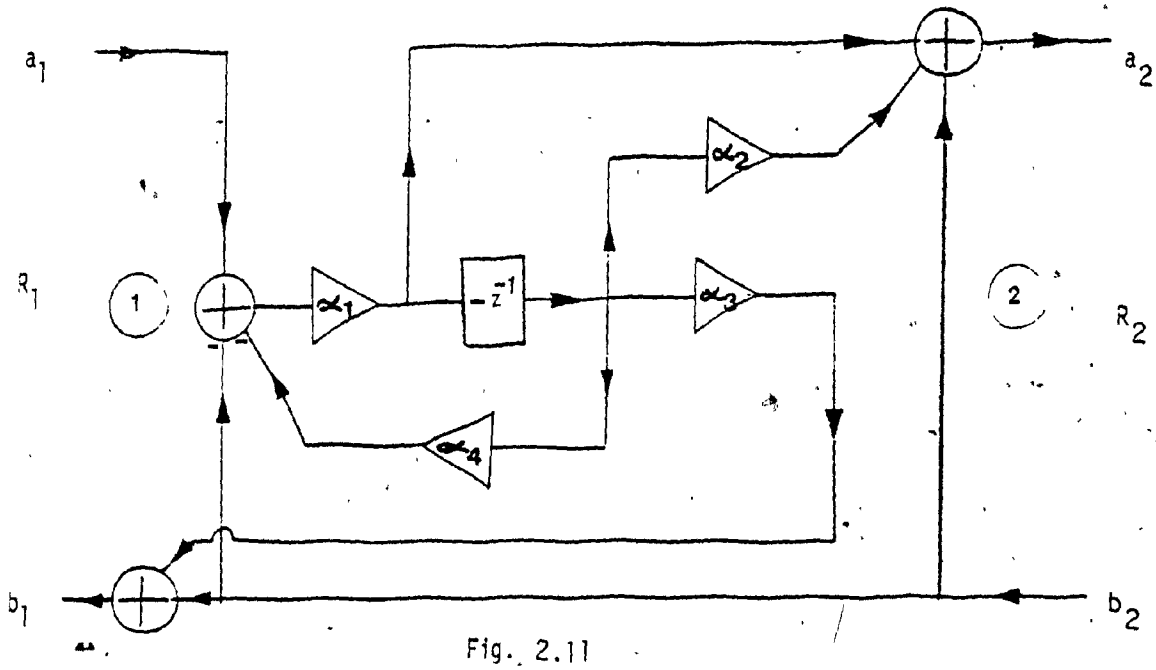

Fig. 2.11

Two-Port Digital Realization for Analog Network of Fig. 2.10

Table 2-1

Two-Port Wave Digital Realization of Different Combinations of Resistances and Reactive Elements in the Series Arm of Analog Network

Element	Corresponding 2-port Wave Digital Realization	Relations
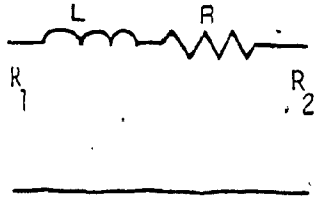	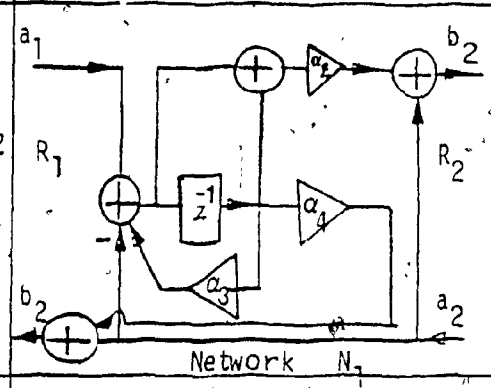 Network N_1	$\alpha_2 = \frac{R_2}{R_1}$ $\alpha_3 = \frac{R_1}{R + R_2}$ $\alpha_4 = \frac{R_1}{R_2}$
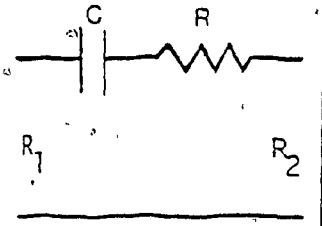	Same as Network N_1 with z^{-1} replaced by z_1^{-1} and L replaced by $\frac{1}{C}$ Network N_2	$\alpha_2 = \frac{R_2}{R + R_1}$ $\alpha_3 = \frac{R + R_2}{R + R_1}$ $\alpha_4 = \frac{RC - 1}{RC + 1}$
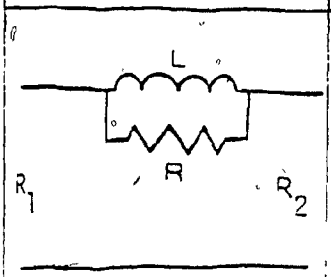	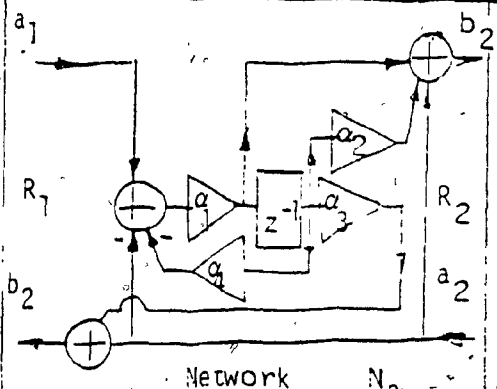 Network N_3	$\alpha_1 = \frac{R_2}{R_1}$ $\alpha_2 = \frac{R - L}{R + L}$ $\alpha_3 = \frac{R(R_2 - R_1)}{R_2}$ $\alpha_4 = \frac{R_1 L + R_2 R}{R_2 (R - L)}$
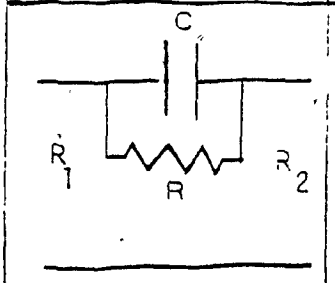	Same as Network N_3 with z^{-1} replaced by $-z^{-1}$ and L replaced by $1/C$ Network N_4	$\alpha_1 = R_2/R_1$ $\alpha_2 = \frac{RC - 1}{RC - 1}$ $\alpha_3 = \frac{R(R_2 - R_1)}{R_2}$ $\alpha_4 = \frac{R_1 + CR_2R}{R_2(RC+1)}$

2.3.2 Realization of the Different Combinations of Resistances and Reactive Elements in the Shunt Arm:

(1) Series Combination of Capacitance (C) and Resistance(R)

From Fig. 2.12,

$$Y'(s) = Cs/(RCs + 1) \text{ with } s = (z - 1)/(z + 1), \tag{2.32}$$

$$Y(z) = C(z - 1)/(RC(z - 1) + z + 1)$$

From Eqn. (2.4),

$$\mu_2 = \frac{Y_b + G_1 + G_2}{2G_1} \tag{2.33}$$

$$= \frac{\{C + (G_1 + G_2)(RC + 1)\} z \quad (G_1 + G_2)(1 - RC) - C}{2G_1 \{(RC + 1)z + (1 - RC)\}} \tag{2.34}$$

$$\nu_2 = 1 - \mu_2$$

$$\frac{\nu_2}{\mu_2} = \frac{\{2G_1(RC + 1) - C - (G_1 + G_2)(RC+1)\} z + 2G_1(1-RC)-(G_1+G_2)(1-RC)+C}{C\{(G_1+G_2)(RC+1)\} Z + (G_1 + G_2)(1-RC) - C} \tag{2.35}$$

Again, to avoid delay-free loops in the realization, it is required that the degree of numerator of $\frac{\nu_2}{\mu_2}$ should be less than that of the denominator and hence,

$$(RC+1)(G_1 - G_2) - C = 0 \tag{2.36}$$

Therefore,

$$\left.\begin{aligned} C &= (RC+1)(G_1 - G_2) \\ G_1 &= G_2 + \frac{C}{RC + 1} \\ G_2 &= G_1 - \frac{C}{RC + 1} \\ R &= \frac{1}{C}\left(\frac{C}{G_1 - G_2} - 1\right) \end{aligned}\right\} \tag{2.37}$$

Substituting Eqn. (2.37) into Eqns.(2.35) and (2.33) we have,

$$\frac{\gamma_2}{\mu_2} = \frac{\dfrac{(G_1 - G_2)}{G_1(RC+1)} z^{-1}}{1 + \dfrac{G_2 + G_1 RC}{G_1 (RC+1)} z^{-1}} \tag{2.38}$$

$$\frac{1}{\mu_2} = \frac{1 + \dfrac{1-RC}{1+RC} z^{-1}}{1 + \dfrac{G_2 + RCG_1}{G_1 (RC+1)} z^{-1}} \tag{2.39}$$

Let,

$$\frac{1 - RC}{1 + RC} = \beta_1$$

$$\frac{G_1 - G_2}{G_1(RC+1)} = \beta_2 \tag{2.40}$$

$$\frac{G_2 + RCG_1}{G_1(RC+1)} = \beta_3$$

Substituting Eqns. (2.38) and (2.39) into Eqn. (2.6) we have,

$$b_1 = a_2\sigma_2 + \frac{\beta_2 z^{-1}}{1 + \beta_3 z^{-1}} \times (a_1 + \sigma_2 a_2) \tag{2.41}$$

$$b_2 = -a_2 + \frac{1 + \beta_1 z^{-1}}{1 + \beta_3 z^{-1}} \times (a_1 + \sigma_2 a_2) \tag{2.42}$$

The corresponding realization is shown in Fig. (2.13).

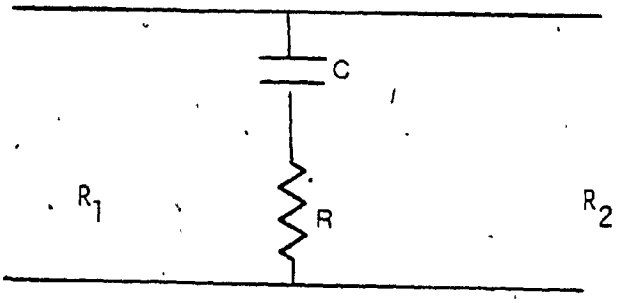

Fig. 2.12

Series Combination of Capacitance and Resistance in the Shunt Arm

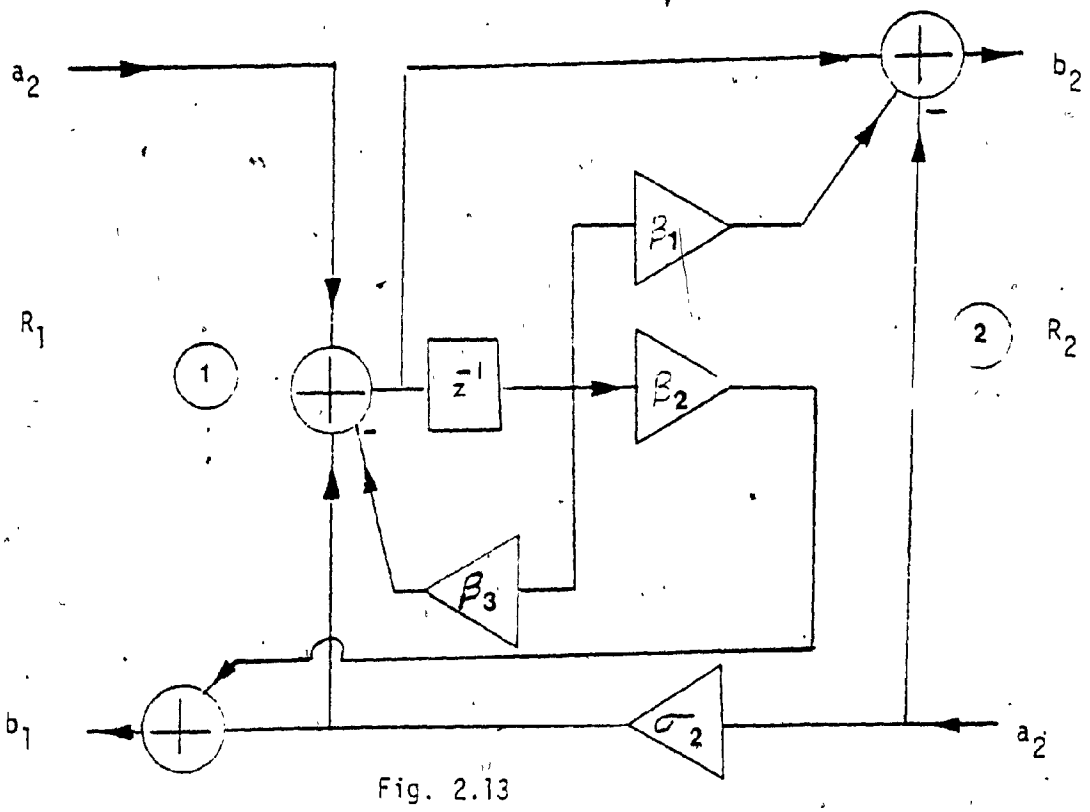

Fig. 2.13

Digital Realization Corresponding to Fig. 2.12

(2) Series combination of an inductance (L) and a resistance (R) in the shunt arm:

From Fig. 2.14. we have,

$$Y(s) = \frac{1}{Ls + R} \tag{2.43}$$

Let us make the transformation $L \rightarrow \frac{1}{C}$ and $s \rightarrow \frac{1}{s}$

then,

$$Y(s) = \frac{Cs}{RCs + 1} \tag{2.44}$$

Eqn. (2.44) is the same as Eqn. (2.32). Hence realization of Fig. 2.14 is the same as that of Fig. 2.13 with z^{-1} is replaced by $-z^{-1}$ and C is replaced by $\frac{1}{L}$ ..

Two-port wave digital realization is shown in Fig. 2.15.

(3) Parallel combination of capacitance (C) and resistance (R) in the shunt arm:

From Fig. 2.16, it is clear that the shunt resistance is in parallel with output load resistance or output port resistance hence the total resistance is given as,

$$R_t = R \times R_L/(R+R_L)$$

Realization is carried out as if only C is in shunt arm and output port resistance is equal to R_t.

Two-Port Wave Digital Realization is shown in Fig. 2.17.

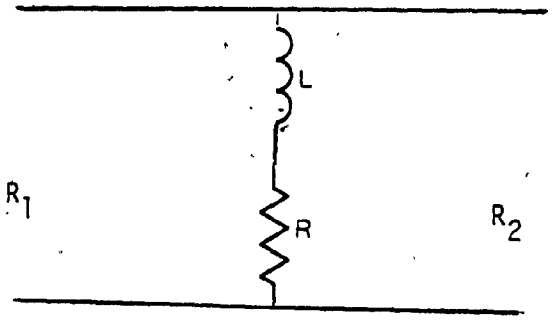

Fig. 2.14

Series Combination of an Inductance (L) and a Resistance (R) in the Shunt Arm

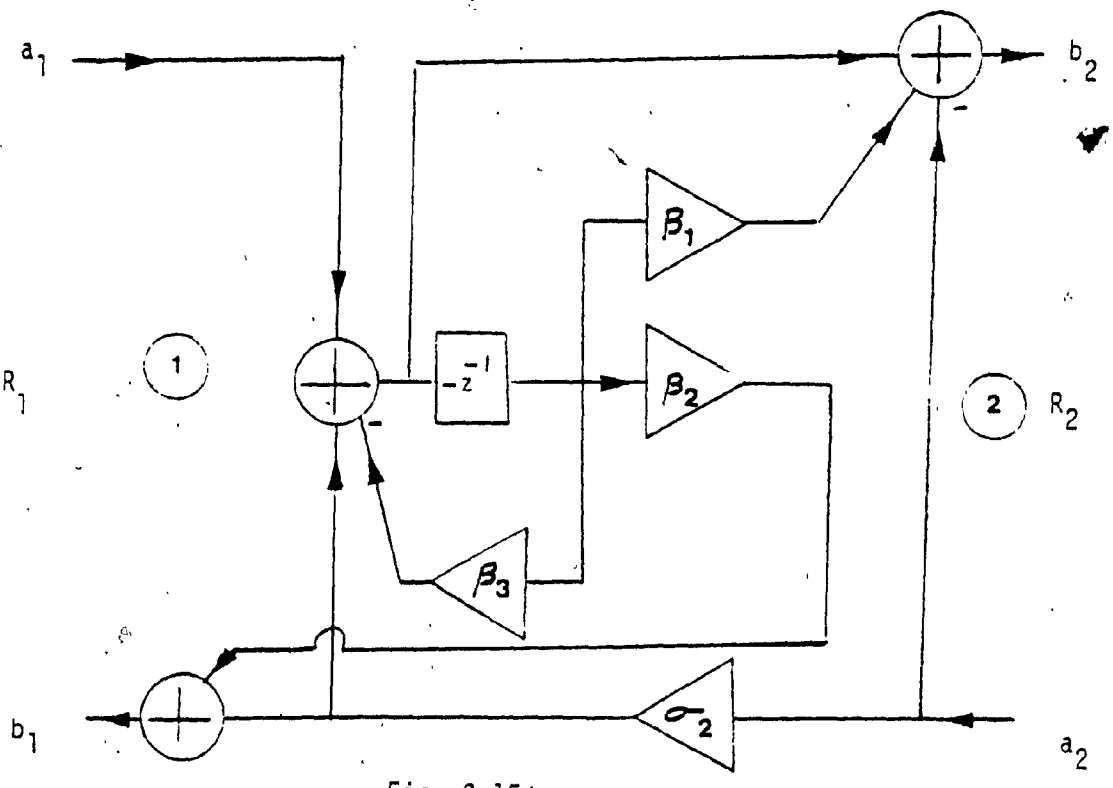

Fig. 2.15

Two-Port Wave Digital Realization of Network Shown in Fig. 2.14

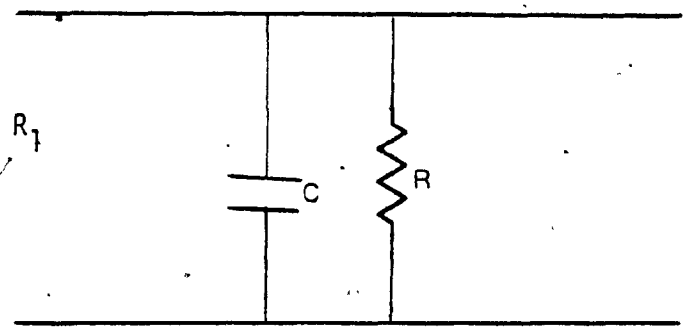

Fig. 2.16

Parallel Combination of Capacitance (C) and Resistance (R) in shunt Arm

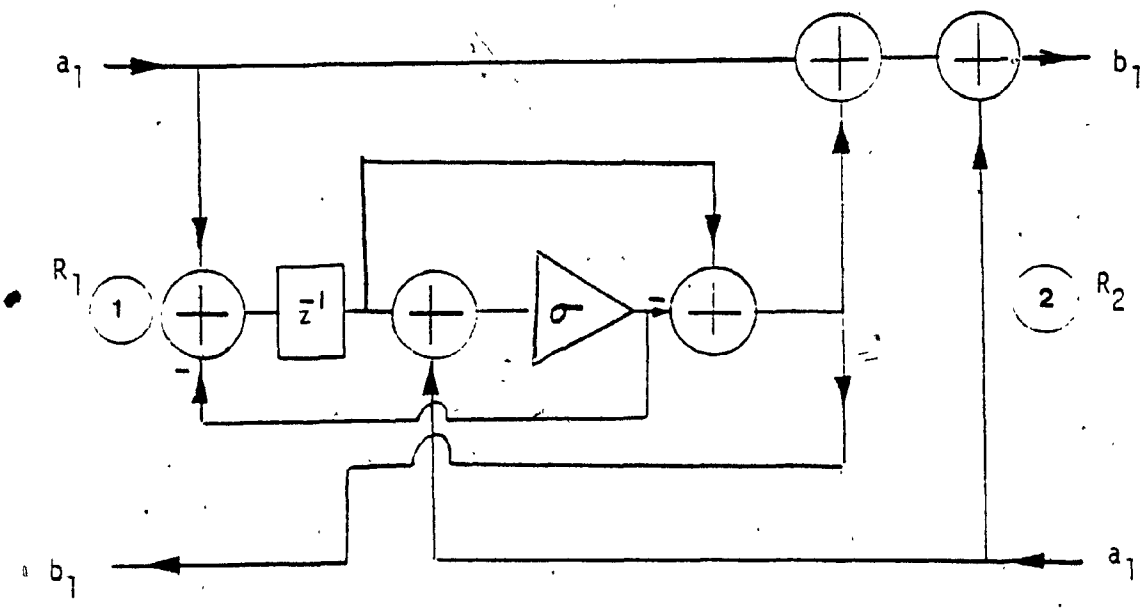

Fig. 2.17

Two-Port Wave Digital Realization of Network Shown in Fig. 2.16

(4) Parallel Combination of an inductance (L) and Resistance (R) in the shunt arm:

From Fig. 2.18, it is clear that the shunt resistance is in parallel with output port resistance. Hence wave digital realization can be carried out as if only (L) is in shunt with output port resistance is R_t where,

$$R_t = R R_L/(R+R_L)$$

Two-port wave digital realization is shown in Fig. 2.19.

Table 2.2 shows wave digital realization for combination of reactive and resistive elements in the shunt branch of the analog network ($\bar{N}$). It must be stated that in both Tables 2.1 and 2.2, only one digital realization corresponding to a combination in any arm is given. Other possibilities exist.

Now, we shall discuss the utilization of these results for the exact realization of PSTFs.

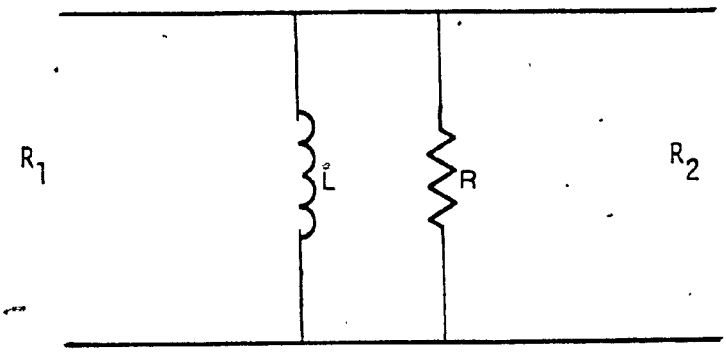

Fig. 2.18

Parallel Combination of an Inductance (L) and a Resistance (R) in the shunt Arm

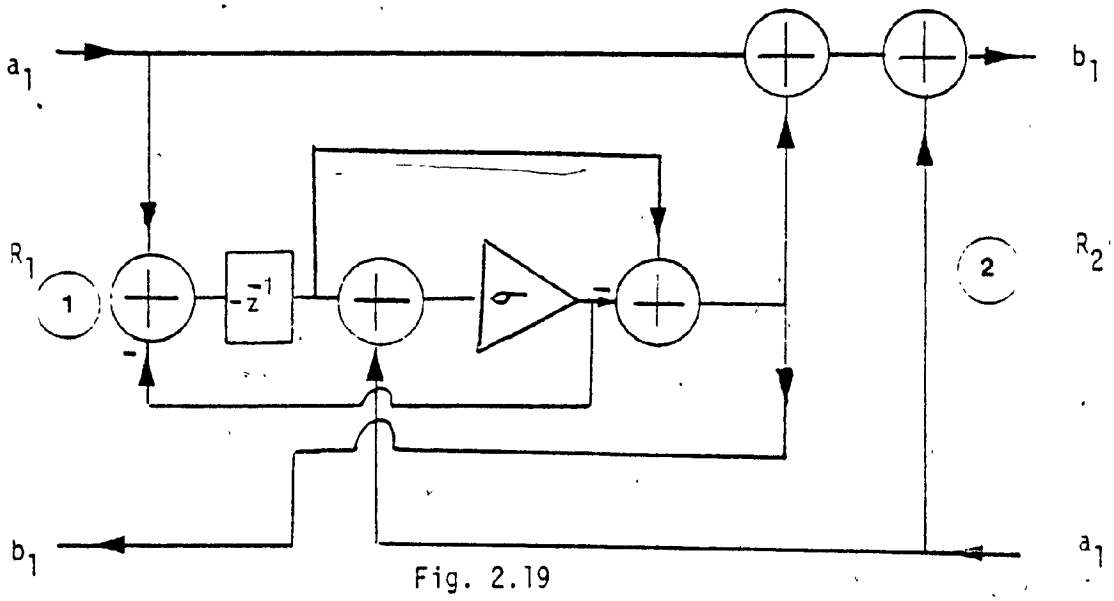

Fig. 2.19

Two port-Wave Digital Realization of Network Shown in Fig. 2.18

Table 2.2

Two-port Wave Digital Realizations of Different Combinations of Resistances and Reactive Elements in the Shunt Arm of Analog Network

Element	Corresponding wave Digital 2-port Realization	Relations
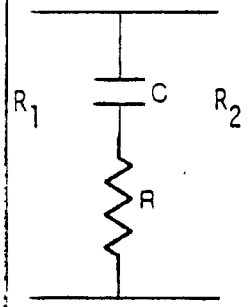	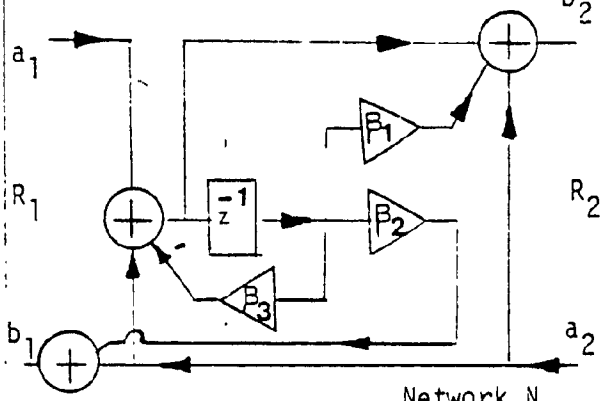 Network N_5	$G_1 = G_2 + \frac{C}{RC+1}$ $\sigma_2 = R_2/R_1$ $\beta_1 = \frac{1-RC}{1+RC}$ $\beta_2 = \frac{G_1-G_2}{G_1(RC+1)}$ $\beta_3 = \frac{G_2+RCG_1}{G_1(RC+1)}$
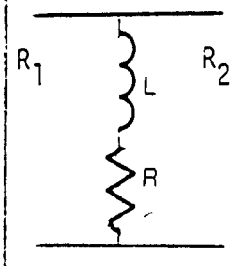	Same as Network N_5 with z^{-1} replaced by $-z^{-1}$ Network N_6	Multipliers, same as above with C replaced by 1/L
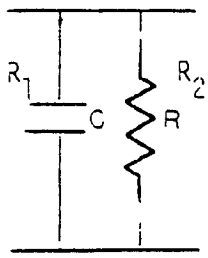	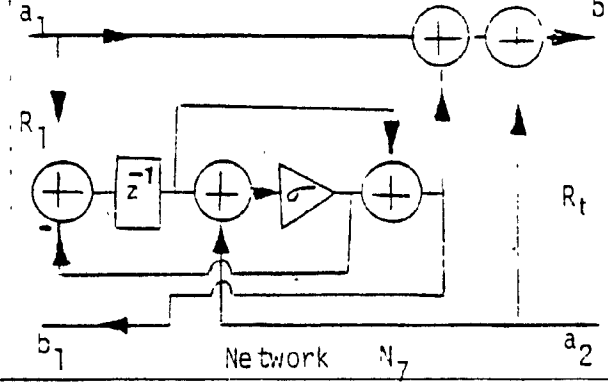 Network N_7	$R_t = \frac{R \times R_2}{R + R_2}$ $G_1 = G_2 + C$ $\sigma = G_2/G_1$
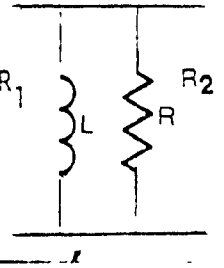	Same as Network N_7 with z^{-1} replaced by $-z^{-1}$ Network N_8	$R_t = \frac{R \times R_2}{R + R_2}$ $\sigma = G_2/G_1$ $G_1 = G_2 + 1/L$

2.4 Product Separable Transfer Function Realization:

For the sake of completeness, we shall discuss both approximate and exact realizations of PSTFs.

2.4.1 Approximate Realization of PSTF:

Let us start with Nth order doubly terminated L-C ladder network of two-variables s_1 and s_2. Reactive elements of network can be associated with either variable s_1 or variable s_2 as shown in Fig. 2.20.

Let the chain matrix of Network 1 be represented as,

$$\begin{bmatrix} a_1 & b_1 \\ c_1 & d_1 \end{bmatrix}$$

and let the chain matrix of Network 2 be represented as,

$$\begin{bmatrix} a_2 & b_2 \\ c_2 & d_2 \end{bmatrix}$$

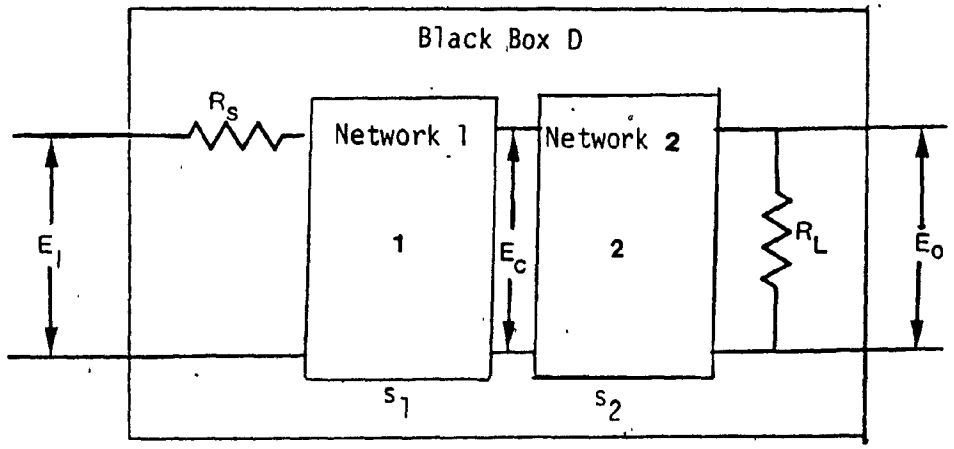

Fig. 2.20

Two-Variable Cascade Analog Network

$$\frac{E_c}{E_1} = h(s_1) = \frac{n_1(s_1)}{d_1(s_1)}$$

$$\frac{E_o}{E_c} = h_1(s_1) = \frac{n_2(s_2)}{d_2(s_2)}$$

Tho ABCD matrix of black box D is given by

$$\begin{bmatrix} A & B \\ C & D \end{bmatrix} = \begin{bmatrix} 1 & R_s \\ o & 1 \end{bmatrix} \times \begin{bmatrix} a & b \\ c & d \end{bmatrix} \times \begin{bmatrix} 1 & 0 \\ R_L & 1 \end{bmatrix}$$

(2.46)

The transfer function of the black box D is given by $H(s_1,s_2) = 1/A$ which is,

$$H(s_1,s_2) = \frac{1}{a + R_s c + R_L b + R_s R_L d} \qquad (2.47)$$

It is clear from Eqn. (2.47), that by cascading two analog sections of different variables (s_1 and s_2), it does not realize exact product separable digital filter transfer function.

One can approximate Eqn. (2.47) as a product separable transfer function. To make it clear, let us consider a network shown in Fig. 2.21,

The transfer function is given by,

$$H(s_1,s_2) = \frac{\frac{1}{L_1L_2C_1C_2}}{(s_1^2+\frac{R_s}{L_1}s_1+\frac{1}{L_1C_1})(s_2^2+\frac{R_L}{C_2}s_2+\frac{1}{L_2C_2})+C_2L_1(s_1+\frac{R_s}{L_1})(s_2+\frac{R_L}{C_2})} \qquad (2.48)$$

The coefficients of different terms are shown in Table 2.3. By assuming $C_2L_1(s_1+\frac{R_s}{L_1})(s_2+\frac{R_L}{C_2})$ is very small then Eqn. (2.48) can be approximated as,

$$H(s_1,s_2) = \frac{\frac{1}{L_1C_2C_1C_2}}{(s_1^2+\frac{R_s}{L_1}s_1+\frac{1}{L_1C_1})(s_2^2+\frac{R_L}{C_2}s_2+\frac{1}{C_2L_2})} \qquad (2.49)$$

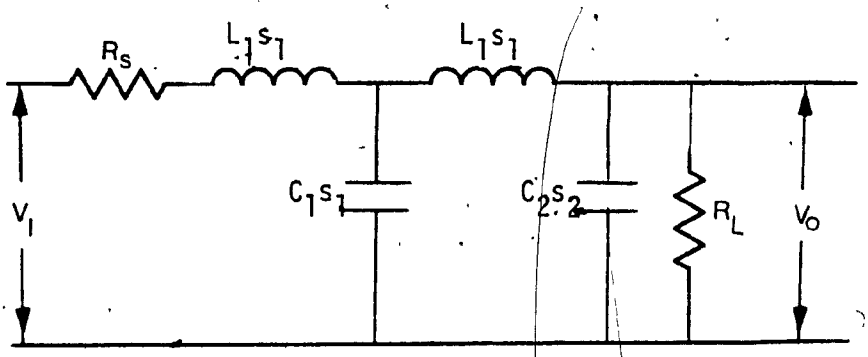

Fig. 2.21

A Second order doubly Terminated Cascade-decomposable Analog Network

$$H(s_1, s_2) = \frac{V_o}{V_1} = \frac{\frac{1}{L_1 L_2 C_1 C_2}}{(s_1^2 + \frac{R_s}{L_1} s_1 + \frac{1}{L_1 C_1})(s_2^2 + \frac{R_L}{C_2} s_2 + \frac{1}{L_2 C_2}) + C_2 L_1 (s_1 + \frac{R_s}{L_1})(s_2 + \frac{R_L}{C_2})}$$

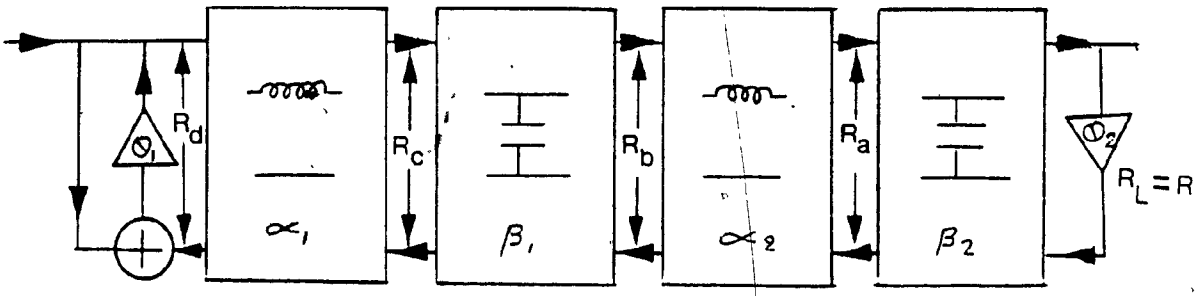

Fig. 2.22

Two-port Digital Realization Corresponding to Network of Fig. 2.21

Table 2.3

Coefficients of the different powers in Eqns. (2.48) and (2.49)

No.	Term (a)	Coefficients of Eqn(2.44) (b)	Coefficients of Eqn(2.44) (c)	Difference (b)-(c)
1	$s_1^2 s_2^2$	1	1	0
2	$s_1^2 s_2$	$\frac{R_L}{C_2}$	$\frac{R_L}{C_2}$	0
3	s_1^2	$\frac{1}{L_2C_2}$	$\frac{1}{L_2C_2}$	0
4	$s_1 s_2^2$	$\frac{R_s}{L_1}$	$\frac{R_s}{L_1}$	0
5	$s_1 s_2$	$\frac{1}{L_2C_1} + \frac{R_sR_L}{L_1C_2}$	$\frac{R_sR_L}{L_1C_2}$	$\frac{1}{L_2C_1}$
6	s_1	$\frac{R_s}{C_2L_1L_2} + \frac{R_L}{L_2C_1C_2}$	$\frac{R_s}{L_1L_2C_2}$	$\frac{R_L}{L_2C_1C_2}$
7	s_2^2	$\frac{1}{L_1C_1}$	$\frac{1}{L_1C_1}$	0
8	s_2	$\frac{R_s}{L_1C_1L_2} + \frac{R_L}{L_1C_1C_2}$	$\frac{R_L}{L_1C_1C_2}$	$\frac{R_s}{C_1L_1L_2}$
9	1	$\frac{1}{L_1L_2C_1C_2} + \frac{R_LR_s}{L_1L_2C_1C_2}$	$\frac{1}{L_1L_2C_1C_2}$	$\frac{R_LR_s}{L_1L_2C_1C_2}$

To satisfy the assumption, one has to make $C_2L_1(s_1+\frac{R_s}{L_1})(s_2+\frac{R_L}{C_2})$ as small as possible. This can be achieved by fulfilling the following conditions which are given from Table 2.3.

$$\frac{1}{L_2C_1} << \frac{R_sR_L}{C_2L_1C_2} \qquad (a)$$

$$\frac{R_L}{L_2C_1C_2} << \frac{R_s}{L_1L_2C_2} \qquad (b)$$

$$\frac{R_s}{L_1L_2C_1} << \frac{R_L}{L_1C_1C_2} \qquad (c)$$

$$\frac{R_LR_s}{L_1L_2C_1C_2} << \frac{1}{L_1L_2C_1C_2} \qquad (d)$$

From these conditions it can be concluded that to consider Eqn. (2.47) as an approximate product separable transfer function, network of Fig. 2.21 must satisfy the following conditions.

(1) $R_s \simeq R_L$

(2) $C_1 >> L_1$

(3) $L_2 >> C_2$

2.4.2 Exact realization of PSTF:

Our aim here is to realize exact digital filter PSTF. One of the methods we are applying here is to cascade parallel sections of different variables with the realization shown in section 2.4.1. Due to cancellation of terms this overall structure gives a realization of product separable digital filter transfer function.

For cascade separable analog network (Fig. 2.20) the transfer function will be of the form [19] to [21] .

$$H_a(s_1,s_2) = \frac{\{n_1(s_1) \quad n_2(s_2)\}}{n_1(s_1)d_2(s_2) + d_1(s_1)n_2(s_2)} \tag{2.50}$$

After making the double bilinear transformation, the 2-D digital transfer function will be of the type,

$$H_{d_1}(z_1,z_2) = \frac{n_d(z_1,z_2)}{n_{d_1}(z_1)d_{d_2}(z_2) + n_{d_2}(z_2)d_{d_1}(z_1)} \tag{2.51}$$

In order to obtain realization of a exact PSTF, a parallel realization of a digital transfer function,

$$H_{d_2}(z_1,z_2) = \frac{n_{d_1}(z_1)}{d_{d_1}(z_1)} + \frac{n_{d_2}(z_2)}{d_{d_2}(z_2)} \tag{2.52}$$

$$= P_1(z_1) + P_2(z_2)(\text{say})$$

is so connected in cascade with $H_{d_1}(z_1,z_2)$ so that the overall 2-D digital transfer function will be

$$H_d(z_1,z_2) = \frac{n_d(z_1z_2)}{d_{d_1}(z_1)d_{d_2}(z_2)} \tag{2.53}$$

The corresponding realization is shown in Fig. 2.23.

For the realization of Eqn. (2.50) by the network shown in Fig. 2.20, we can make the identification,

$$y_{22_1}(s_1) = \frac{n_1(s_1)}{d_1(s_1)} \quad \text{and} \quad y_{11_2}(s_2) = \frac{n_2(s_2)}{d_2(s_2)} \tag{2.54}$$

$$-y_{12_1}(s_2) = \frac{n_{a_1}(s_1)}{d_1(s_1)} \qquad -y_{12_2}(s_2) = \frac{n_{a_2}(s_2)}{d_2(s_2)}$$

Where the y_{22_1} and $-y_{12_1}$ are the Y parameters of the network of variables s_1 and y_{11_2} and $-y_{12_2}$ are the Y parameters of the network of variable s_2.

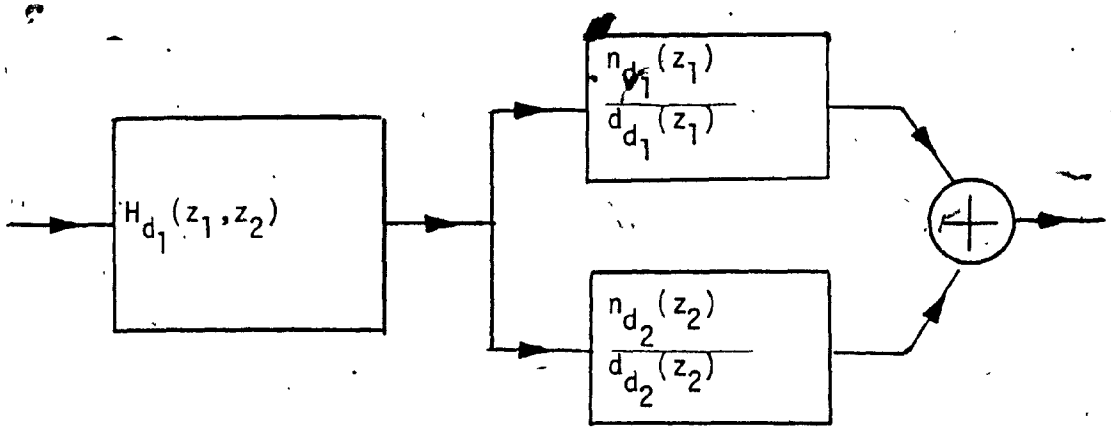

Fig. 2.23

Overall Realization of $H_d(z_1,z_2)$, a PSTF

Both y_{11_2} and y_{22_1} are positive real functions and will be reactance functions in the case of lossless networks. $P_1(z_1)$ and $P_2(z_2)$ are the digital transfer functions obtained from $y_{22_1}(s_1)$ and $y_{11_2}(s_2)$ after the corresponding bilinear transformations. If the starting analog networks have to be in the form of ladder networks from which the digital filter realizations are obtained, then $y_{22_1}(s_1)$ and $y_{11_2}(s_2)$ shall have special forms. It has to be pointed out that other realizations are possible.

Since higher order PSTFs can be realized by having a cascade connection of lower order building blocks, we shall consider the realization of second order $y_{22_1}(s_1)$ and $y_{11_2}(s_2)$, in which case the functions $d_{d_1}(z_1)$ and $d_{d_2}(z_2)$ are each of second order. Therefore, it is essential that Fig. 2.21 has to be rearranged. Two possible rearrangements are given below (It has to be emphasized that other realizations are possible).

Fig. 2.24(a) and Fig. 2.24(b) are the two possibilities given. Fig. 2.24(c) and Fig. 2.24(d) are some of the other possiblities to realize Eqn. (2.50). It is to be noted here that y_{12_1} and y_{12_2} of Fig. 2.24(c) and 2.24(a) are not all pole functions and y_{22_1} and y_{11_2} have same degree numerators and denominators polynomial. So in this method it is not possible to get all-pole analog 2-D transfer function. When higher order filters are designed, this method appears to be powerful and therefore be adopted. However, in such realizations, stability can be guaranteed.

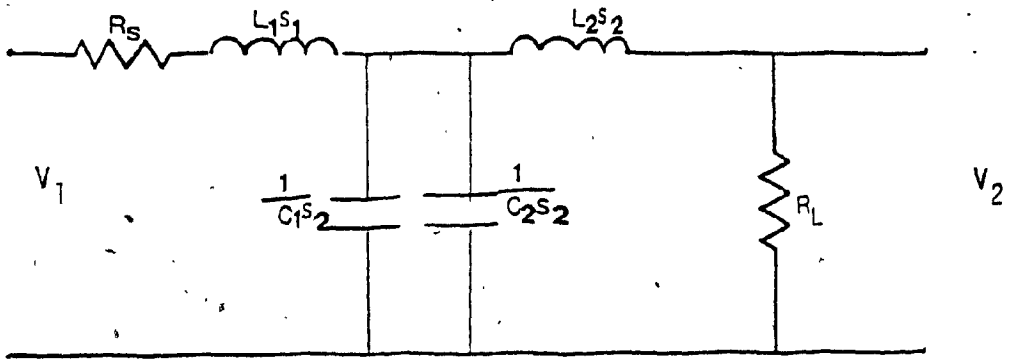

Fig. 2.24(a)

Rearrangement of the Network shown in Fig. 2.21

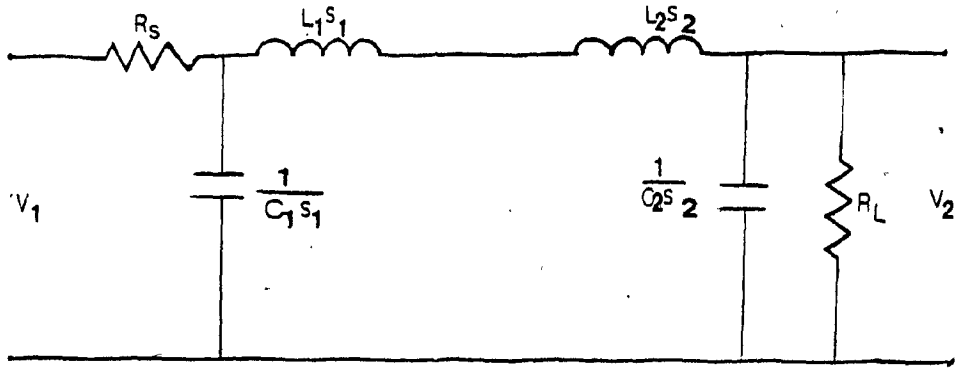

Fig. 2.24(b)

Rearrangement of the Network shown in Fig. 2.21

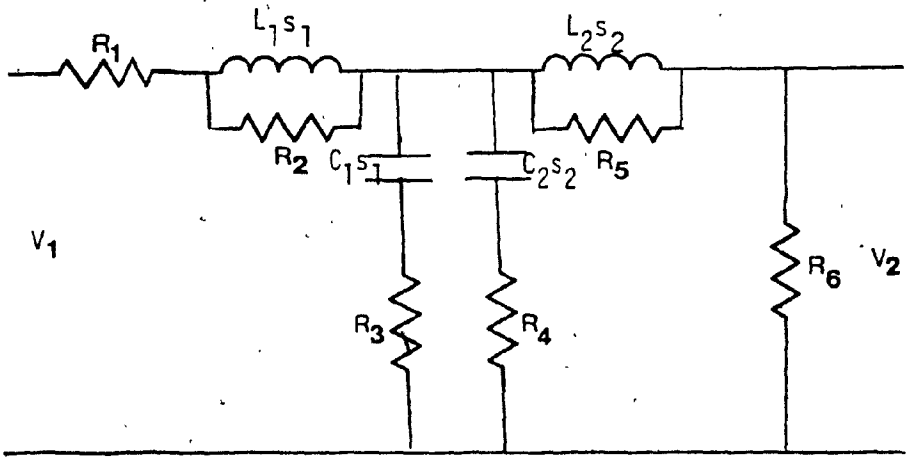

Fig. 2.24(c)

Realization of Eqn. (2.50)

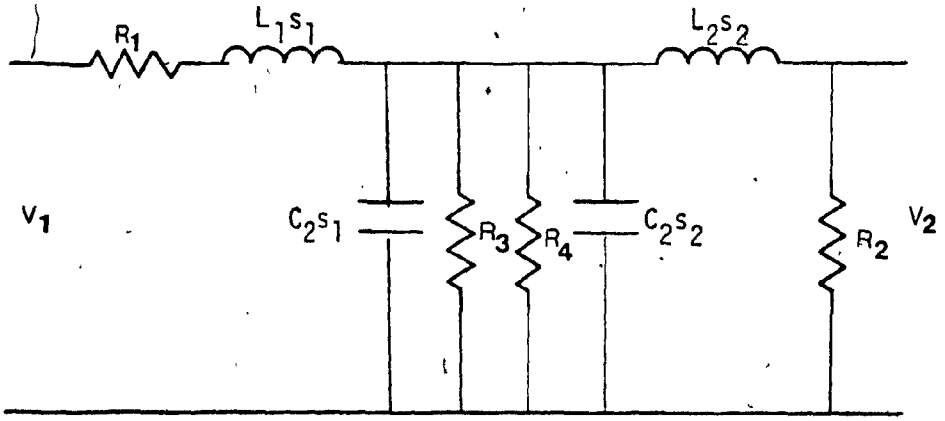

Fig. 2.24(d)

Realization of Eqn. (2.50)

The analog transfer function in the case of network of Fig. 2.24(a) will be,

$$\frac{V_2}{V_1} = H_c(s_1,s_2) =$$

$$\frac{R_L}{(L_1 C_1 s_1^2 + R_s C_1 s_1 + 1)(L_2 s_2 + R_L) + (L_1 s_1 + R_s)(L_2 C_2 s_2^2 + R_L C_2 s_2 + 1)}$$

where,

$$\frac{1}{Y_{22_1}(s_1)} = \frac{n_1(s_1)}{d_1(s_1)} = \frac{L_1 s_1 + R_s}{L_1 C_1 s_1^2 + R_s C_1 s_1 + 1}$$

$$\frac{1}{Y_{11_2}(s_2)} = \frac{n_2(s_2)}{d_2(s_2)} = \frac{L_2 s_2 + R_L}{L_2 C_2 s_2^2 + R_L C_2 s_2 + 1}$$

The transfer functions $P_1(z_1)$ and $P_2(z_2)$ are

$$P_1(z_1) = \frac{1}{Y_{22_1}(s_1)} \Bigg|_{s_1 = \frac{z_1 - 1}{z_1 + 1}} \qquad (2.56a)$$

and

$$P_2(z_2) = \frac{1}{Y_{11_2}(s_2)} \Bigg|_{s_2 = \frac{z_2 - 1}{z_2 + 1}} \qquad (2.56b)$$

The corresponding analog realizations for Fig. 2.24(a) and Fig. 2.24(b) are shown in Figs. 2.25(a) and 2.25(b).

The two-port digital realizations of networks in Figs. 2.24 and 2.25 are shown in Figs. 2.26 and 2.27. Cascading digital networks of Figs. 2.26 and 2.27 as shown in Fig. 2.28, It gives overall exact realization of second order PSTF given in Eqn. (2.53) with,

$$n_d(z_1,z_2) = k(z_1+1)^2(z_2+1)^2,$$

where k is a positive constant.

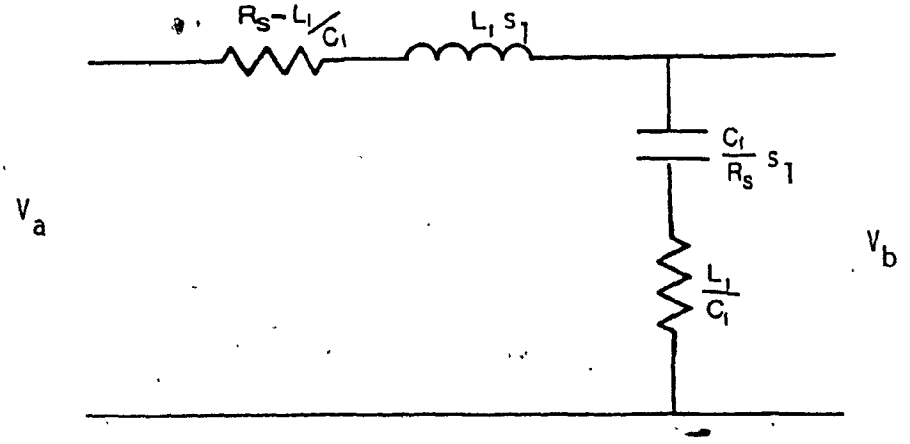

Fig. 2.25(a)
The Analog Realizations of the Transfer Function of Eqn. (2.56a)

$$\frac{V_b}{V_a} = h_1(s_1) = \frac{L_1 s_1 + R_s}{L_1 C_1 s_1^2 + R_s C_1 s_1 + R_s} = \frac{n_1(s_1)}{d_1(s_1)}$$

$$= \frac{1}{Y_{22_1}(s_1)}$$

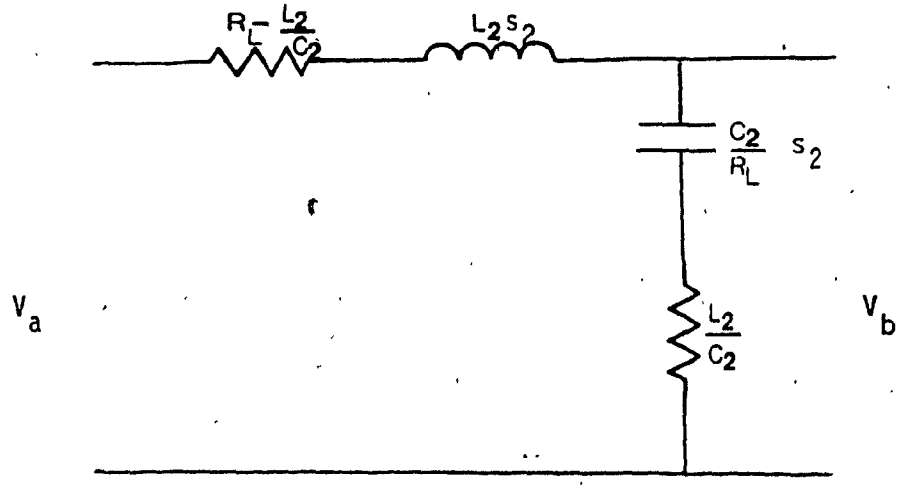

Fig. 2.25(b)
The Analog Realizations of the Transfer Function of Eqn. (2.56b)

$$\frac{V_b}{V_a} = h_2(s_2) = \frac{L_2 s_2 + R_L}{L_2 C_2 s_2^2 + R L_1 C_2 s_2 + R_L} = \frac{n_2(s_1)}{d_2(s_2)} = \frac{1}{Y_{11_2}(s_2)}$$

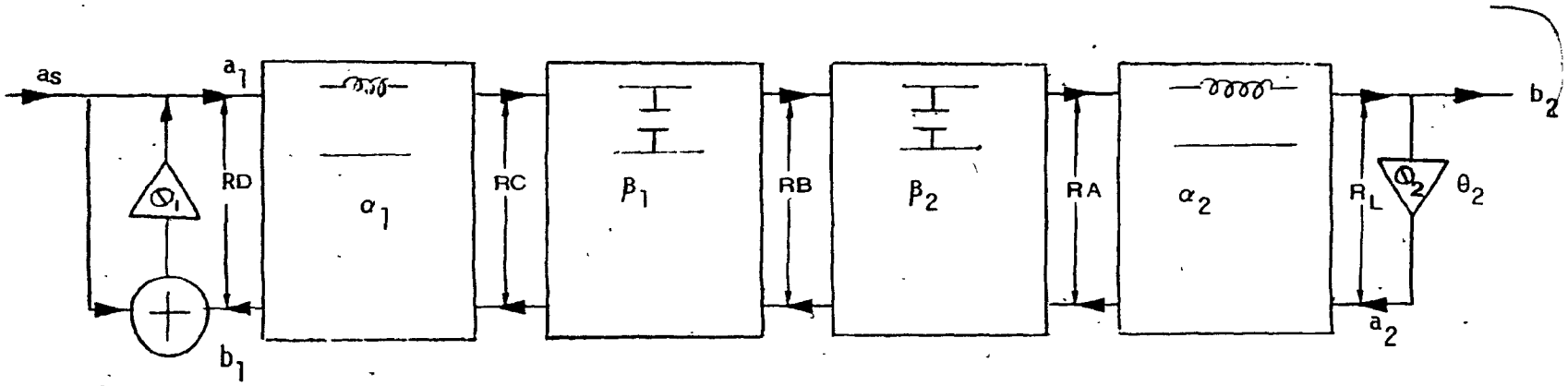

Fig. 2.26

Two-port digital Realization of Analog Network shown in Fig. 2.24

$$\frac{b_2}{as} = H_c(z_1, z_2)$$

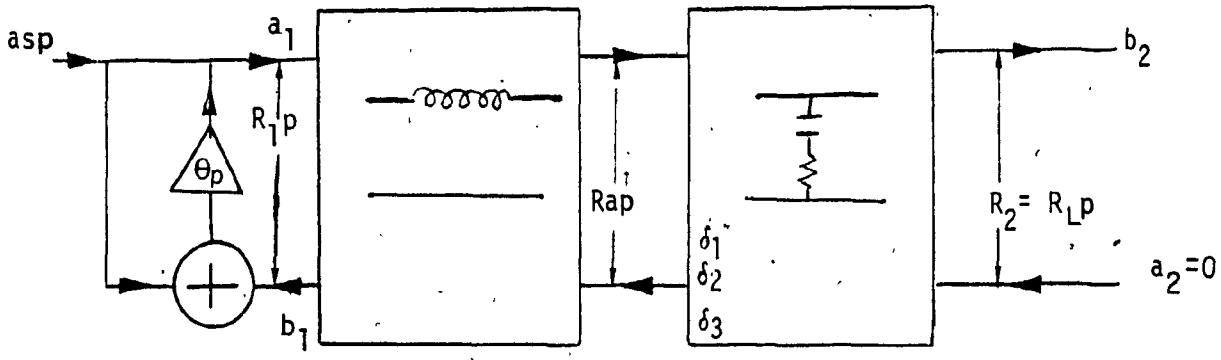

Fig. 2.27

Two-Port Digital Realization of Analog Network Shown in Fig. 2.25

$$\frac{b_2}{asp} = H_p(z_i),\ i = 1,2$$

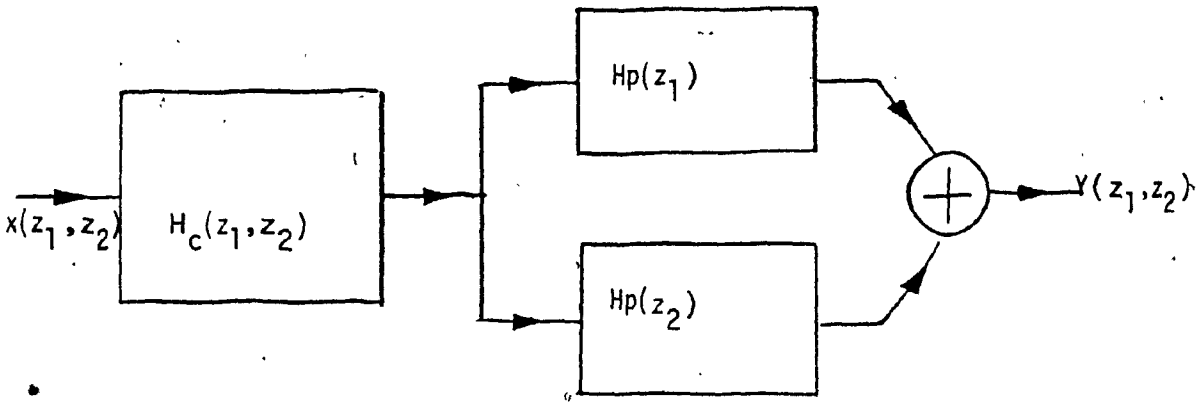

Fig. 2.28

Overall Realization of PSTF

$$\frac{Y(z_1,z_2)}{X(z_1,z_2)} = H(z_1,z_2) = \left\{\frac{K}{D_1(z_1) \times D_2(z_2)}\right\}$$

2.5 Summary and Discussion:

In this chapter, a new way of product separable digital filter transfer function realization has been proposed. This will be a cascade connection of a digital realization corresponding to a doubly-terminated two-variable cascade-decomposable network and a parallel digital realization of suitable single-variable transfer functions. Since higher order functions can be realized using lower order building blocks, a realization corresponding to second degree in each variable is discussed in detail. To accomplish this, it is shown that the wave digital realization corresponding to lossy reactive elements in the series and shunt arms of the analog ladder network is required. Such realizations have been discussed.

Chapter 3

THE DIFFEPENT FILTER RESPONSES FOR PSTF REALIZATIONS

3.1 Introduction

Here we examine the magnitude responses of the approximate and exact realizations of PSTFs having different pole locations. According to these locations we will have different types of two variable product separable denominator polynomials. A similar approach can be applied for higher order PSTF realizations.

We would check now magnitude responses for low-pass normalized approximate and exact PSTFs of the following types:

(a) Butterworth

(b) Chebyshev

(c) Bessel

(d) Different combinations of the above four cases.

We would also check magnitude responses for higher order PSTF of different digital filters.

3.2 Examples

It is shown in Eqn. (1.9) that 2-D PSTF $H(s_1, s_2)$ is given by,

$$H(s_1, s_2) = h_1(s_1) \times h_2(s_2) \qquad (3.1)$$

We consider approximate digital realization of PSTF $H(s_1, s_2)$ shown in Fig. 2.21(b) and exact digital realization shown in Fig. 2.28

(which incorporates the realizations shown in Figs. 2.24(a), 2.25(a), 2.25(b).

Let, R_I be the realization of Fig. 2.21 (b)

and R_{II} be the realization of Fig. 2.28 with Figs. 2.24(a), 2.25(a) and 2.25(b)

3.2.1 Low-Pass Butterworth PSTF Response

The overall PSTF will be

$$H_a(s_1,s_2) = \frac{K}{(s_1^2 + 1.4s_1 + 1)(s_2^2 + 1.4s_2 + 1)} \qquad (3.2)$$

Fig. 3.1 shows the response of the realization of R_I.

Fig. 3.2(a) and 3.2(b) shows the response of the realization of R_{II}.

Fig. 3.3 shows the response 3-D plotting of the realization of R_{II}.

The data for Figs. 2.24 (a), 2.26 and 2.27 are given in Appendix - I.

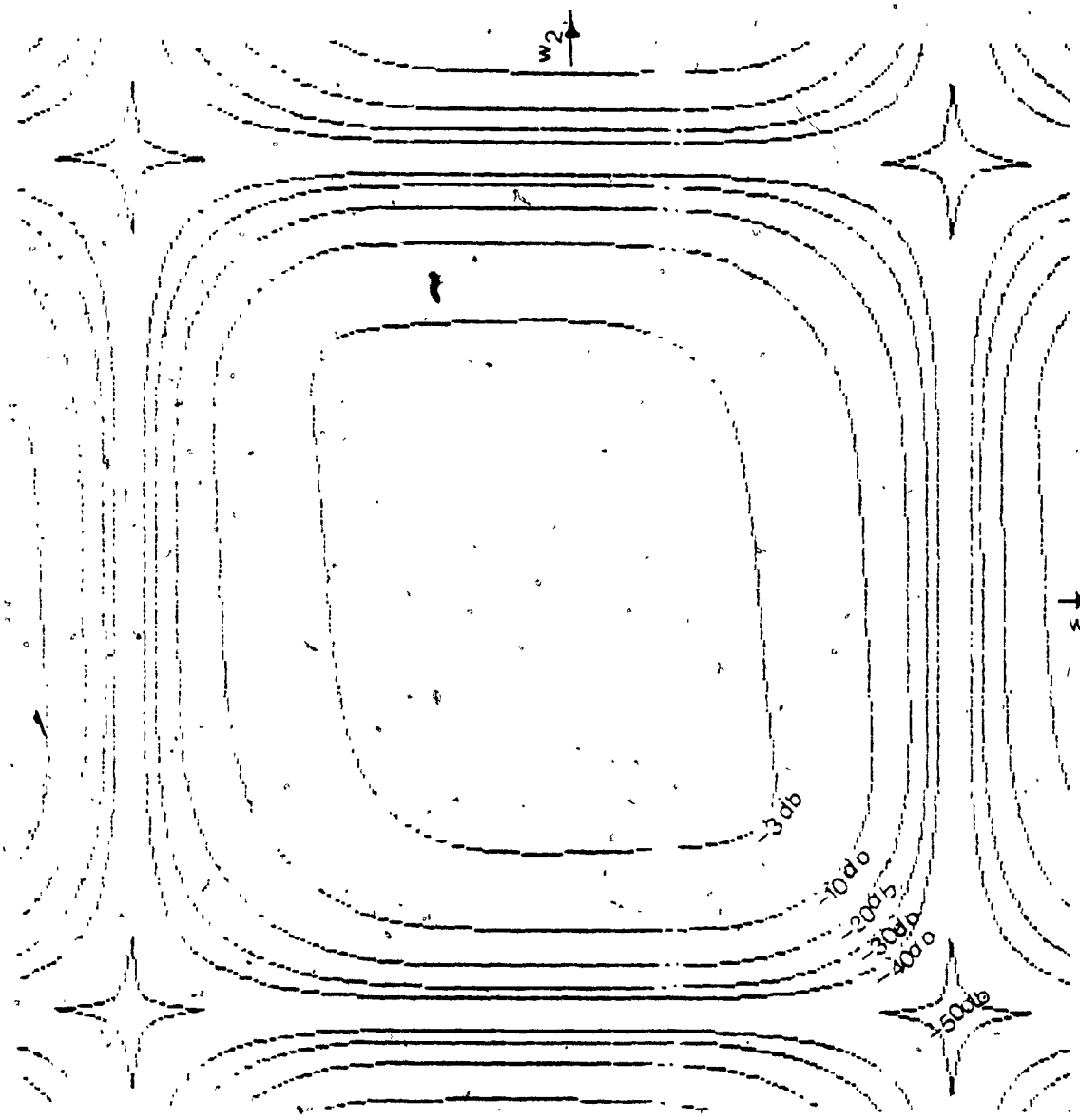

Fig. 3.1

Magnitude Response contours of R_I for Eqn. (3.2)

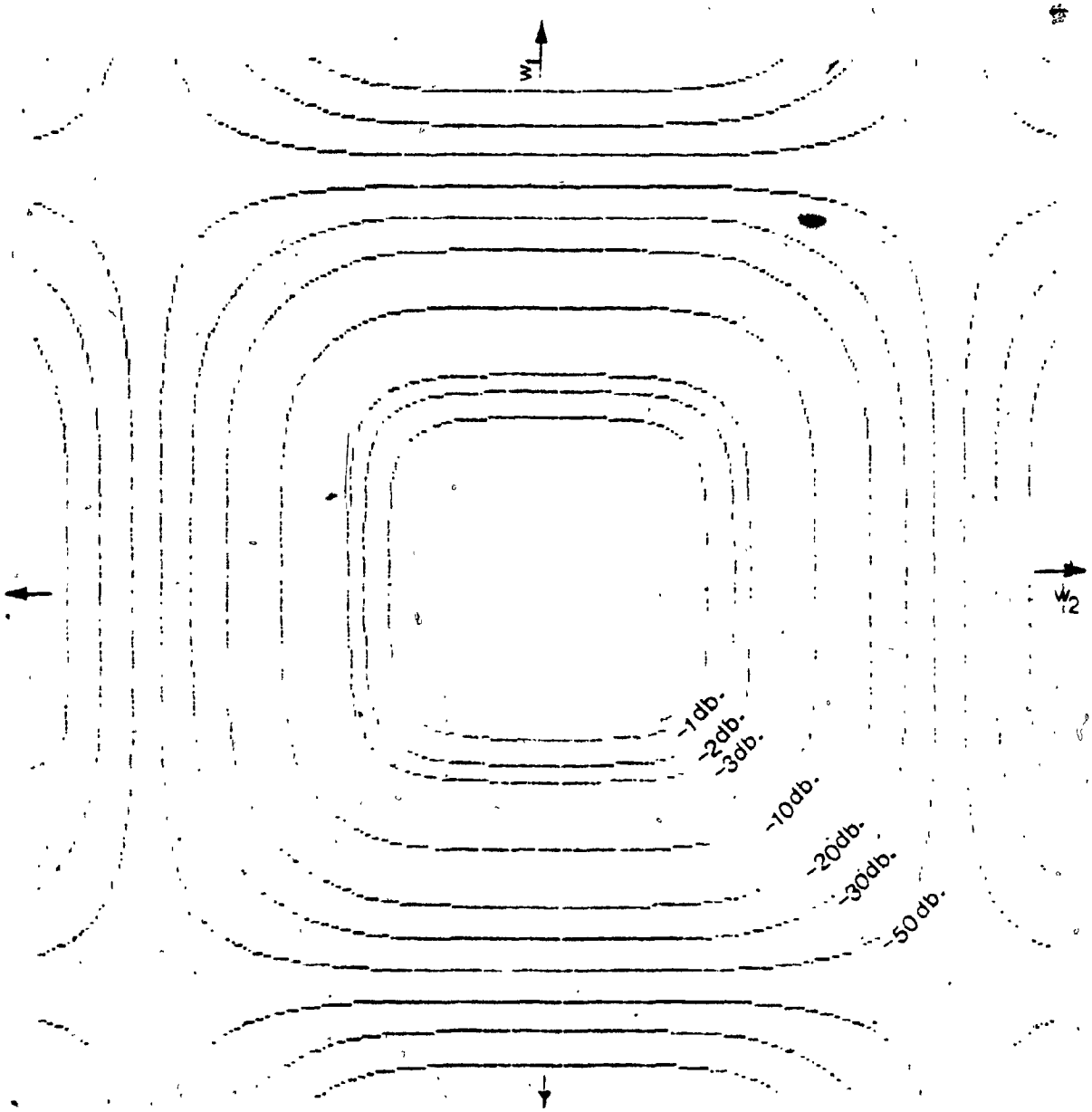

Fig. 3.2(a)

Magnitude Response Contours of R_{II} for Eqn. (3.2)

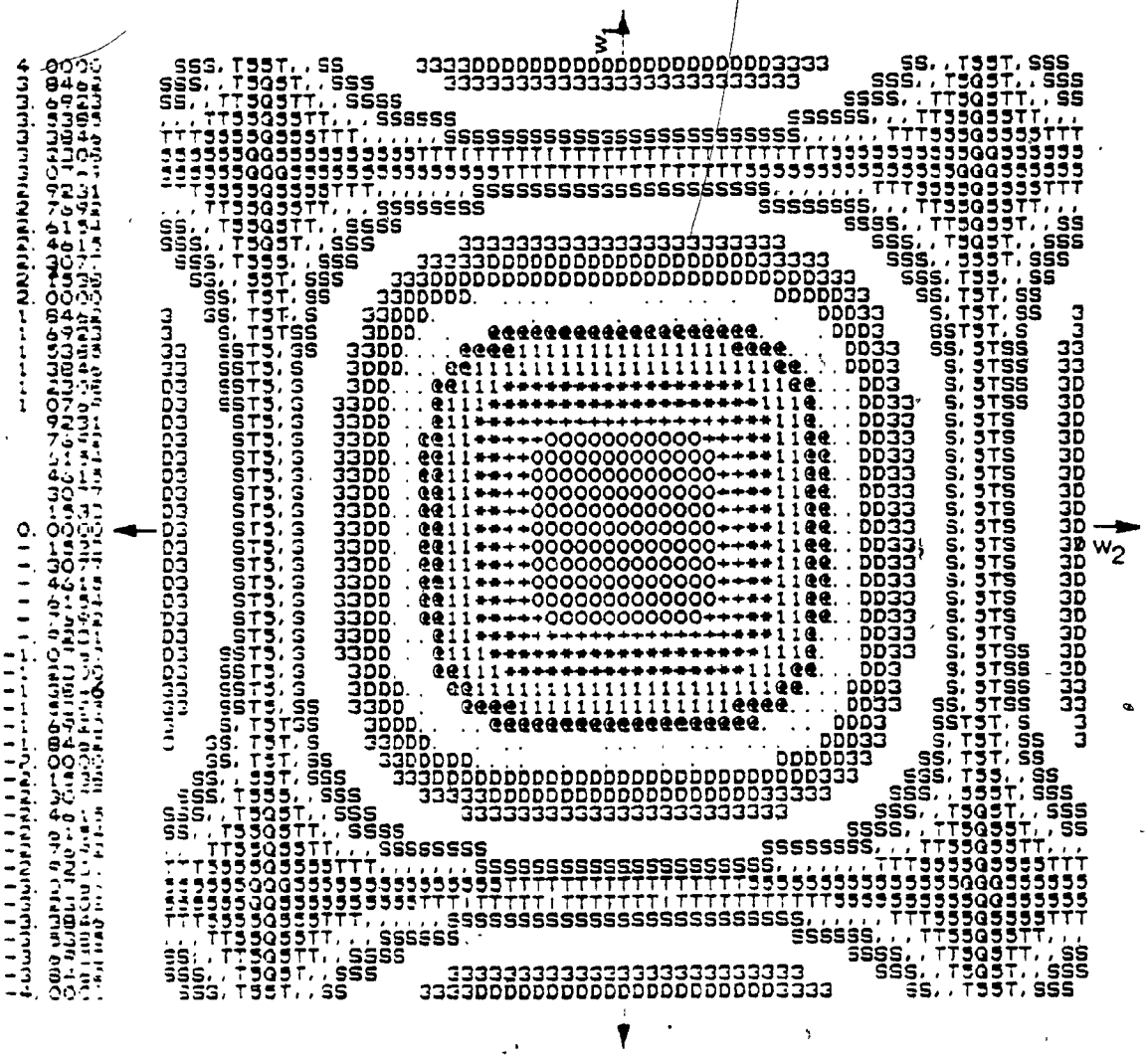

Fig. 3.2(b)

Magnitude Response Contours of R_{II} for Eqn. (3.2)

(Magnitude is in-db.)

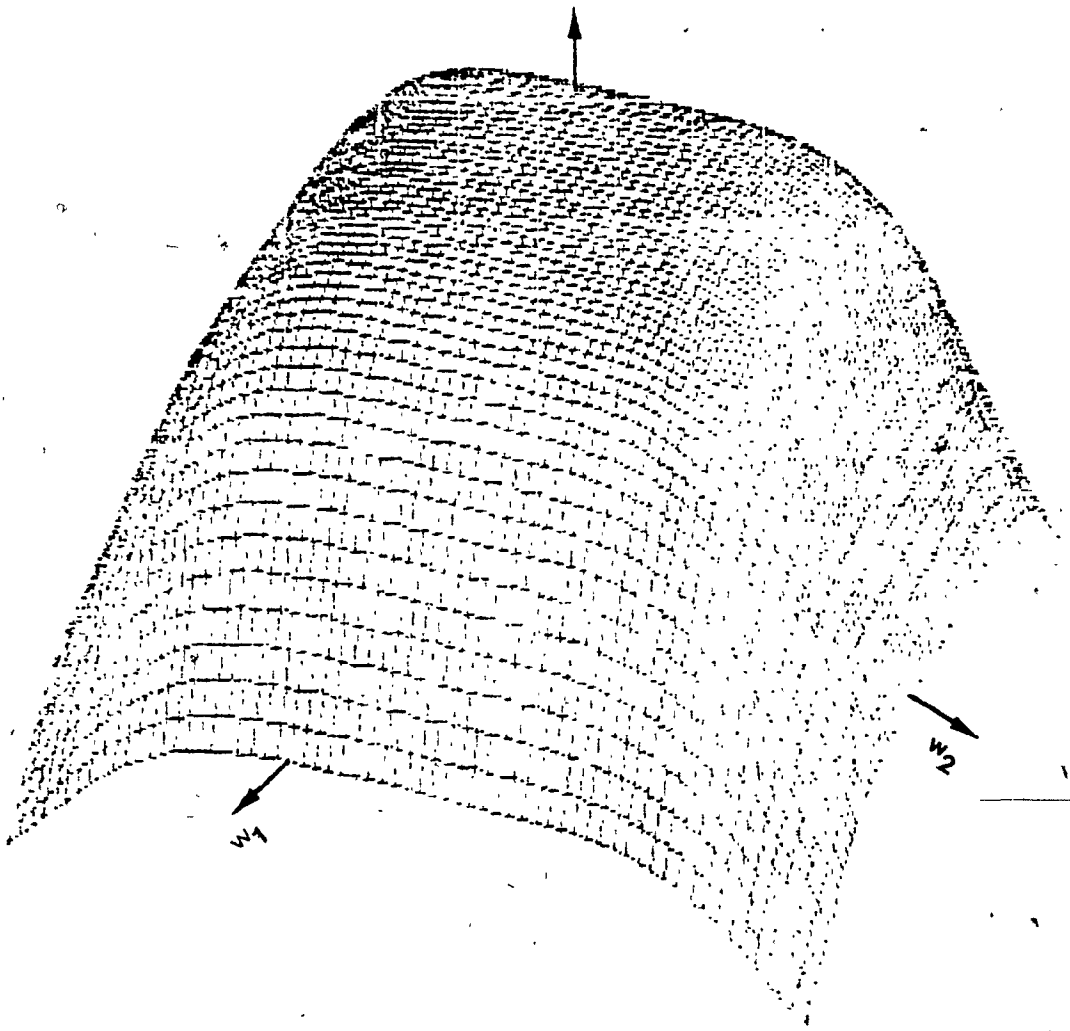

Fig. 3.3

3-D. Plotting of Magnitude Response of R_{II} for Eqn. (3.2)

3.2.2 Low-Pass Chebyshev PSTF Response

Here we will consider an example of low-pass chebyshev filter having o.5 db ripple in its pass-band. The overall PSTF will be,

$$H_a(s_1,s_2) = \frac{K}{(s_1^2 + 2.05s_1 + 0.785)(s_2^2 + 2.05s_2 + 0.785)} \quad (3.3)$$

Fig. 3.4 shows the response contours of the realization of R_I.

Fig. 3.5(a) and 3.5(b) show the response contour of the realization of R_{II}.

Fig. 3.6 shows response 3-D plotting of the realization of R_{II}.

The required data for Figs. 2.24(a), 2.26 and 2.27 are given in Appendix II.

3.2.3 Low-pass Bessel PSTF response:

The overall PSTF will be

$$H_a(s_1,s_2) = \frac{K}{(s_1^2 + 4.4s_1 + 1.62)\quad(s_2^2 + 4.4s_2 - 1.62)} \quad (3\text{-}4)$$

Fig. 3.7 shows the response contours of R_I

Fig. 3.8(a) and 3.8(b) shows the response contours of R_{II}

Fig. 3.9 shows response 3-D ploting of R_{II}

The required data for PSTF for Figs. 2.23(a), 2.26 and 2.27 are given the Appendix III.

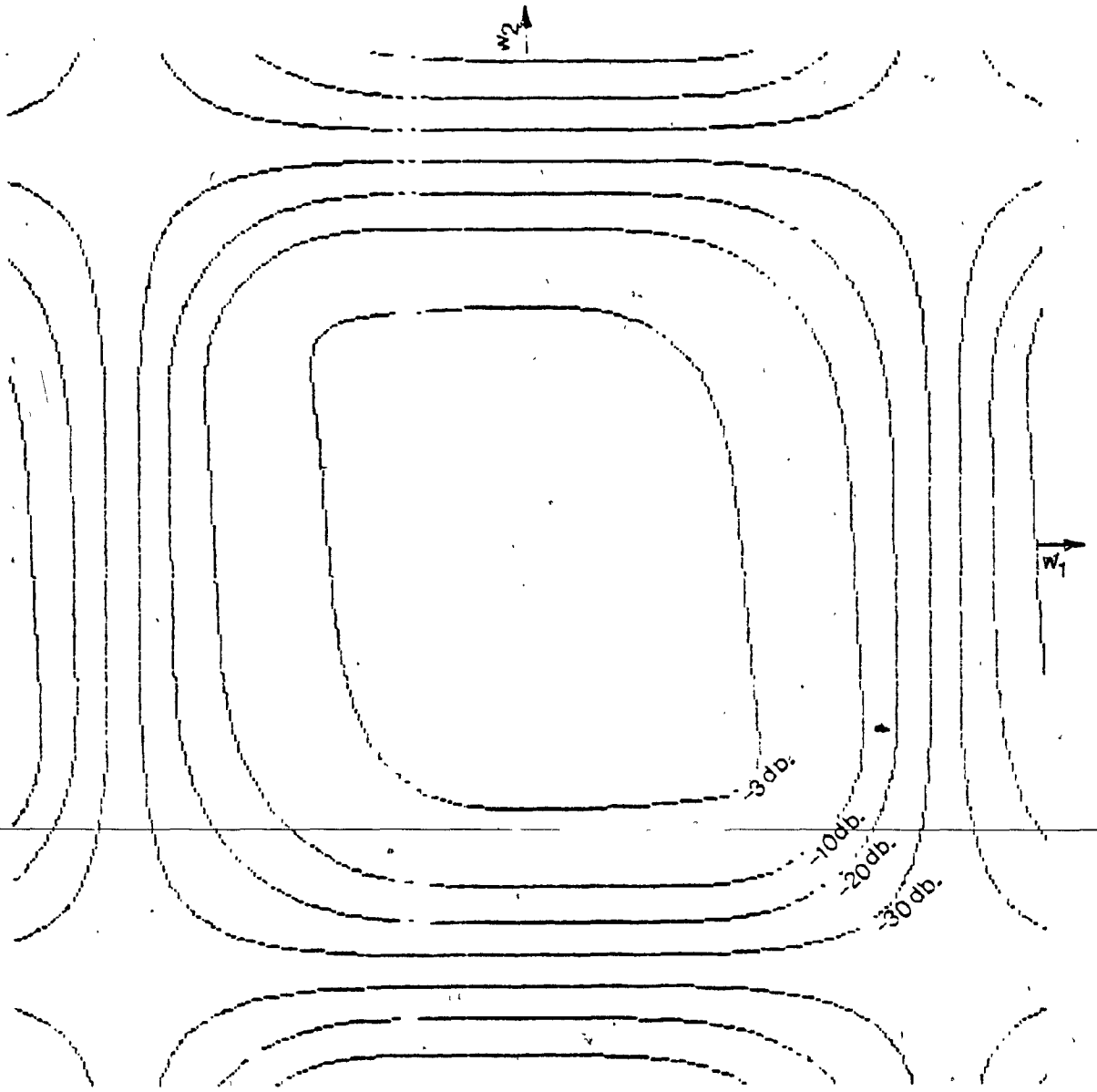

Fig. 3.4

Magnitude Response Contours of R_I for Eqn. (3.3)

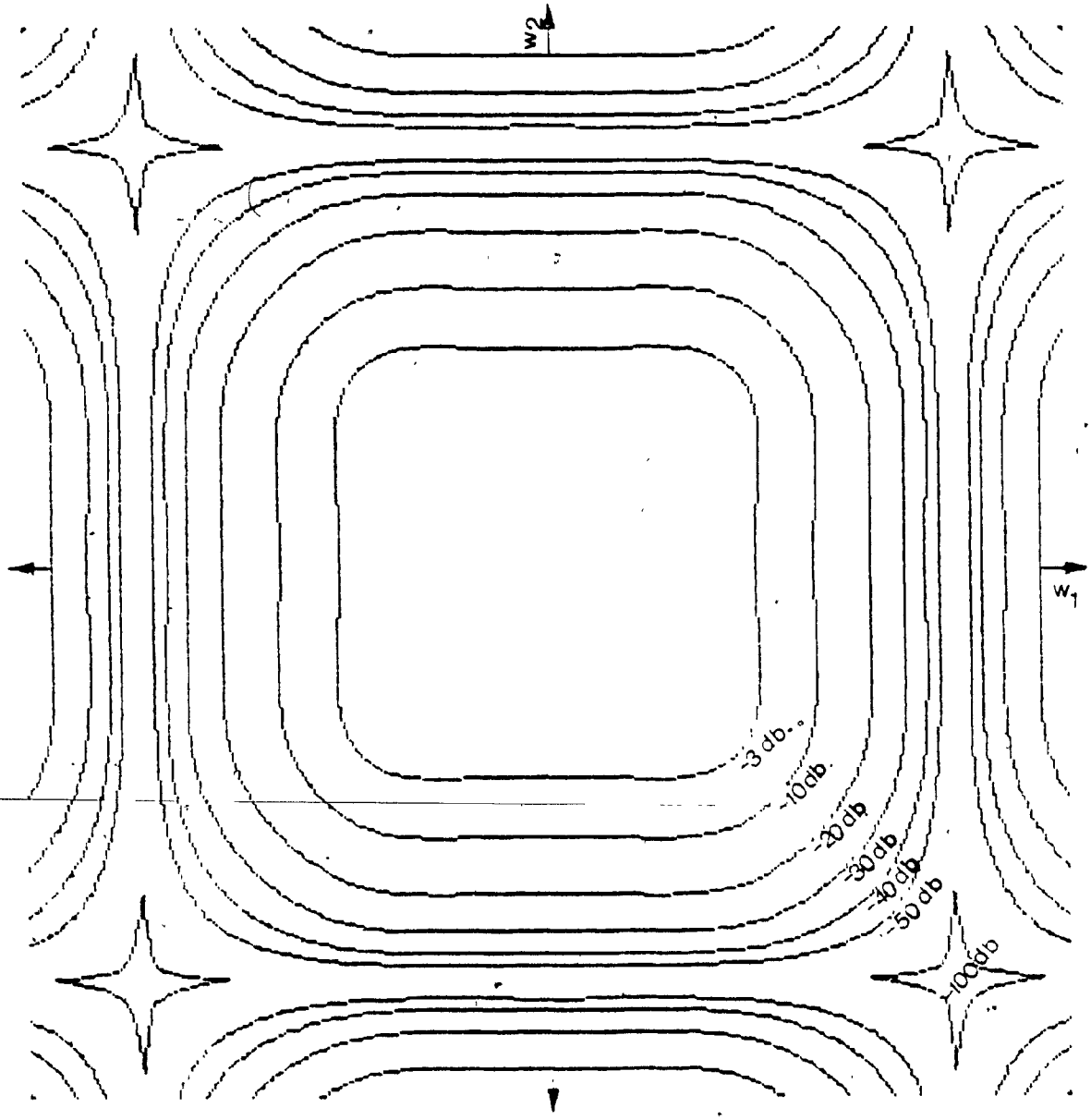

Fig. 3.5(a)

Magnitude Response Contours of R_{Ii} for Eqn. (3.3)

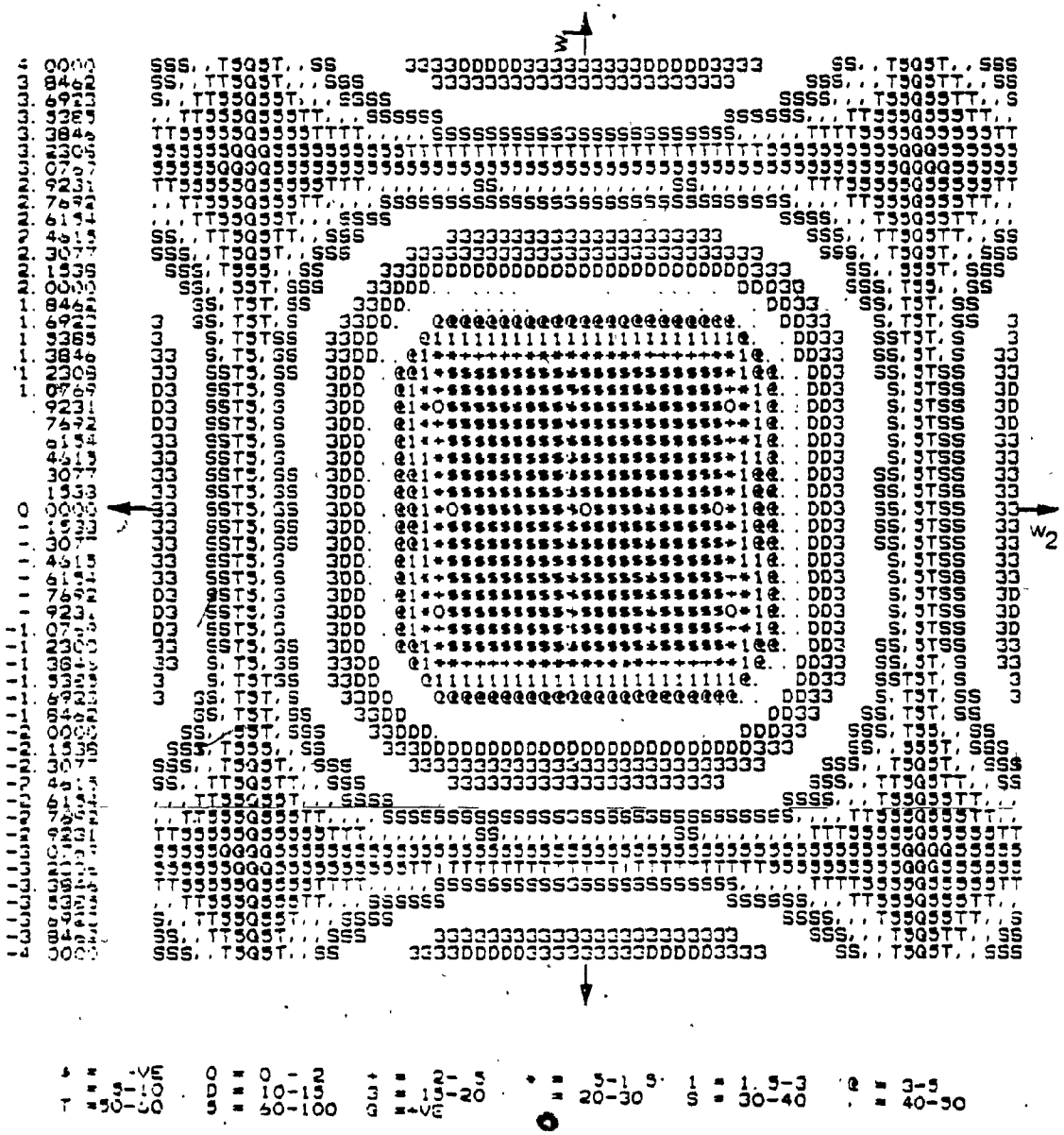

* = -VE 0 = 0 - 2 + = 2- 5 • = 5-1 5 1 = 1 5-3 @ = 3-5
= 5-10 D = 10-15 3 = 15-20 = 20-30 S = 30-40 . = 40-50
T =50-60 5 = 60-100 G =+VE

Fig. 3.5(b)

Magnitude Response Contours of R_{II} for Eqn.(3.3)

(Magnitude is in-db)

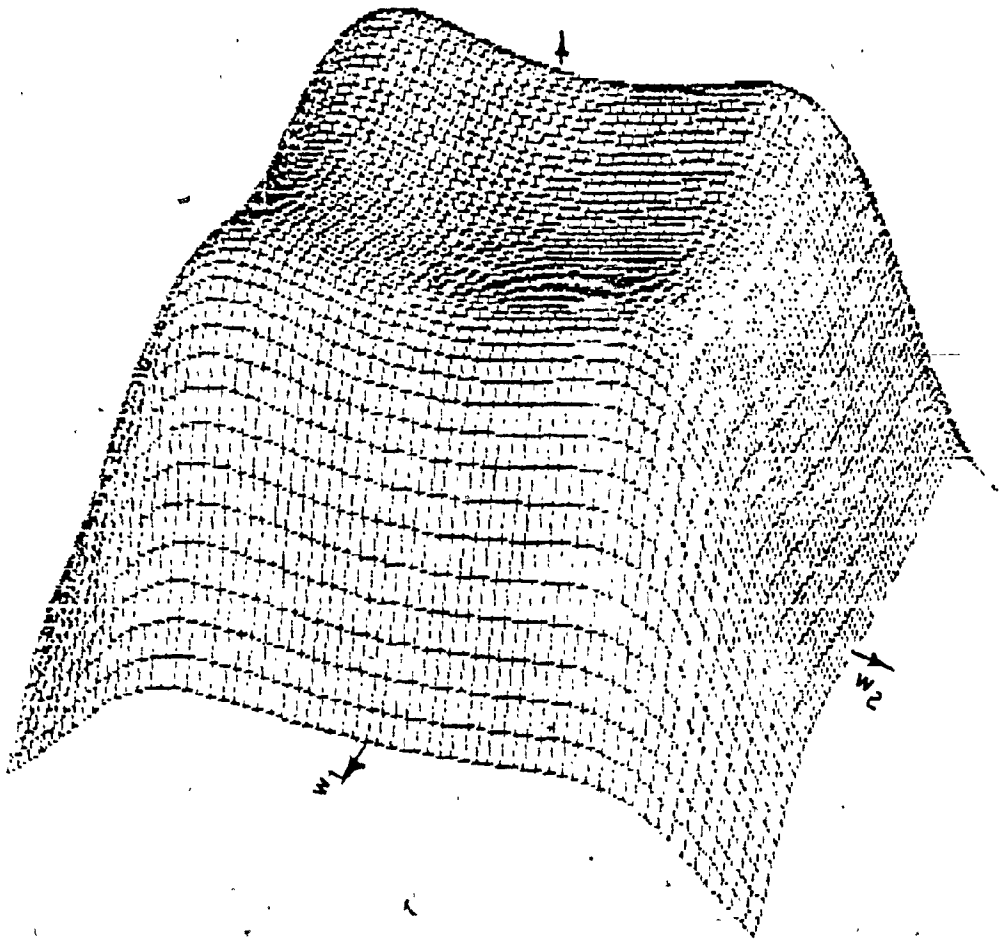

Fig. 3.6

3-D. Plotting of Magnitude Response of R_{II} for Eqn. (3.3)

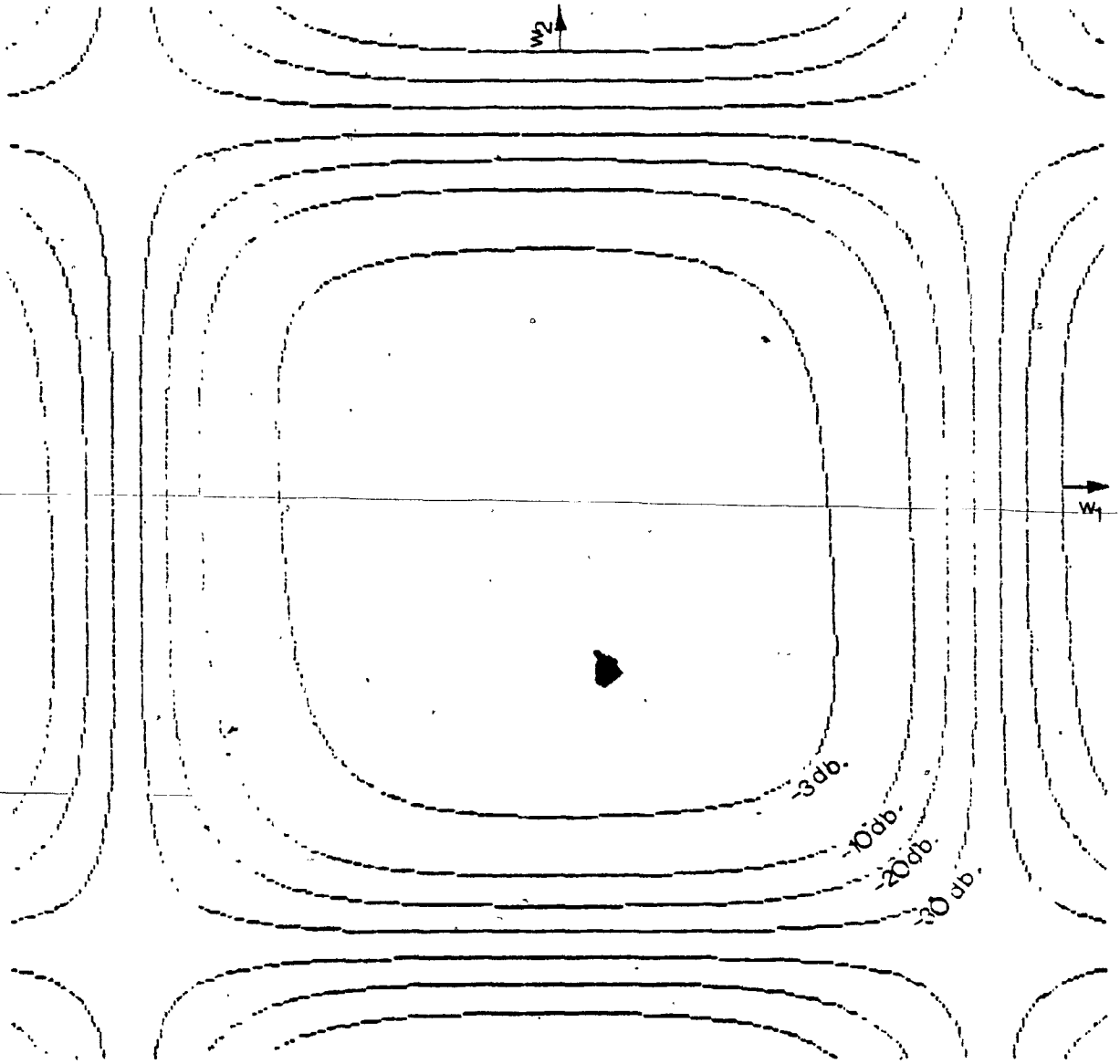

Fig. 3.7

Magnitude response contours of R_I for Eqn. (3.4)

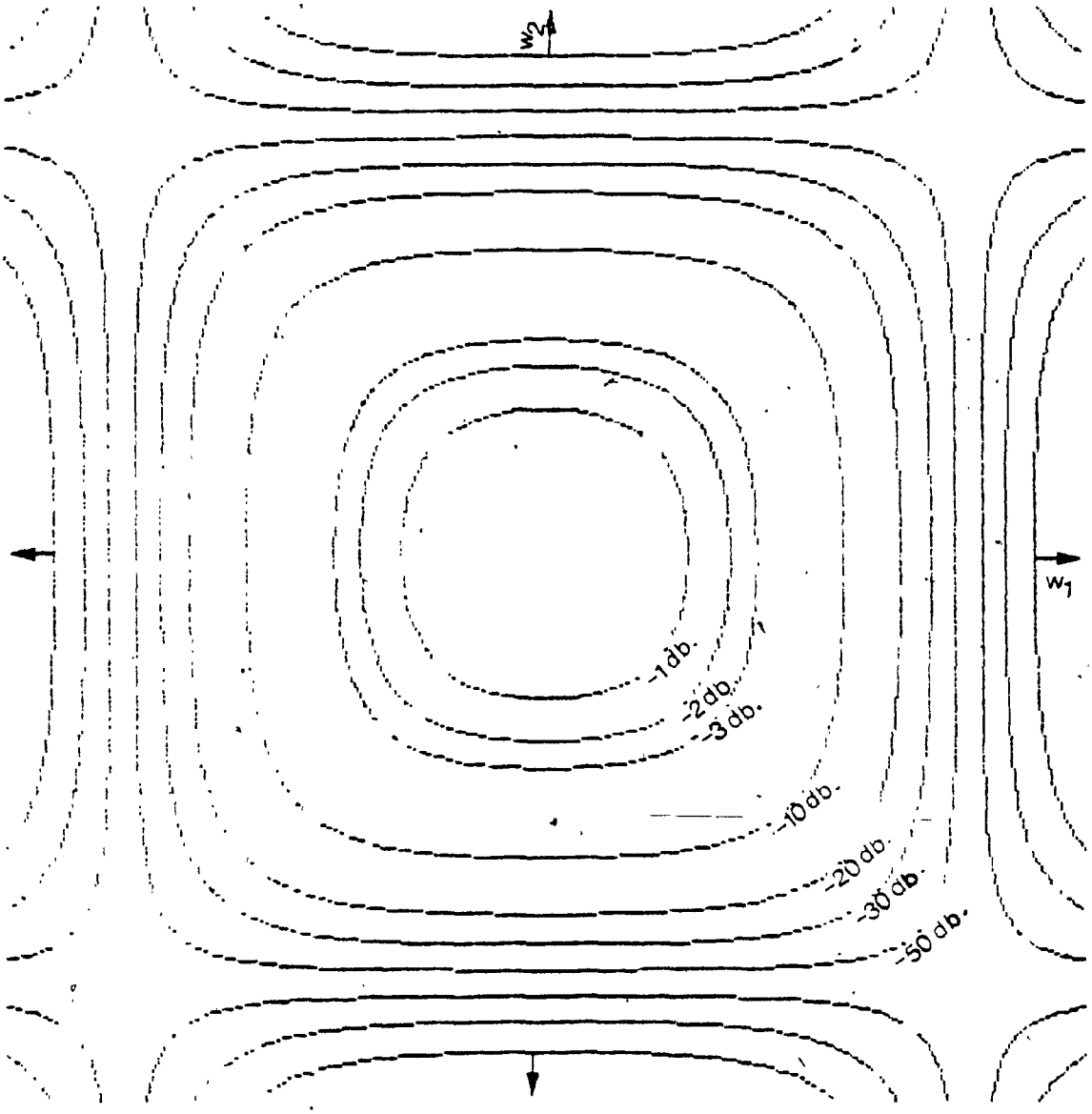

Fig. 3.8(a)

Magnitude response contours of R_{II} for Eqn.(3.4)

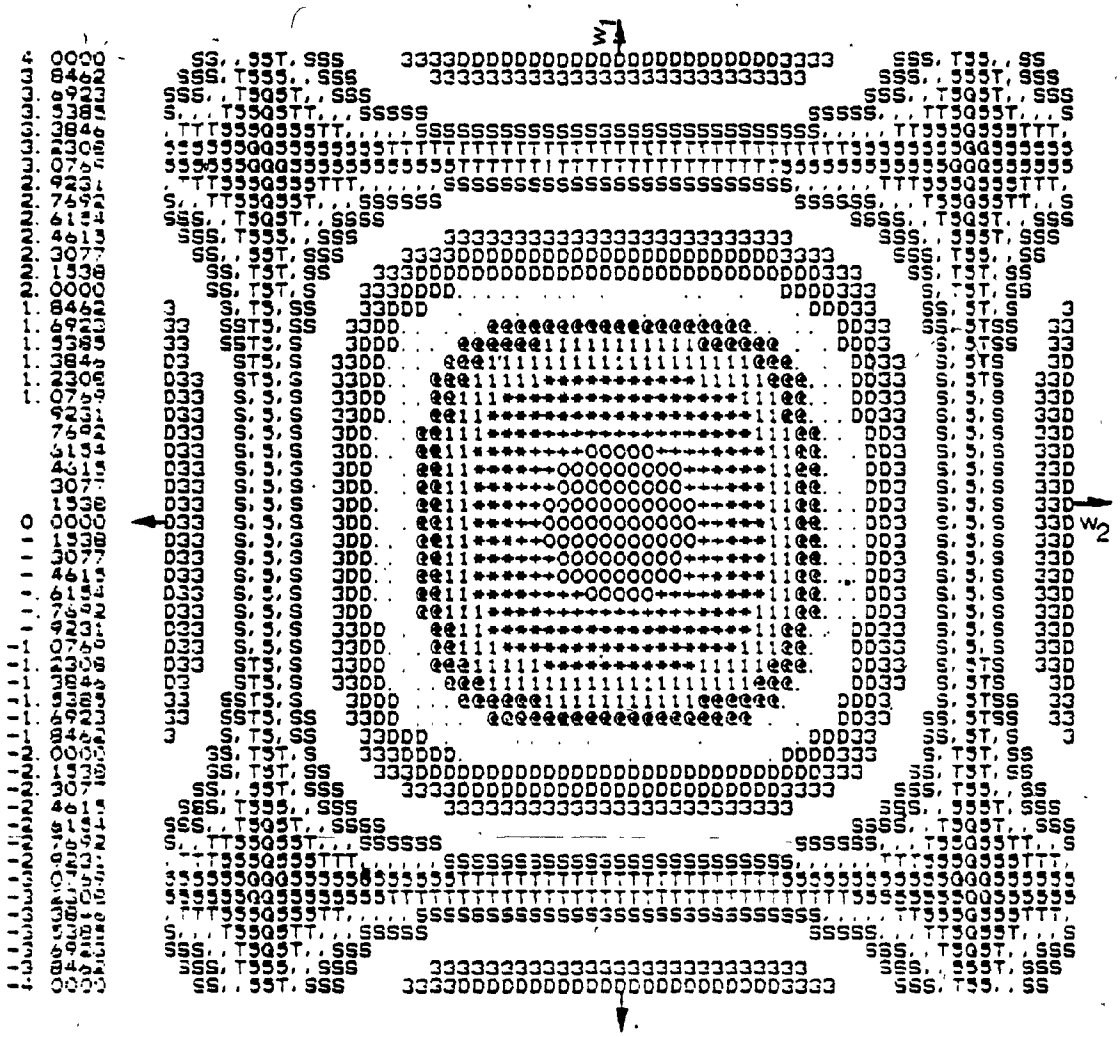

Fig. 3.8(b)

Magnitude response contours of R_{II} for Eqn.(3.4)(Magnitude is in-db)

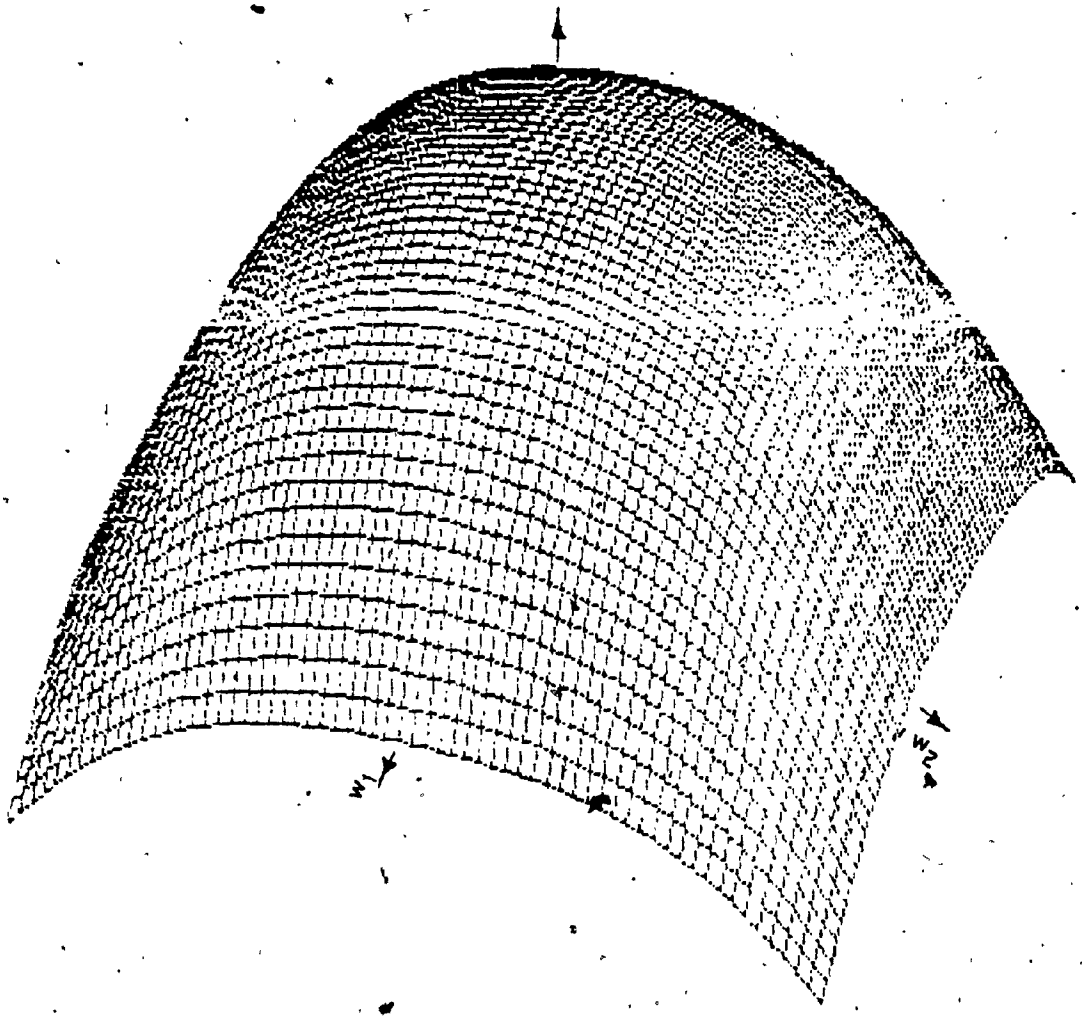

Fig. 3.9

3-D. ploting of Magnitude response of R_{II} for Eqn.(3.4)

3.2.4 Combination of Low-pass Butterworth and Chebyshev PSTF response

The overall PSTF will be

$$H_a(s_1,s_2) = \frac{K}{(s_1^2 + 2.05s_1 + .78)(s_2^2 + 1.41s_2 + 1)} \quad (3.5)$$

Fig. 3.10 shows response contours of R_I.

Figs. 3.12(a) and 3.12(b) shows response contours of R_{II}.

Fig. 3.12 shows response 3 - D plotting of R_{II}. The required data for PSTF for Figs. 2.24(a), 2.26 and 2.27 are given in the Appendix IV.

3.2.5 Combination of Low-pass Chebyshev and Bessel PSTF response

The overall PSTF will be,

$$H_a(s_1,s_2) = \frac{K}{(s_1^2 + 2.05s_1 + 0.785)(s_2^2 + 4.4s_2 + 1.6)} \quad (3.6)$$

Fig. 3.13 shows response contours of R_I.

Fig. 3.14 (a) and 3.14(b) show response contours of R_{II}.

Fig. 3.15 shows response 3 - D plotting of R_{II}. The required data for PSTF for Figs. 2.24(a), 2.26 and 2.27 are given in the Appendix V.

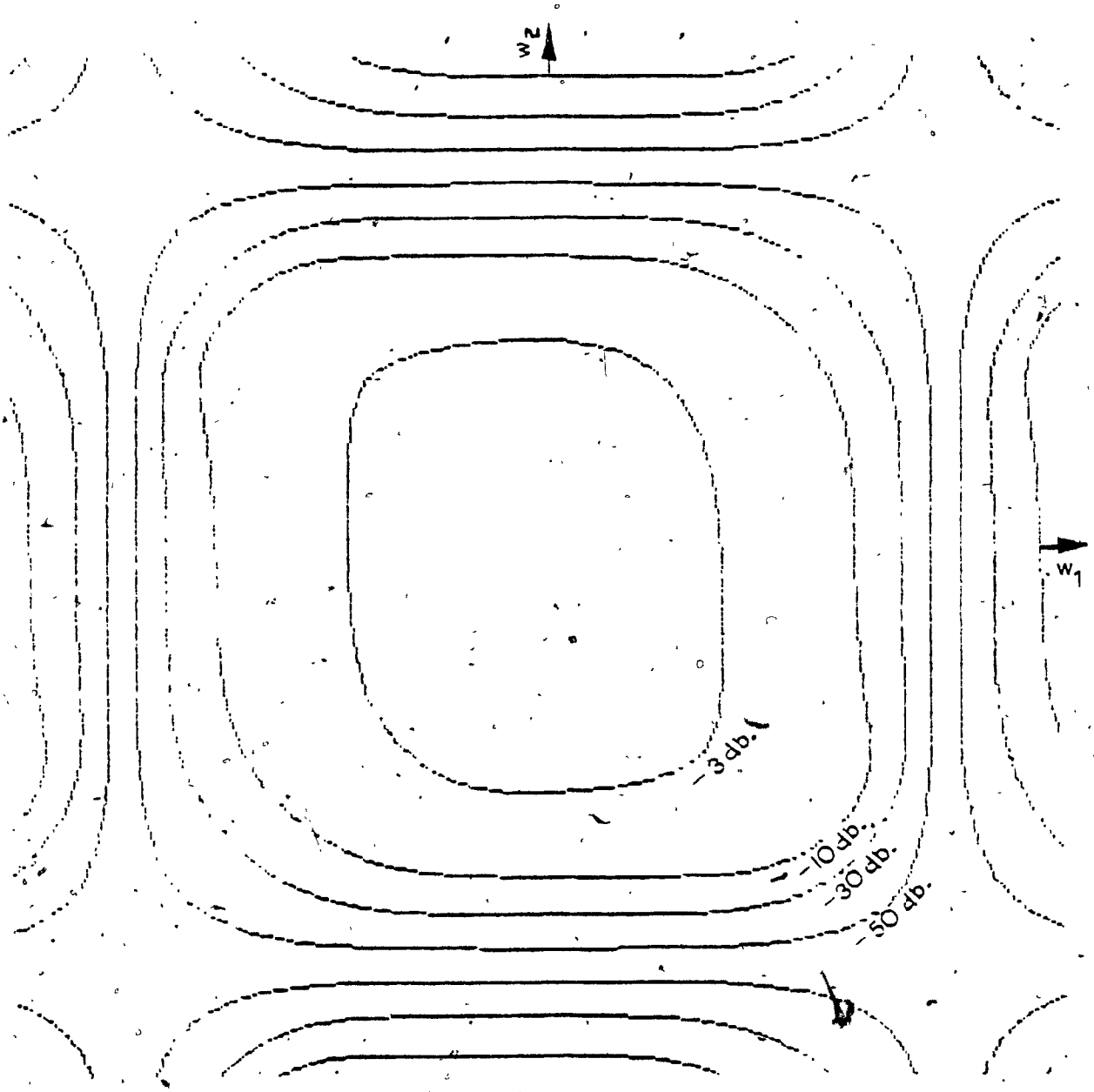

Fig. 3.10

Magnitude Response Contours of R_I for Eqn. (3.5)

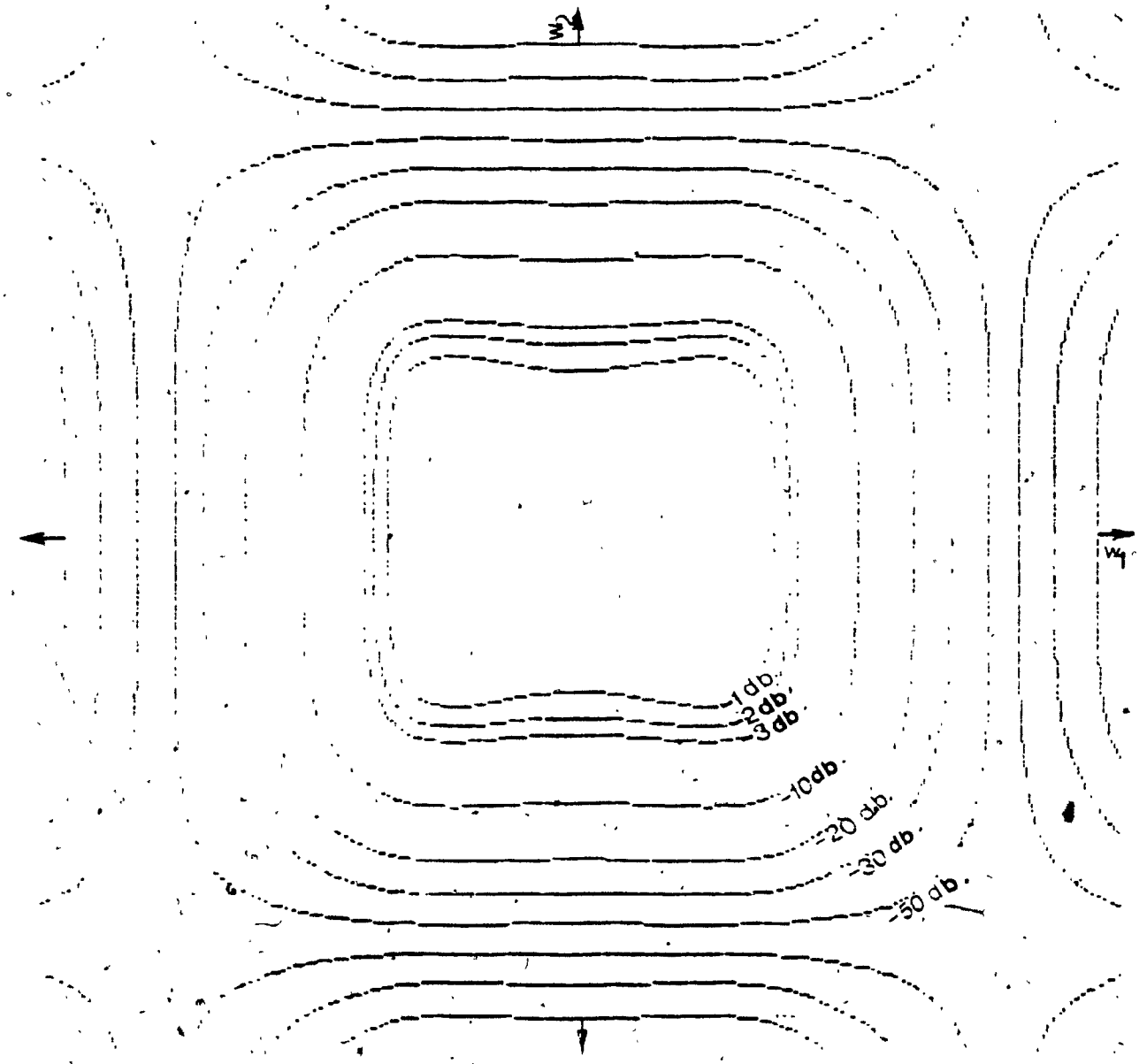

Fig. 3.11 (a)

Magnitude Response Contours of R_{II} for Eqn. (3.5)

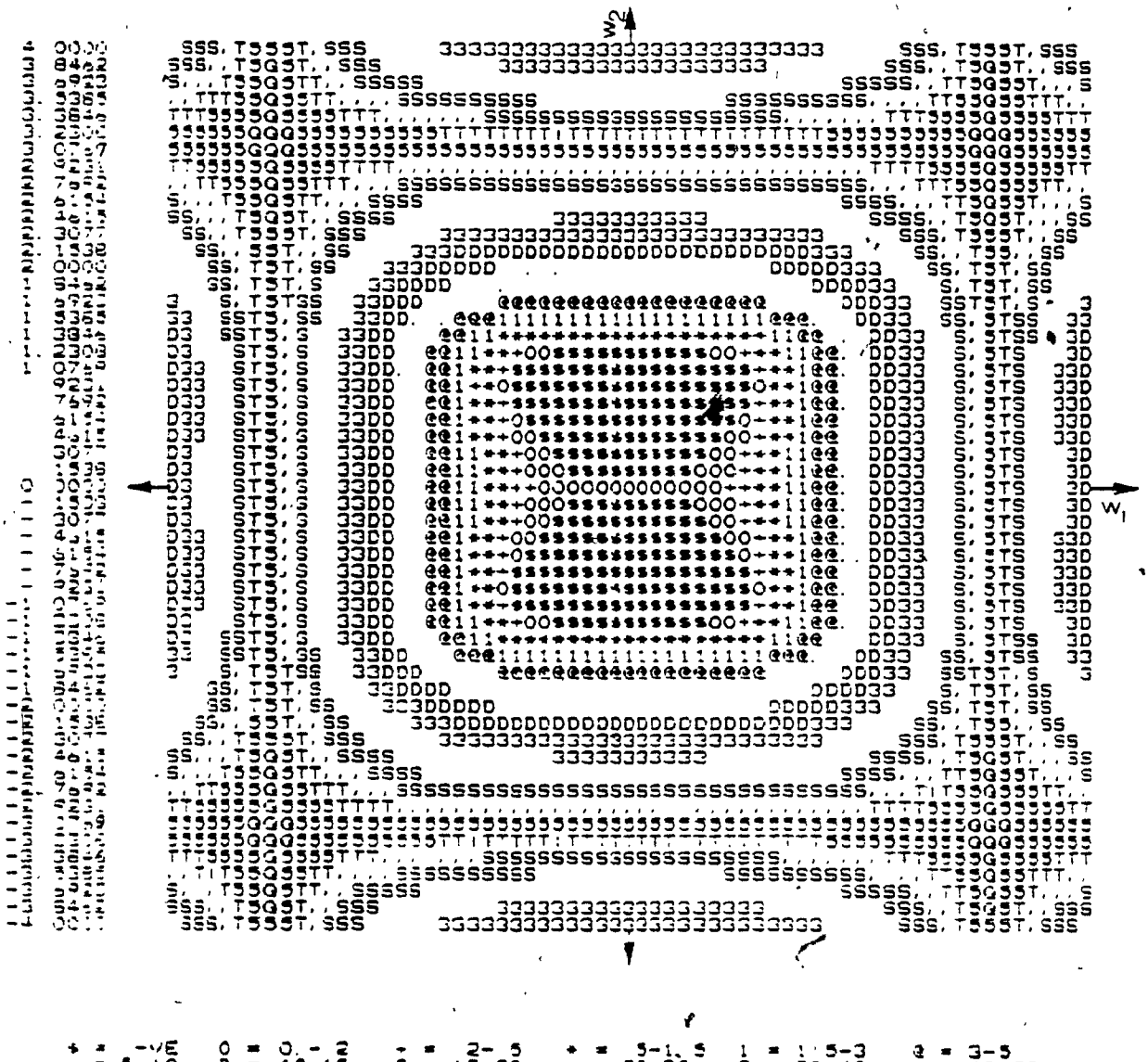

Fig. 3.11(b)

Magnitude Response Contours of R_{II} for Eqn. (3.5)

(Magnitude is in-db.)

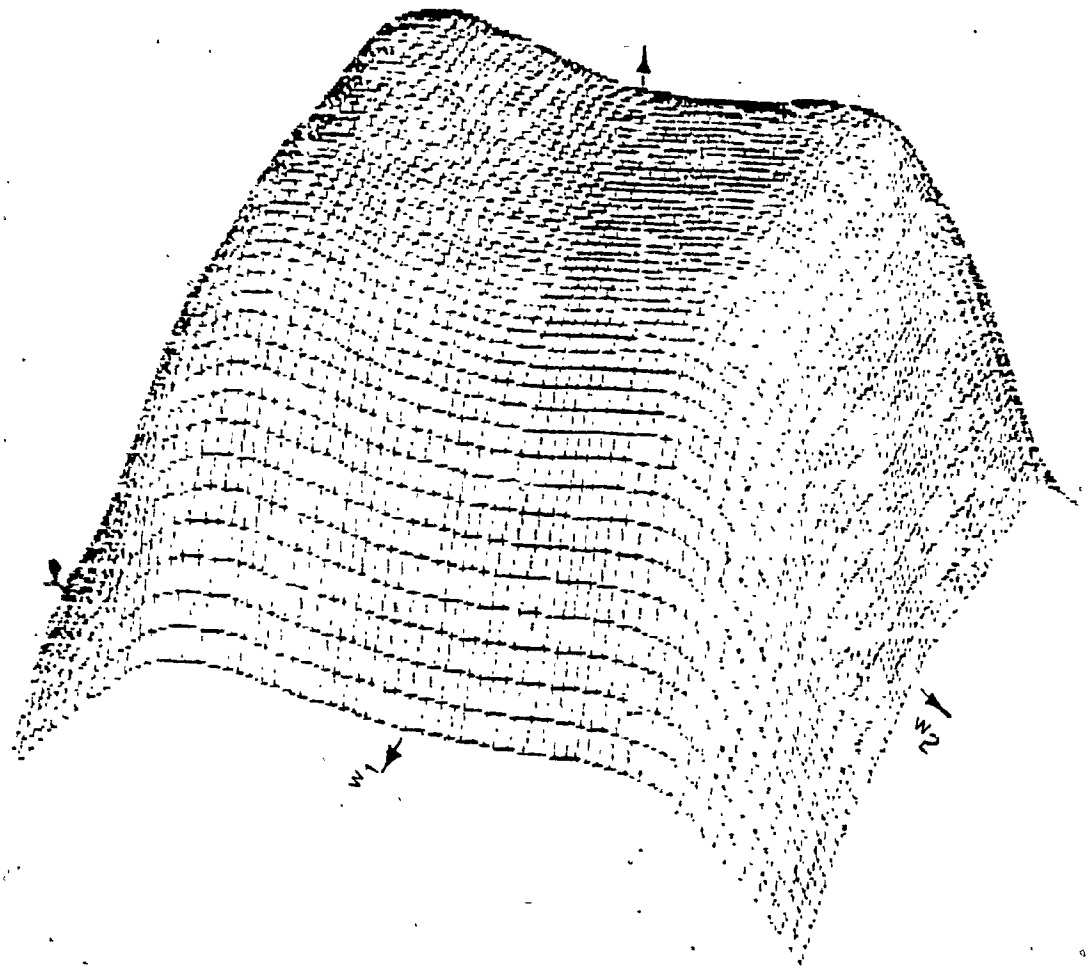

Fig. 3.12

3-D. Plotting of Magnitude Response of R_{II} for Eqn. (3.5)

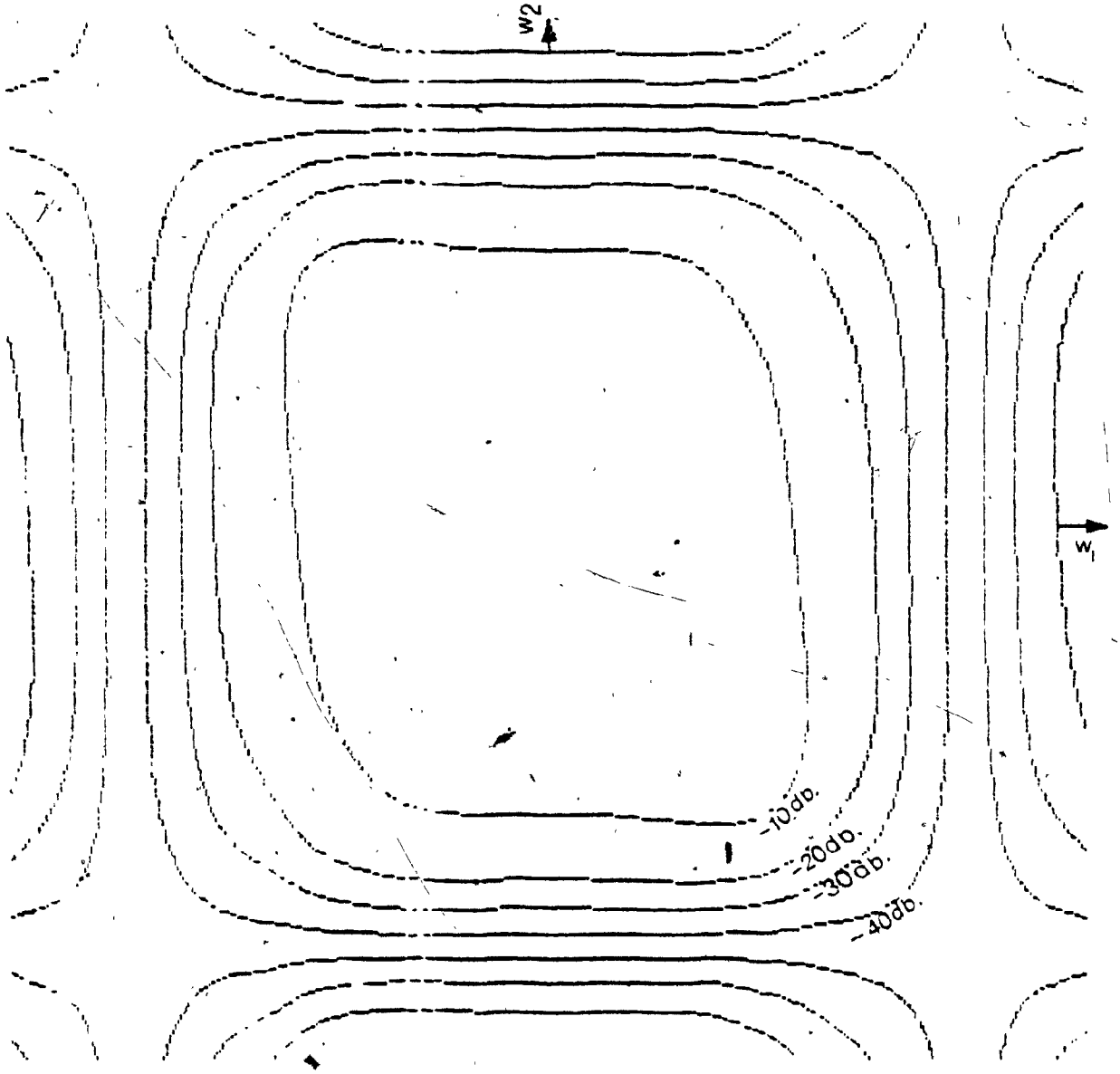

Fig. 3.13

Magnitude Response Contours of R_I for Eqn. (3.6)

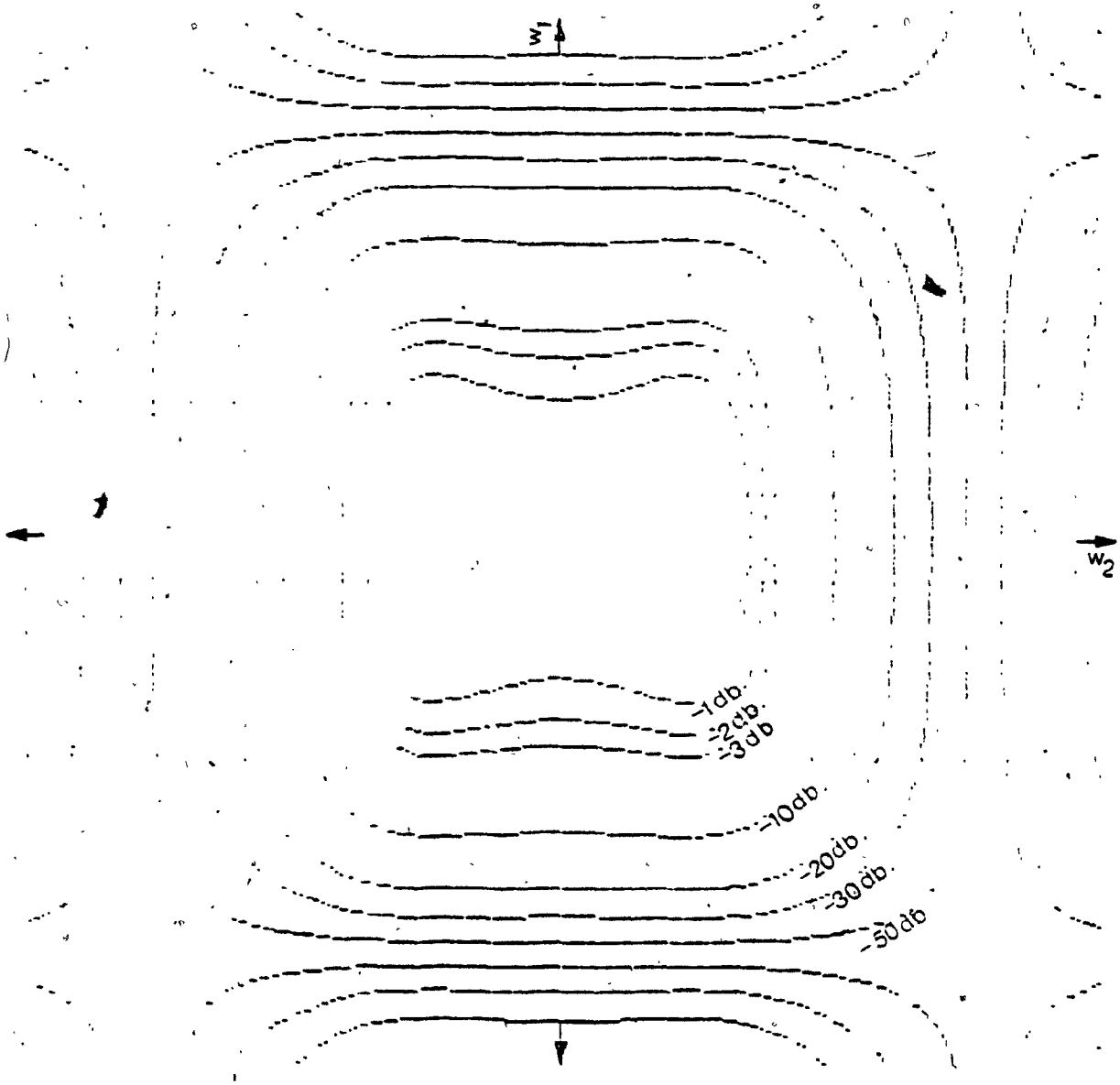

Fig. 3.14(a)

Magnitude Response Contours of R_{II} for Eqn. (3.6)

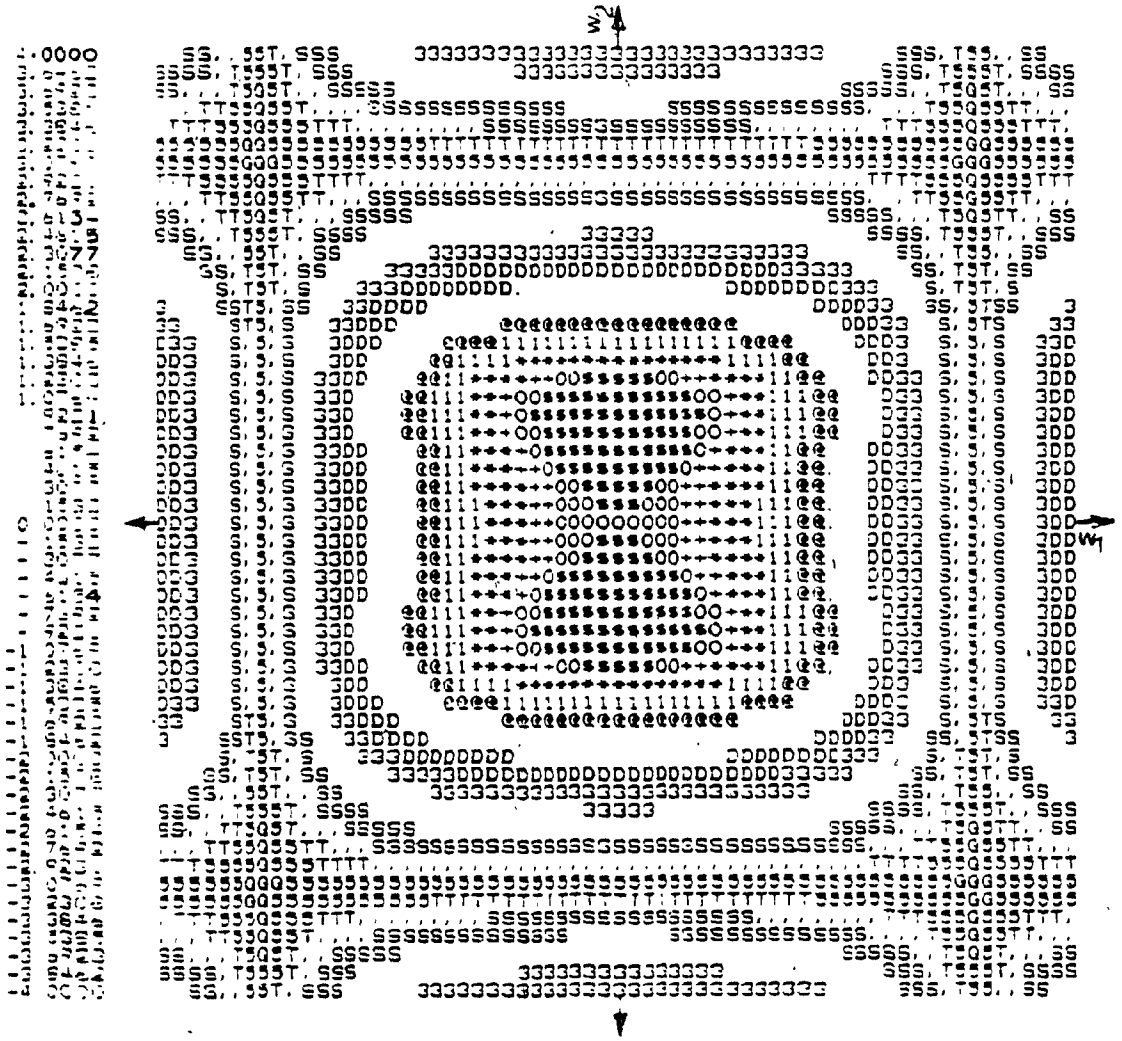

* = -VE 0 = 0 - 2 + = 2- 5 • = 5-1 5 : = 1 5-3 @ = 3-5
= 5-10 D = 10-15 3 = 15-20 = 20-30 S = 30-40 . = 40-50
+ =50-6 5 = 60-100 G =+VE

Fig. 3.14(b)

Magnitude Response Contours of R_{II} for Eqn.(3.6)

(Magnitude is in-db)

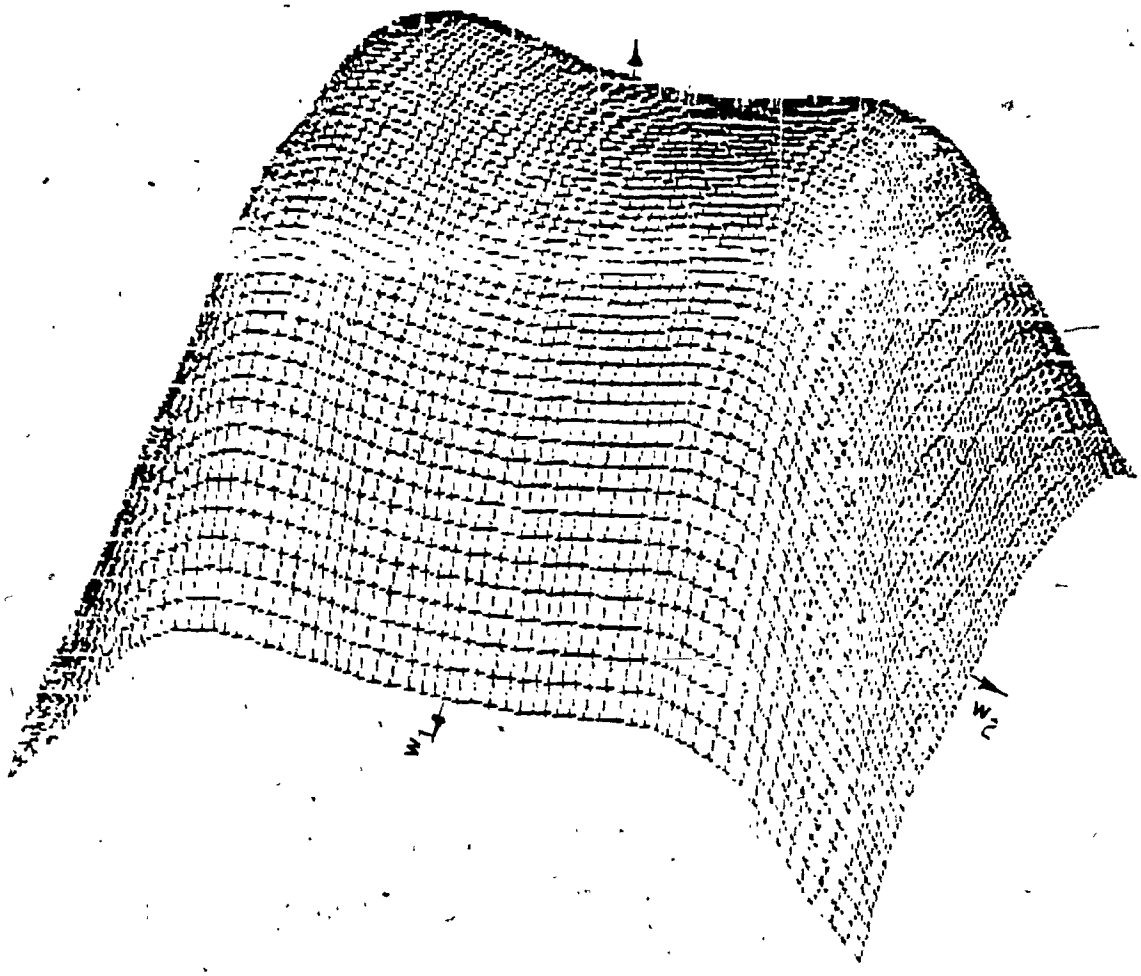

Fig. 3.15

3-D. Plotting of Magnitude Response of R_{II} for Eqn. (3.6)

3.3 Higher Order Digital PSTF Responses:

3.3.1 4th order low-pass Butterworth PSTF response:

The overall PSTF will be,

$$H_a(s_1, s_2) \frac{1}{(s_1^4 + 2.613\, s_1^3 + 3.41 s_1^2 + 2.613 s_1 - 1) \times} \quad (3.7)$$

$$(s_2^4 + 2.613 s_2^3 + 3.41 s_2^2 + 2.61 s_2 + 1)$$

This can be expressed as,

$$H_a(s_1, s_2) = \frac{1}{(s_1 + .92 \pm j.38)(s_1 + .38 \pm j.92) \times} \quad (3.8)$$

$$(s_2 + .92 \pm j.38)(s_2 + .38 \pm j.92)$$

Fig. 3.16 shows response contours of exact realization of Eqn. (3.7).

3.3.2 5th Order Low-pass Butterworth PSTF response:

The overall PSTF will be,

$$H_a(s_1, s_2) = \frac{1}{(s_1^5 + 3.23 s_1^4 + 5.23 s_1^3 + 5.23 s_1^2 + 3.23 s_1 + 1) \times} \quad (3.9)$$

$$(s_2^5 + 3.23 s_2^4 + 5.23 s_2^3 + 5.23 s_2^2 + 3.23 s_2 + 1)$$

poles of this function are,

$$(s_i + 1)(s_i + .81 \pm j.59)(s_i + .31 \pm j.95), \; i = 1, 2$$

Fig. 3.17 shows response contours of exact realization of Eqn. (3.8).

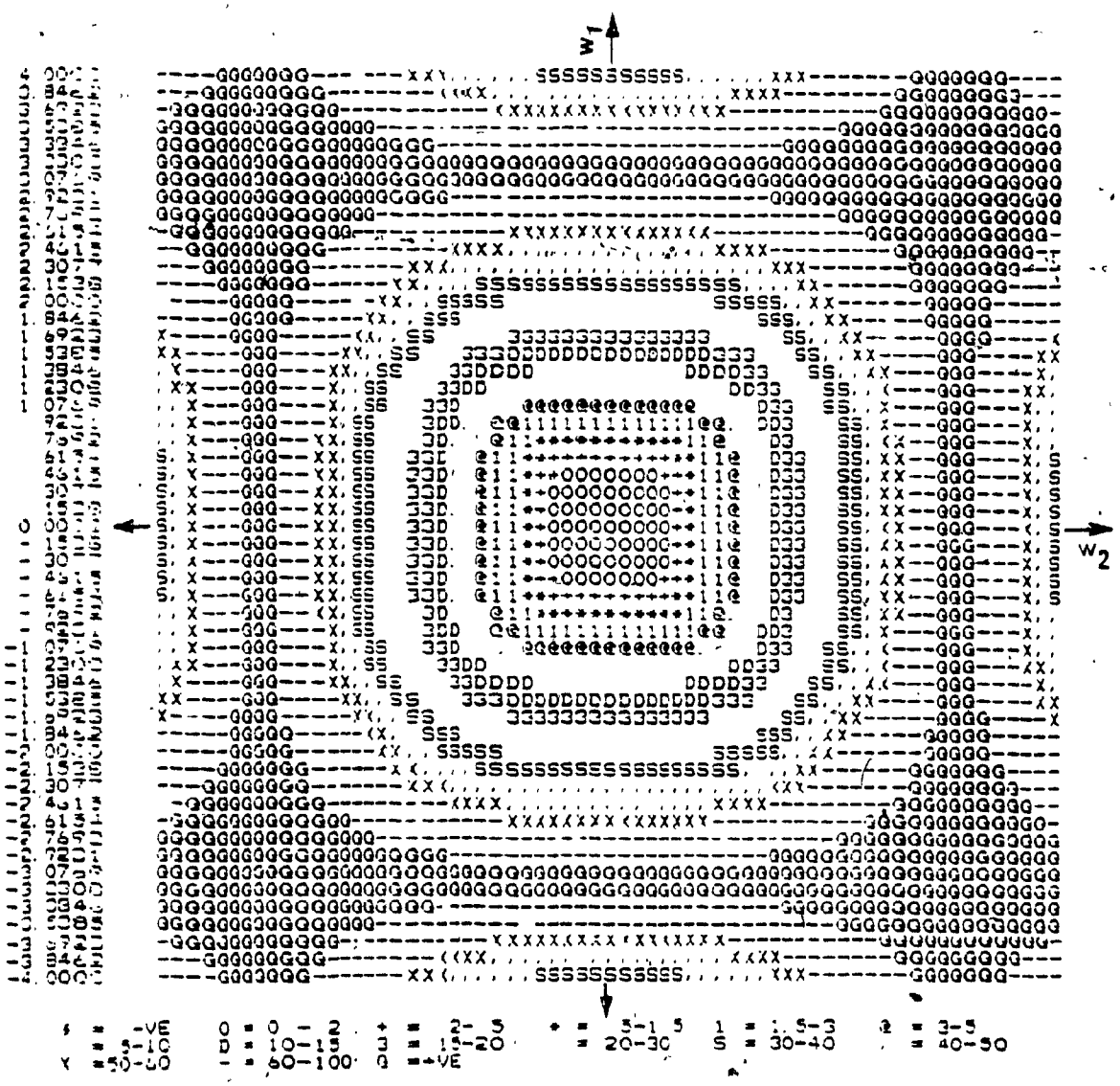

Fig. 3.16

Magnitude Response Contours of 4th Order 2-D PSTF of Eqn. (3.7)

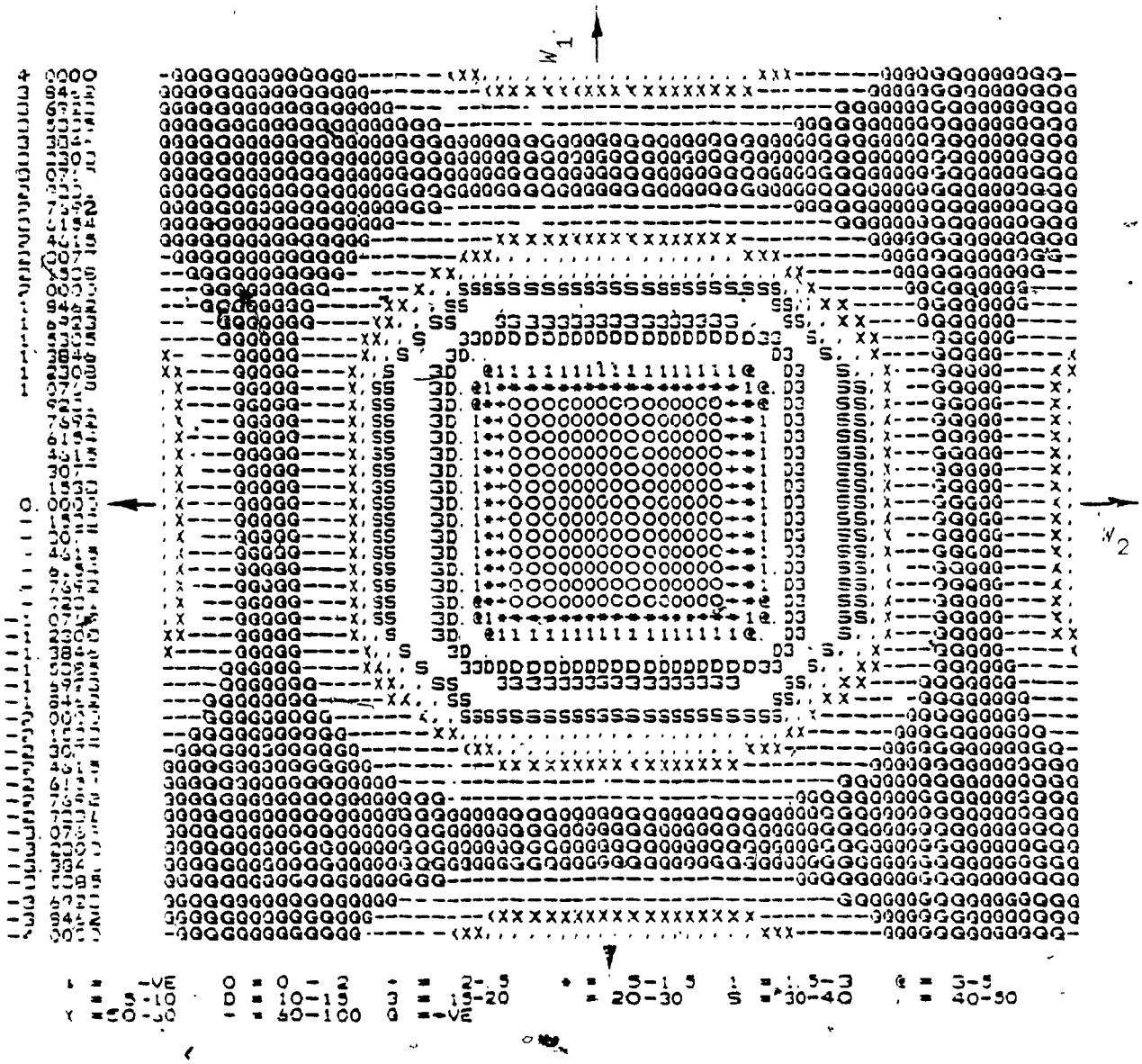

Fig. 3.17

Magnitude Response Contours of 5th Order

2-D PSTF of Eqn.(3.9)

3.3.3 4th order Low-pass Chebychev PSTF response:

(ripple in passband is 0.3 db.)

The overall PSTF will be,

$$H_a(s_1,s_2)= \frac{K_4}{(s_1^4+1.38s_1^3+1.95s_1^2+1.28s_1+.484)(s_2^4 - +1.38s_2^3+1.95S_2^2+1.28s_2+.484)} \quad (3.10)$$

poles of transfer function are,

$s_i = -0.20 \pm j\ 1.04$ And

$-0.489 \pm jo.433, i= 1,2$

Fig. 3.18 shows response contours of exact realization of Eqn. (3.9).

3.3.4 5th Order Low-pass Chebychev PSTF response:

(ripple in pass band is 0.3 db.)

The overall PSTF will be,

$$H_a(s_1,s_2) = \frac{K_5}{(s_1^5+1.35s_1^4+2.16S^3+1.6s_1^2-.92s_1-.234) \times (s_2^5+1.35s_2^4+2.16s_2^3+1.6s_2^2-.92s_2-.234)} \quad (3.11)$$

poles of transfer function are,

$s_i = -0.417,$

$(-.13 \pm j\ 1.03),$

$(-.338 \pm j.637)$ For $i = 1,2$

Fig. 3.19 shows response contours of exact realization of Eqn. (3.10).

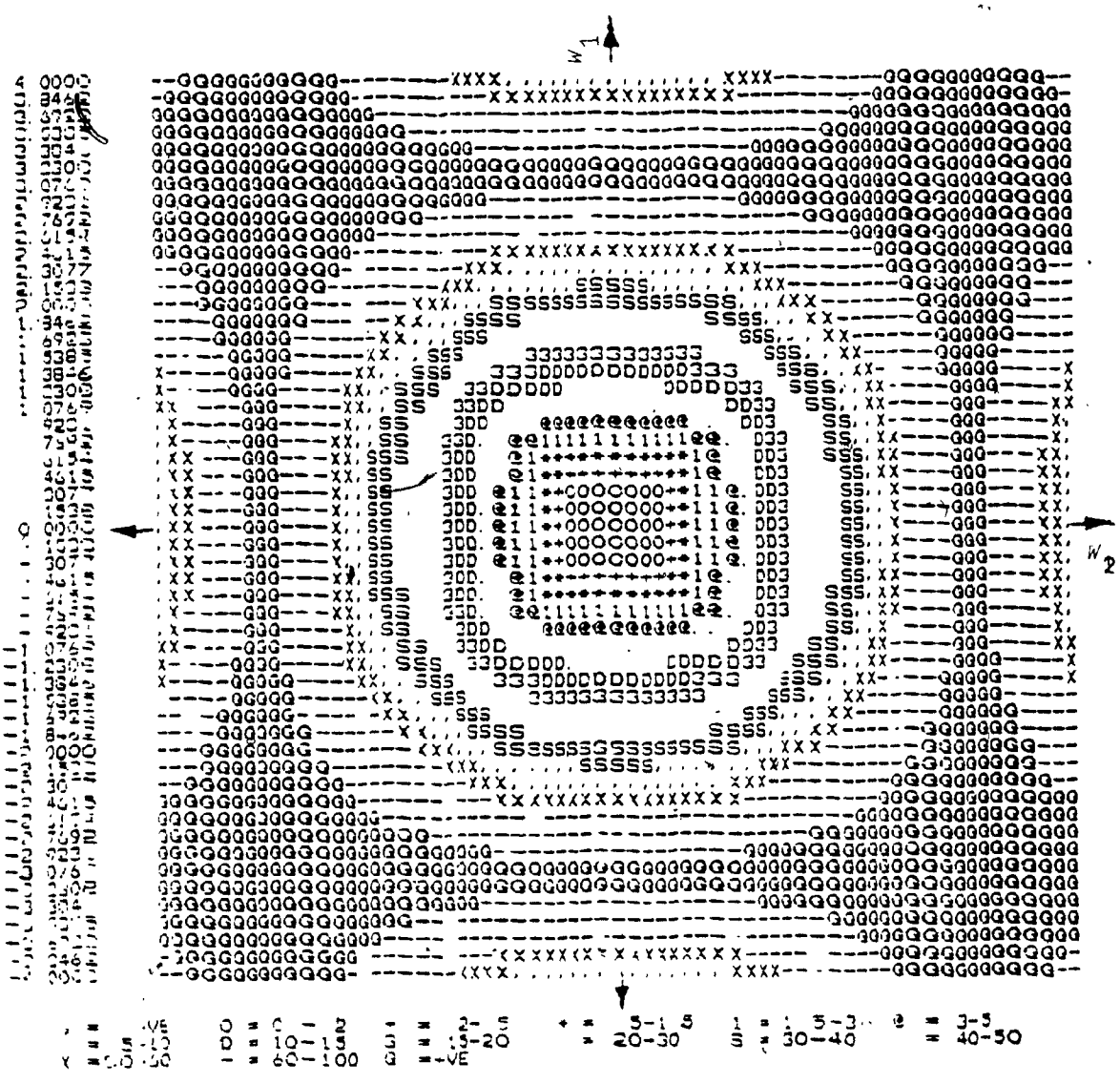

Fig. 3.18

Magnitude Response Contours of 4th Order 2-D PSTF of Eqn. (3.10)

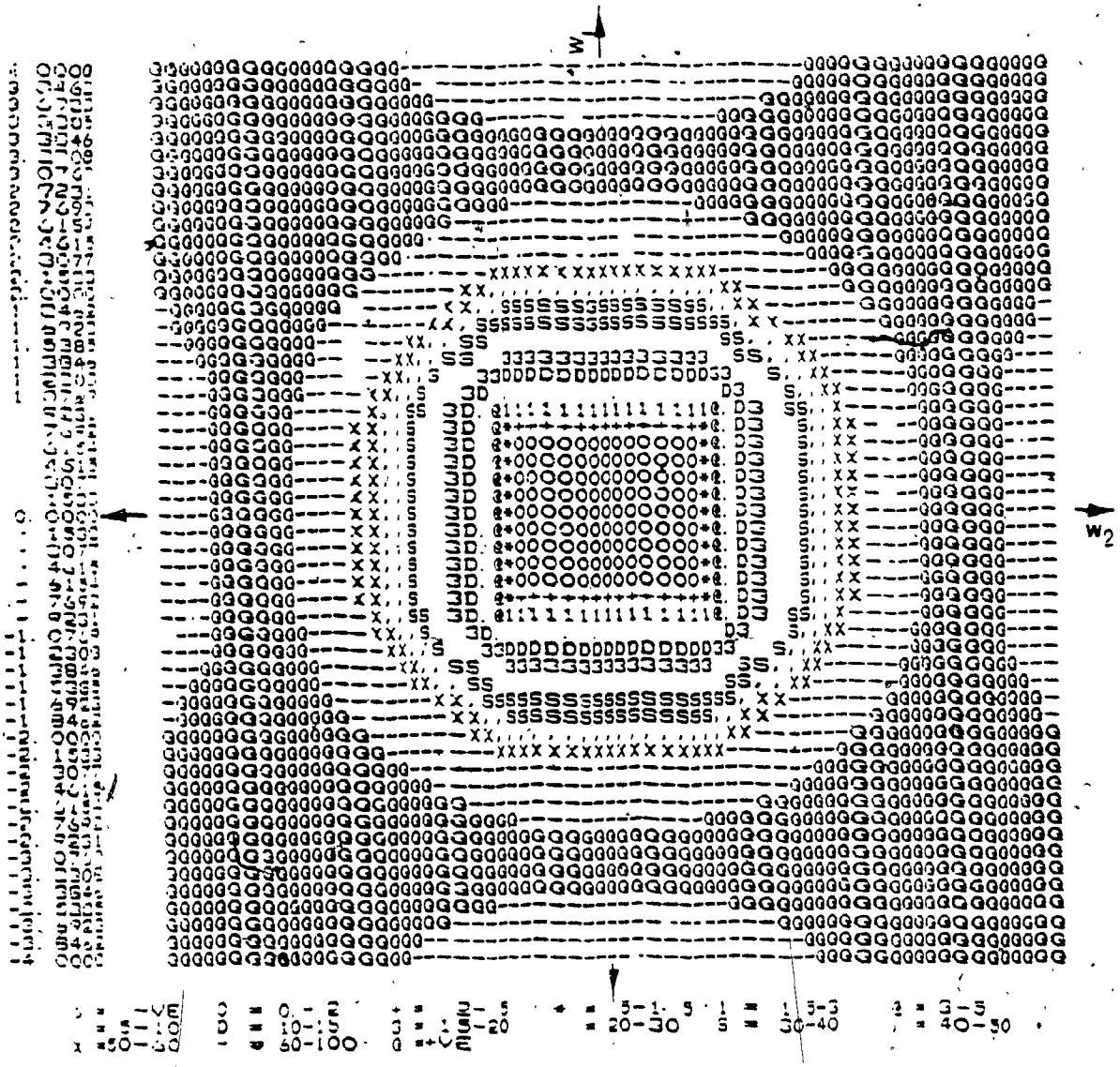

Fig. 3.19

Magnitude Response Contours of 5th Order 2-D PSTF of Eqn. (3.11)

3.4 Summary and Discussion

In this chapter, we have considered the different filter responses when the PSTFs are realized in accordance with the discussions in Chapter II. As is to be expected, the symmetry in the case of exact realizations is found to be better as compared to that in the case of approximate realizations.

CHAPTER 4

EFFECTS OF QUANTIZATION ON THE PROPOSED DIGITAL FILTERS

4.1 Introduction:

In this chapter, we shall determine the effects of quantization on the digital filters proposed earlier in the thesis. Comparison will be made with other known structures. Specifically, the following structures were considered:

(a) Realization of PSTF shown in Fig. 4.1, where $h_1(z_1)$ and $h_2(z_2)$ are realized by direct canonic structures, referred to as CD I.

(b) Realization of PSTF shown in Fig. 4.2, where $h_1(z_1)$ and $h_2(z_2)$ are realized by wave - digital structures, referred to as W C I.

(c) Realization of PSTF shown in Fig. 4.3, which is discussed in chapter 2. Only two realizations R_I and R_{II} are, considered.

There are two main criteria for evaluating and choosing a digital filter realization structure, and these are as follows:

(a) Sensitivity of the structure to coefficient quantization.

(b) Output noise level due to product quantization.

Using these criteria, we now compare the above realizations.

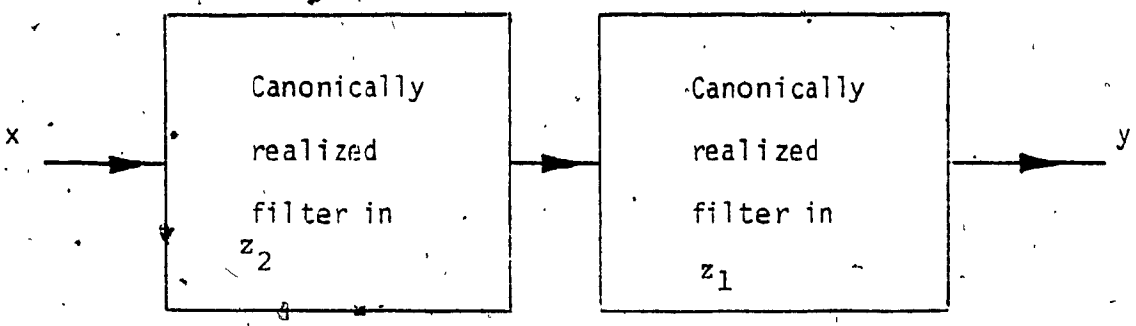

Fig. 4.1

Realization of C D I

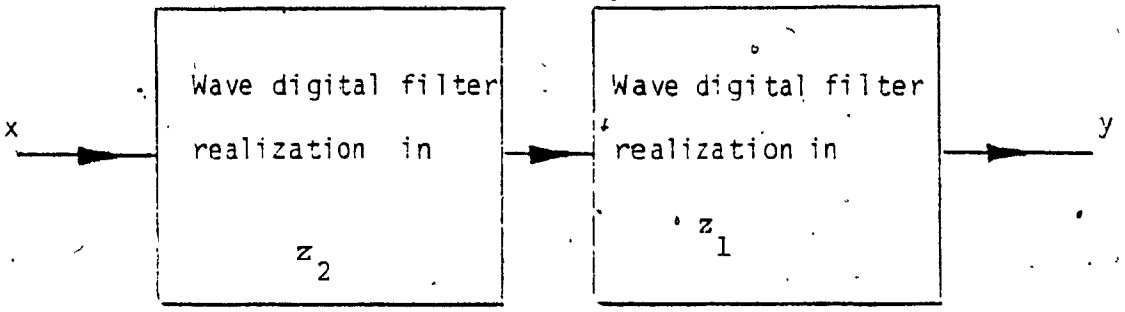

Fig. 4.2

Realization of W C I

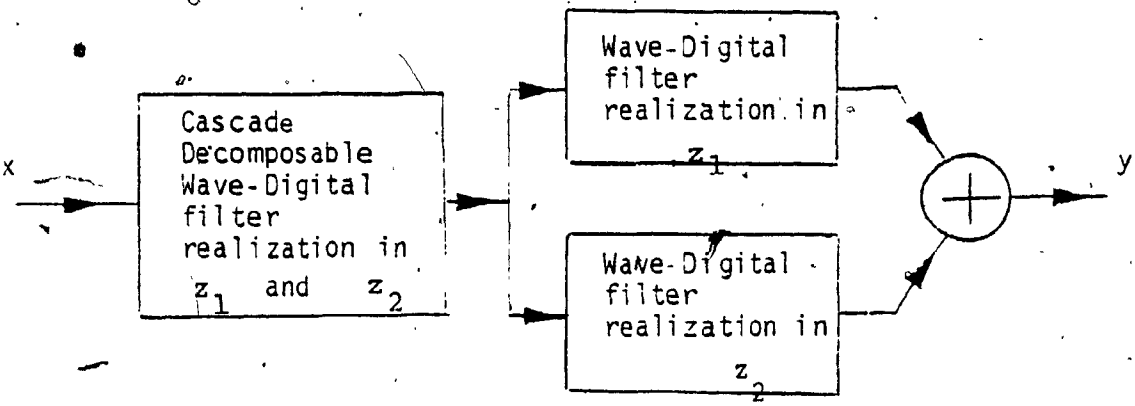

Fig. 4.3

Proposed Realization of PSTF

4.2 Sensitivity and Coefficient Quantization Error:

(1) Sensitivity:

The sensitivity of digital filter network is the vector of partial derivaties (gradients) of the transfer function $H(z)$ with respect to its multiplier coefficients $m_1, m_2 \ldots m_n$ [9] [22] [23] . i.e.

$$S^{H}_{M_i}(z) = \frac{\partial H(z)}{\partial m_i} \qquad i = k, 2 \ldots n \tag{4.1}$$

For complicated network structures, it is often difficult to compute sensitivity. For such networks, the model shown in Fig. 4.4, the sensitivity of $H(z)$ with respect to variations in coefficient m is defined as,

$$S^{H}_{m(z)} = \lim_{\Delta m \to 0} \frac{\Delta H_{12}}{\Delta m} = H_{14}(z) \; H_{32}(z) \tag{4.2}$$

From the above equation, it is clear that sensitivity to variations in any multiplier constant m_1 can be formed by multiplying the transfer function from the input of the network to the input of the multiplier by the transfer function from the output of the multiplier to the output of the network.

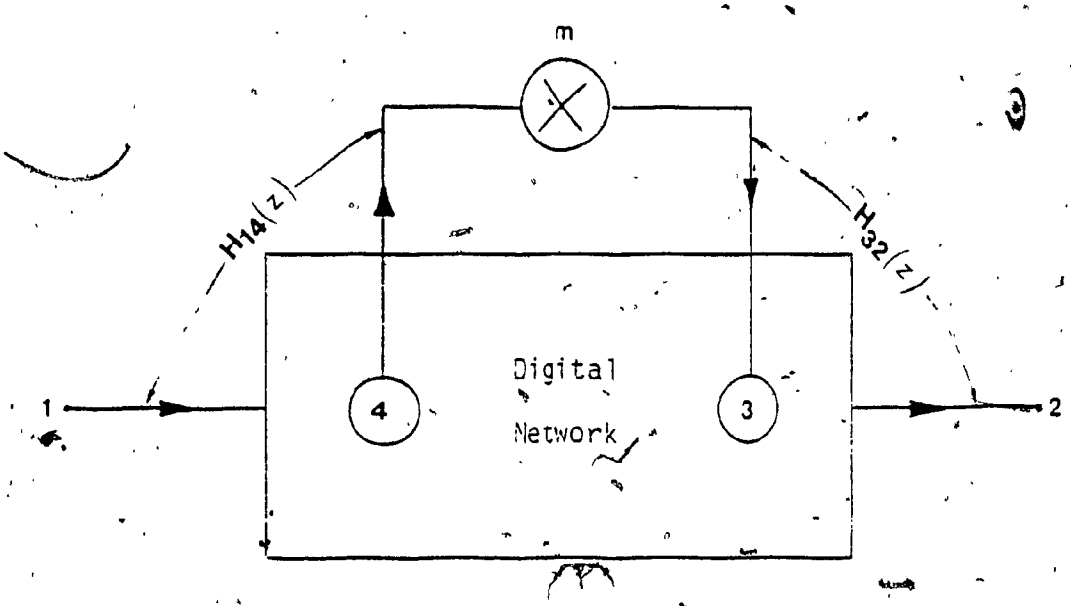

Fig. 4.1

Model of the network used to compute sensitivity.

(2) Coefficient quantization error

Coefficient quantization error introduces perturbation in the zeros and poles of the transfer function, which in turn manifest themselves as error in the frequency response. The problem is closly associated with the choice of the filter structure and its sensitivity properties.

Here we take statistical approach suggested by Crochiere[24] to compute the coefficient quantization error for different digital filter networks. This method leads to a fairly accurate estimate for the required wordlength. The approach can be summarized as follows:

Consider a fixed-point implementation with coefficients m_1, m_2 .. m_n. Assume that coefficients are to be quantized by rounding. According to Crochiere [24] ,

$$|\Delta M(w)| \leq \Delta M_{max} \tag{4.3}$$

with a confidance factor y given by

$$y = \frac{2}{\sqrt{2\pi}} \int_0^x e^{-x^2/2}\, dx \tag{4.4}$$

Provided that the coefficient word length L is chosen as,

$$L \geq W(w) = 1 + J + \log_2 \left\{ \frac{x S_T}{\sqrt{12}\,\Delta M_{max}} \right\} \tag{4.5}$$

where,

$$S_T = \sqrt{\left\{ \sum_{i=1}^{n} S^2 m_i \right\}}$$

$$Sm_i = \frac{\partial M(w)}{\partial m_i}$$

Constant J in the above equation can be deduced by noting that 2^J is the power of 2 represented by the most significant bit in the largest coefficient m_i.

In our computations the value of x was assumed to be 2, which corresponds to a confidence factor of 0.95 [24]. The quantity $\frac{\partial M(w)}{\partial m_i}$ can be found as follows,

$$\frac{\partial H(e^{jwt})}{\partial m_i} = \frac{\partial \{ M(w)\ e^{j\theta(w)} \}}{\partial m_i} \qquad (4.5\ a)$$

$$= \text{Re}\ \frac{\partial H(e^{jwt})}{\partial m_i} + j\ \text{Im}\left(\frac{\partial H(e^{jwt})}{\partial m_i}\right) \qquad (4.6)$$

After some manipulation Eqn. (4.6) is express as,

$$\frac{\partial M(w)}{\partial m_i} = \text{Cos}\{\theta(w)\}\left[\text{re}\ \frac{\partial H(e^{jwt})}{\partial m_i}\right] + \text{Sin}\{\theta(w)\}\left[\text{im}\ \frac{\partial H(e^{jwt})}{\partial m_i}\right] \qquad (4.7)$$

The quantity $\frac{\partial M(w)}{\partial m_i}$ is known as the sensitivity of the gain with respect to variations in coefficients m_i. The gain sensitivity can be found using the following steps [9].

(1) Form the real and imaginary parts of the quantity by using Eqn. (4.6).

(2) Find the phase angle $\theta(w)$ of $H(e^{jwt})$.

(3) Compute $\frac{\partial M(w)}{\partial m_i}$ by using Eqn. (4.7).

Coefficient quantization in case of 2-D digital filters :

The statistical approach we have just discussed in the case of 1-D digital filter can be applied to 2-D digital filter networks. Here,

$$Q \leq \frac{\sqrt{12}\ \ \Delta M\ \max\ (w_1, w_2)}{x\ S_T} \qquad (4.8)$$

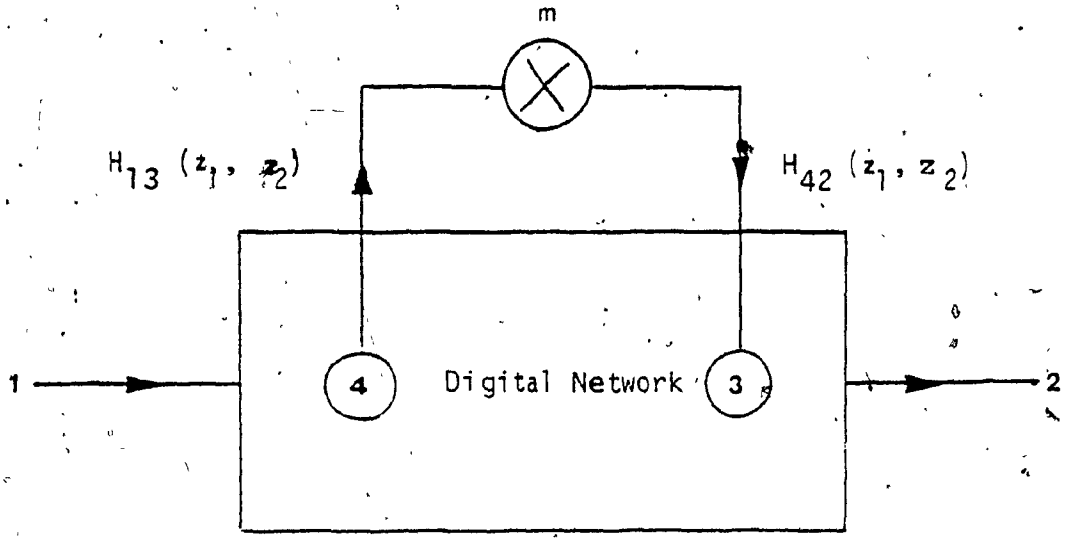

Fig. 4.5

Model for computing sensitivity of a 2-D digital filter

To accommodate the quantized value of the largest coefficient in the register we should have,

$$Q\{\max\ m_i\} = \sum_{i=-k}^{J} bi\,2^i \tag{4.9}$$

Where b_j and $b_k \neq 0$, Then the register wordlength is given by,

$$W = 1 + J + K$$

where,

$$K = \log_2 [1/Q]$$

$$W = 1 + J + \log_2 \left\{ \frac{XS_T}{\sqrt{12}\,\Delta M \max\,(w_1, w_2)} \right\} \tag{4.10}$$

$$S_T = \sqrt{\sum_{i=0}^{n} S^2_{m_i}} \tag{4.11}$$

By assuming X = 2, we have a confidance factor Y = 0.95 which gives a reasonable agreement between the statistical wordlength and exact wordlength [24].

The sensitivity $S^H_{m_i}$ can be computed using the transpose or the adjoint approach. For example, sensitivity for network shown in Fig. (4.5) with respect to coefficient m_i is given by,

$$S^H_{m_i}(z_1,z_2) = \frac{\partial H(z_1,z_2)}{\partial m_i} = H_{13}(z_1,z_2)\, H_{42}(z_1,z_2) \tag{4.12}$$

$H_{13}(z_1,z_2)$ is the transfer function between nodes 1 to 3 and $H_{42}(z_1,z_2)$ is the transfer function between nodes 4 and 2. Therefore we have,

$$S^{H}_{m_i}(e^{jw_1t_1}, e^{jw_2t_2}) = \partial H(e^{jw_1t_1}, e^{jw_2t_2}) / \partial m_i$$

$$= \mathrm{Re}\{S^{H}_{m_i}(e^{jw_1t_1}, e^{jw_2t_2})\} + j\,\mathrm{Im}\{S^{H}_{m_i}(e^{jw_1t_1}, e^{jw_2t_2})\} \quad (4.13)$$

Then we can write,

$$H(e^{jw_1t_1}, e^{jw_2t_2}) = M(w_1,w_2)\, e^{j\theta(w_1,w_2)} \quad (4.14)$$

$$\frac{\partial H(e^{jw_1t_1}, e^{jw_2t_2})}{\partial m_i} = \left\{ e^{j\theta(w_1,w_2)} \frac{\partial M(w_1, w_2)}{\partial m_i} \right\} +$$

$$\left\{ j M(w_1, w_2)\, e^{j\theta(w_1, w_2)} \frac{\partial \theta(w_1, w_2)}{\partial m} \right\} \quad (4.15)$$

From Eqn.(4.13)and(4.15) we find that,

$$\mathrm{Re}\{S^{H}_{m_i}(e^{jw_1t_1}, e^{jw_2t_2})\}$$

$$= \left\{\cos[\theta(w_1, w_2)] \frac{\partial m(w_1, w_2)}{\partial m_i}\right\} - \left\{\sin[\theta(w_1, w_2)]\, M(w_1, w_2) \frac{\partial\theta(w_1, w_2)}{\partial m_i}\right\}, \text{ and } \mathrm{Im}\{S^{H}_{m_i}(e^{jw_1t_1}, e^{jw_2t_2})\} \quad (4.16)$$

$$= \left\{\sin[\theta(w_1,w_2)] \frac{\partial m(w_1, w_2)}{\partial m_i}\right\} + \left\{M(w_1, w_2)\cos[\theta(w_1,w_2)] \frac{\partial\theta(w_1,w_2)}{\partial m_i}\right\} \quad (4.17)$$

and Hence,

$$S^{M}_{m_i} = \{\partial M(w_1, w_2)/\partial m_i\}$$

$$= \cos[\theta(w_1, w_2)]\cdot \mathrm{Re}[S^{H}_{m_1}(e^{jw_1t_1}, e^{jw_2t_2})] +$$

$$\sin[\theta(w_1, w_2)] \mathrm{Im}[S^{H}_{m_i}(e^{jw_1t_1}, e^{jw_2t_2})] \quad (4.18)$$

where $S^{M}_{m_i}$ is the sensitivity of the Magnitude with respect to variations in m_i, hence we can compute S_T in case of 2-D filter as,

$$S_T = \left(\sum_{k=1}^{M} \sum_{j=1}^{N} \sqrt{\sum_{i=1}^{n} S^2_{m_i}} \right) \Big/ (M * N) \qquad (4.19)$$

where n = No. of multiplier coefficients.

Here M and N are No. of frequencies has been taken to find average S_T. Figs. 4.6 to 4.10 show the plots of ΔM_{max} vs. wordlength for the realizations. Comparing these we conclude that W C I is the best of the three while R_{II} is the poorest of the three. This fact can be reasoned as the number of multipliers required to realize R_{II} are much higher than those of the realizations W C I and C D I.

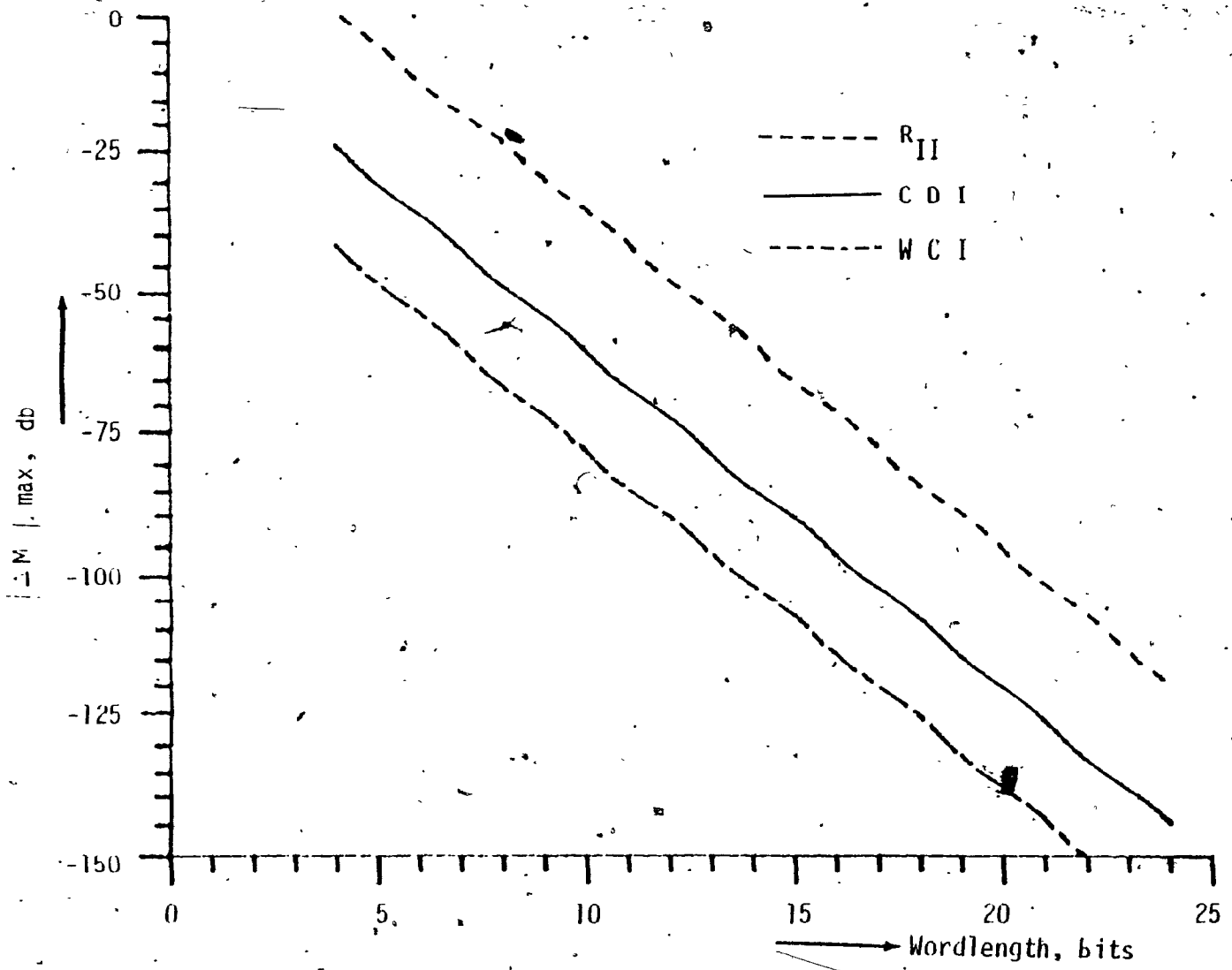

Fig. 4.6

Plot of $|\Delta M|_{max}$ vs. wordlength for different realizations corresponding to PSTFJ of Eqn. (3.2)

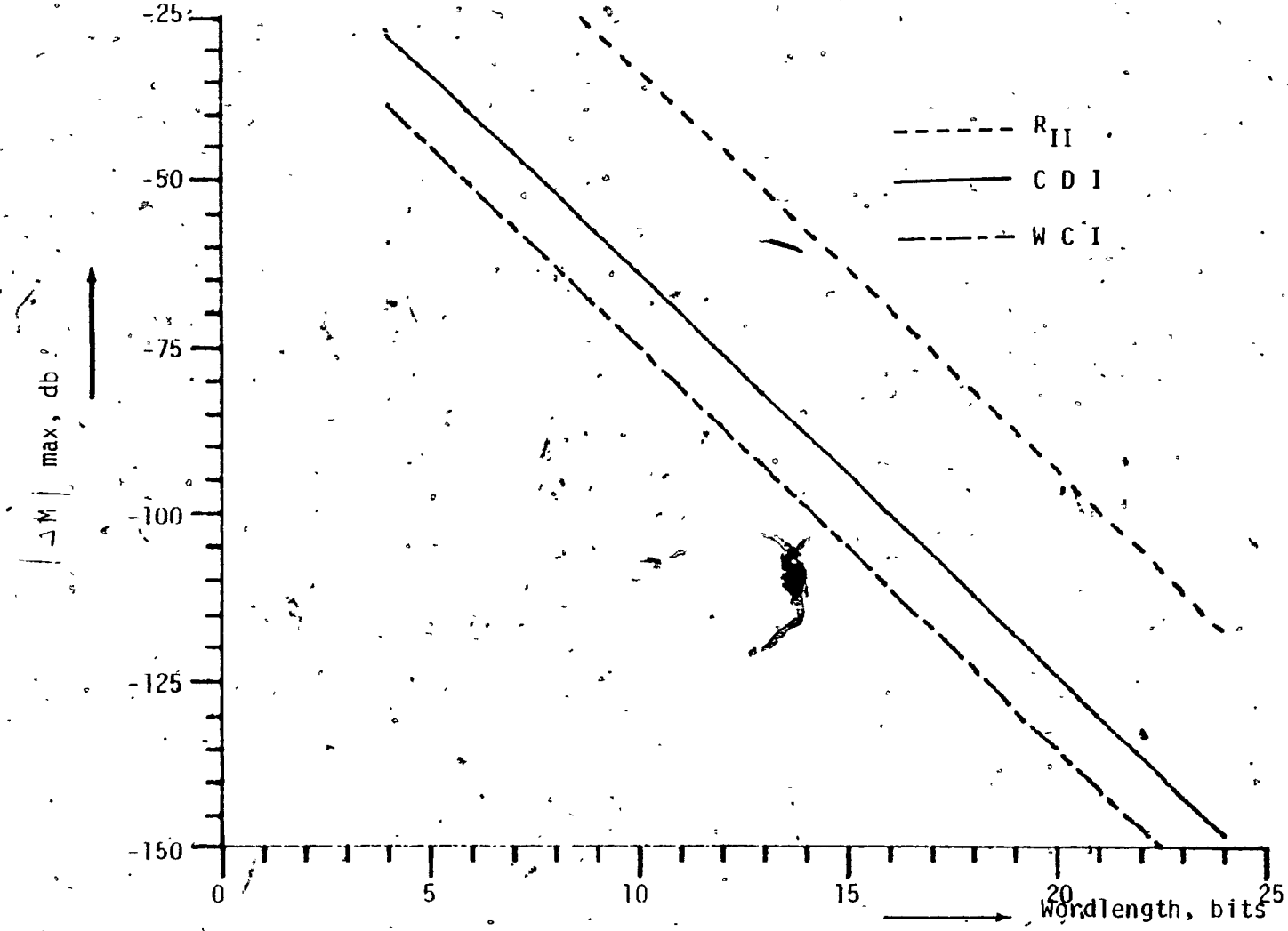

Fig. 4.7

Plot of $|\Delta M|_{max}$ vs. wordlength for different realizations corresponding to PSTF of Eqn. (3.3)

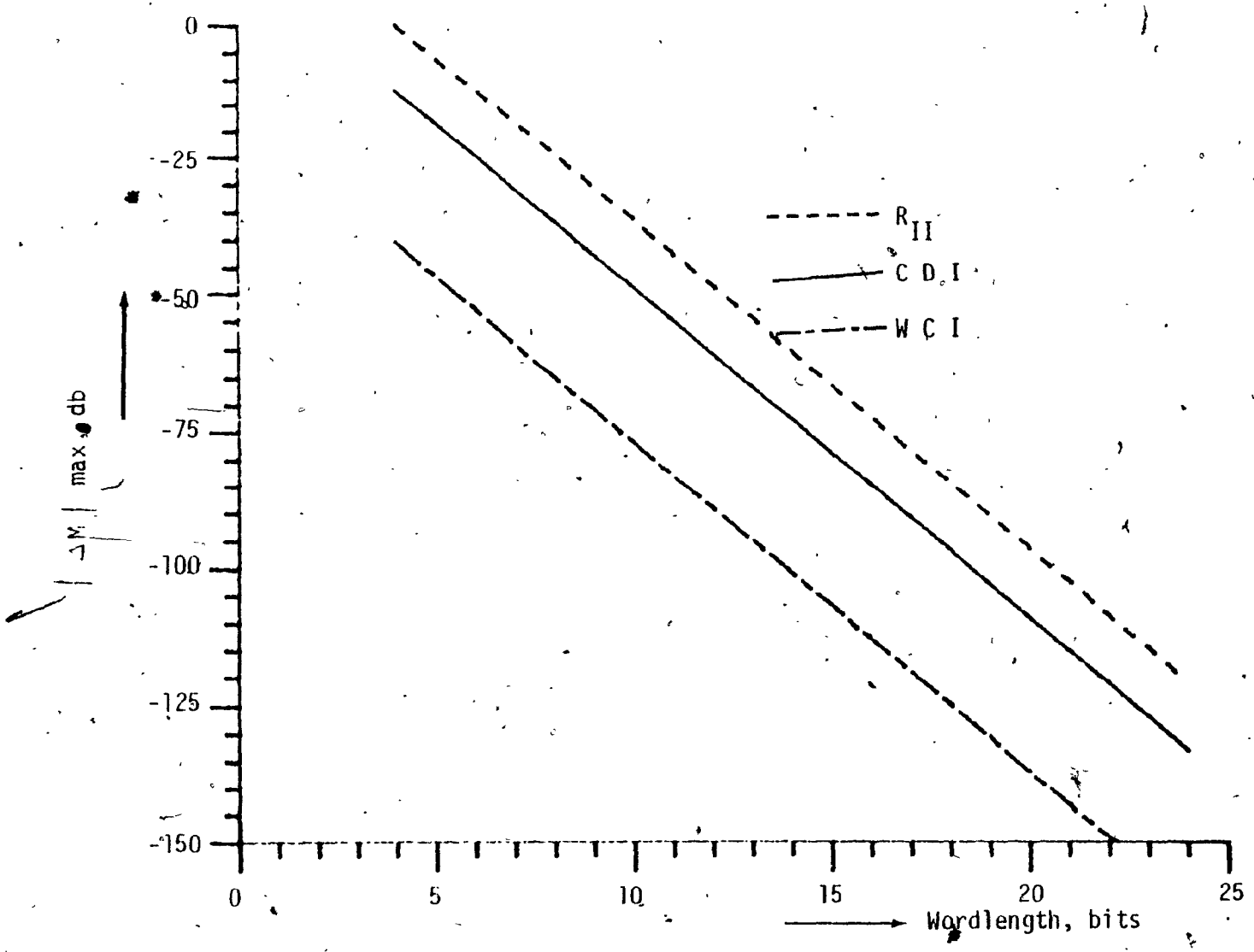

Fig. 4.8

Plot of $|\Delta M|_{max}$ vs. wordlength for different realizations corresponding to PSTF of Eqn. (3.4)

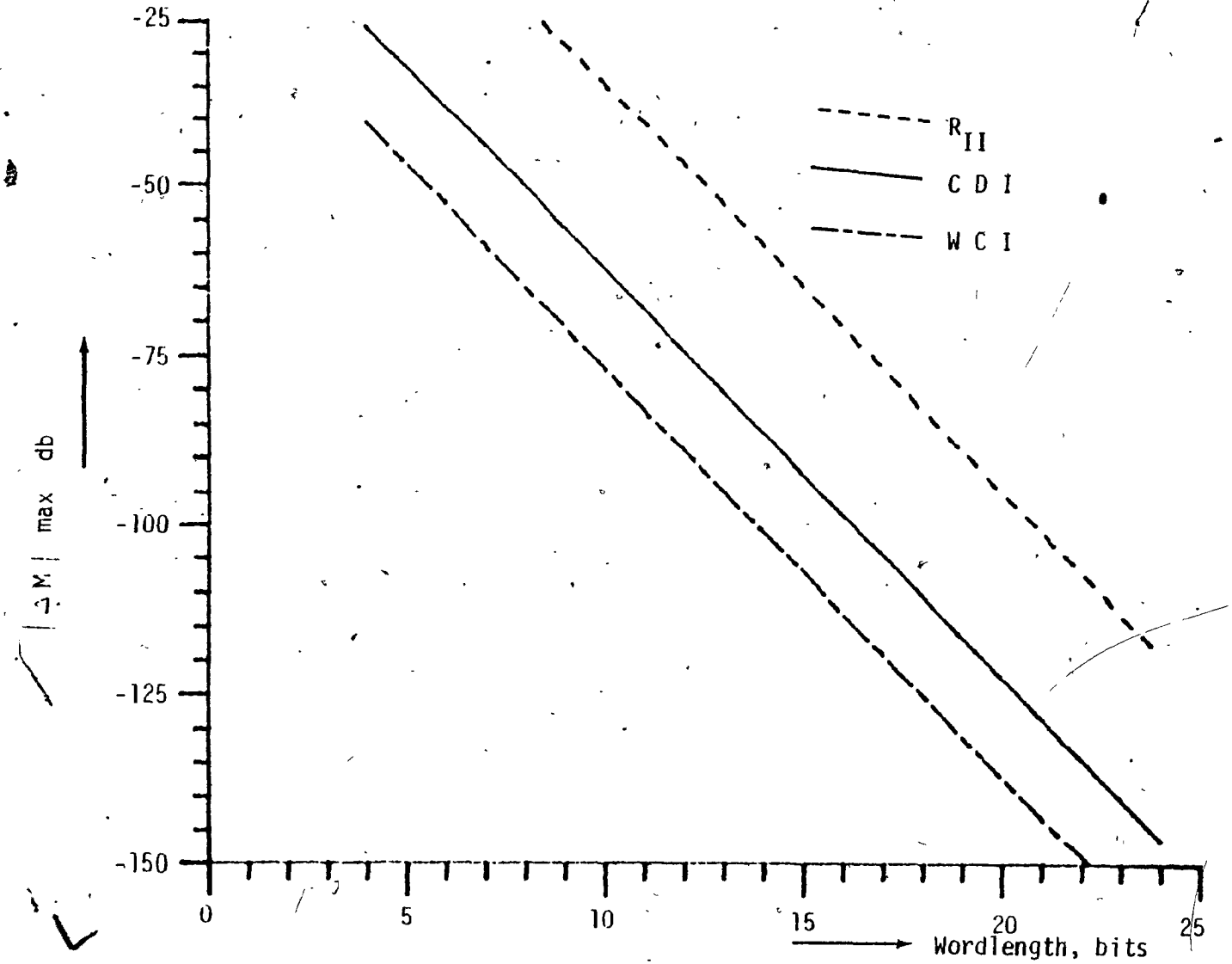

Fig. 4.9

Plot of $|\Delta M|_{max}$ vs. wordlength for different realizations corresponding to PSTF of Eqn. (3.5)

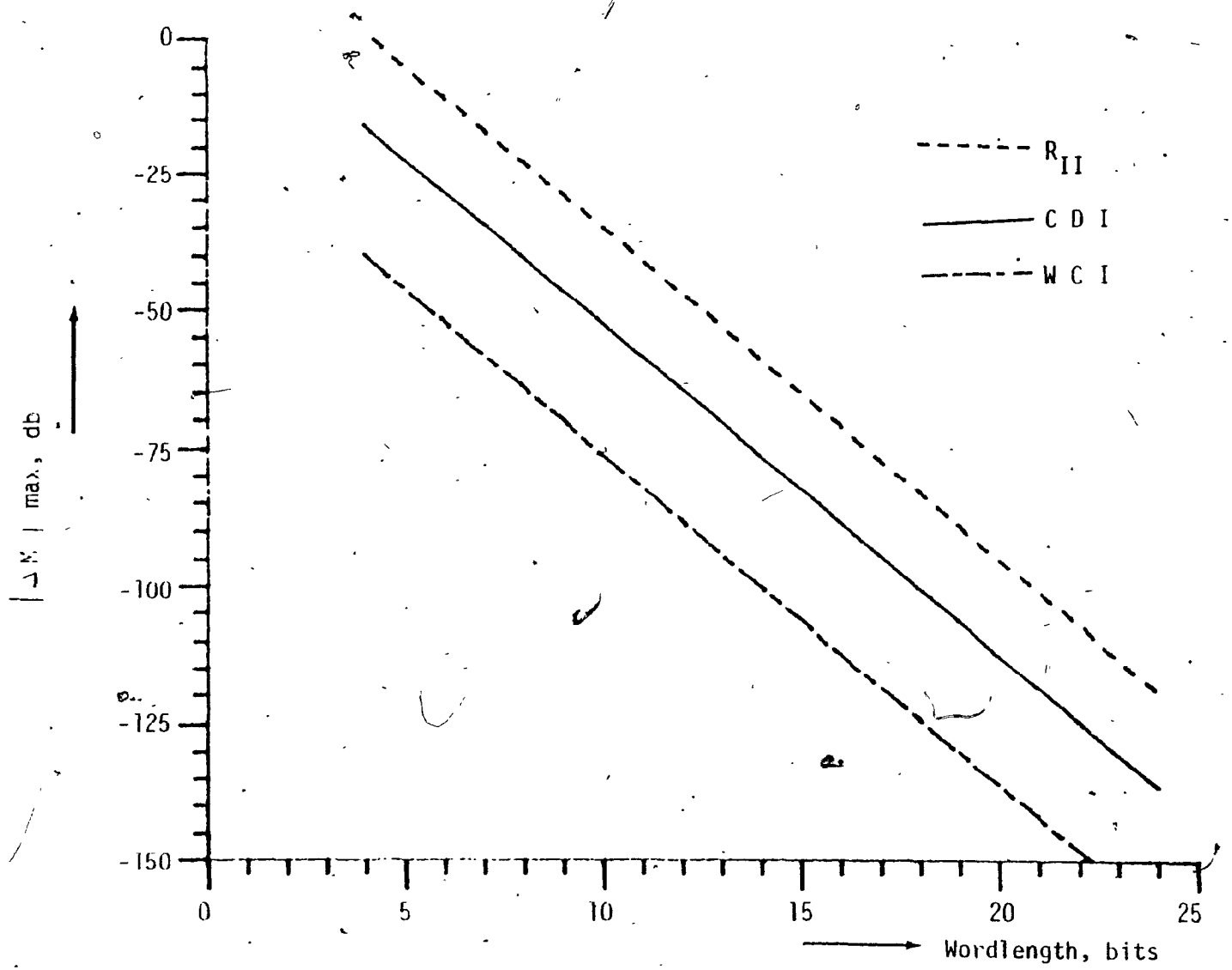

Fig. 4.10

Plot of $|\Delta M|_{max}$ vs. wordlength for different realizations corresponding to PSTF of Eqn. (36)

4.3 Product Quantization Error:

The product resulting from the multiplication of signal represented by N bits and a multiplier coefficient represented by M bits, will have as many as N + M bits, Fig. 4.9. Since a uniform register length is in practice, it would be used throughout the filter. The result of each multiplication must be quantized before processing can be continued, hence quantization errors will arise at the output of multipliers. The effect of this quantization is to inject a noise component at the output of the filter. The output of a finite word length multiplier can be expressed as,

$$Q\ (m_i x(n)\ ) = m_i x(n) + e_i (n) \qquad (4.20)$$

Where,

$m_i\ x\ (n)$ = Exact product.

$e_i\ (n)$ = Quantization error.

This can be represented using model shown in Fig. 4.10 . The effect of product quantization in the various types of filter structures was investigated by computing the output relative power spectral density (RPSD) as a function of frequency. This quantity is given in [9] as,

$$RPSD = 10 \log_{10} \{ S_o (w) / S_m (w) \} \qquad (4.21)$$

Where,

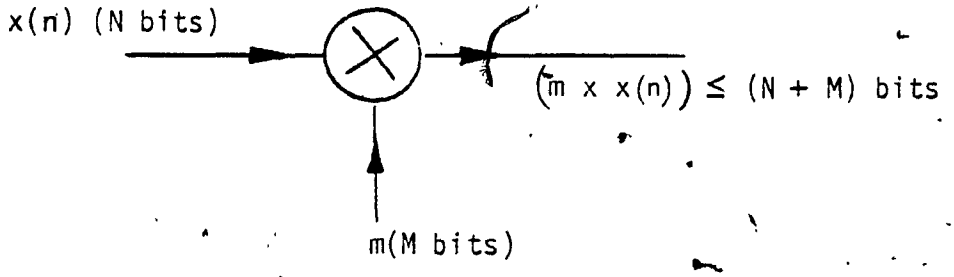

Fig. 4.11

Model to represent production of two signals

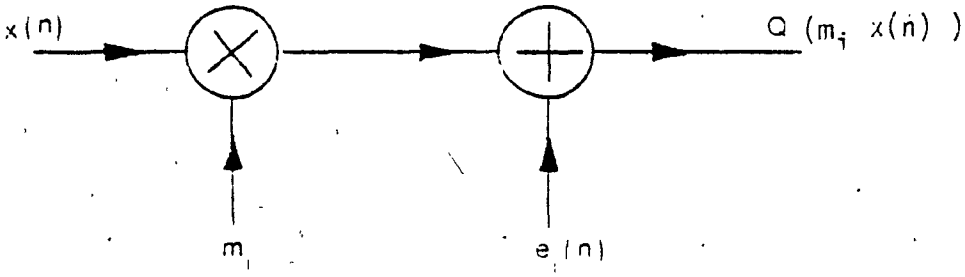

Fig. 4.12

Model of the network to compute product Quantization error

$S_o(w)$ is the absolute power spectral density of the output noise due to product quantization.

$S_m(w)$ is the power spectral density of the noise generated by one multiplier. Assuming fixed-point implementation and quantization by rounding we have,

$$S_m(w) = Q^2/12$$

Where Q is the quantization step.

The power spectral density of the sum of processer $e_i(k)$ and $e_j(k)$ is given by,

$$S\{e_i(k) + e_j(k)\} = S\{e_i(k)\} + S\{e_j(k)\} \qquad (4.22)$$

Because of this statistically independent property, the noise power spectral density at the output of a digital filter can be readilly deduced by using superposition.

For a digital network with input X(k), output Y(k) and transfer function H(z), the input and output PSD's are related as

$$S_Y(z) = H(z)\, H(z^{-1})\, S_X(z) \qquad (4.23)$$

Using Eqn (4.23) one can find RPSD for given digital filter.

Product Quantization Error in Case of 2-D Digital Filters:

The method to find RPSD in case of 1-D digital filter can be exatended to find RPSD in case of 2-D digital filter. A finite word length multiplier gives rise to a quantization output,

$$Q\{m_i\, x(n_1, n_2)\} = m_i\, x(n_1, n_2) + e_i(n_1, n_2) \qquad (4.24)$$

Where.

$m_i\, x(n_1, n_2)$ = Exact product

$e_i(n_1, n_2)$ = quantization error.

If quantization is by rounding, each noise source $e_i(n_1, n_2)$ can be regarded as a random variable of value $-Q/2 \leq e_i(n_1, n_2) \leq Q/2$ where Q is the quantization step.

The mean of $e_i(n_1, n_2)$ is given by,

$$E\{e_i(n_1, n_2)\} = \int_{-\infty}^{\infty} e_i(n_1, n_2)\ P\{e_i(n_1, n_2)\}\ d\{e_i(n_1, n_2)\} \quad (4.25)$$

Where,

$$P(e_i(n_1, n_2) \text{ probability density}) = \begin{cases} 1/Q & \text{for } -Q/2 \leq e_i(n_1, n_2) \leq Q/2 \\ 0 & \text{other wise} \end{cases}$$

The Variance of $e_i(n_1, n_2)$ is given by,

$$\sigma^2_{e_i} = E\left\{ \left[e_i(n_1, n_2) - E\{e_i(n_1, n_2)\} \right]^2 \right\} = Q^2/12 \quad (4.26)$$

The power spectral density (PSD) of $e_i(n_1, n_2)$ is,

$$Se_i(w_1, w_2) = \mathbf{Z}_2\ Q^2/12\ \delta(k_1, k_2) = Q^2/12 \quad (4.27)$$

Where,

$\mathbf{Z}_2$ = 2-D z transform.

$\delta(k_1, k_2)$ = Impulse function.

The autocorrpelation of the of $e_i(n_1, n_2) + e_j(n_1, n_2)$ is,

$$\mathcal{r}e_i(k_1, k_2) + \mathcal{r}e_j(k_1, k_2) = \mathcal{r}e_{(ij)}(k_1, k_2)$$

$$= \frac{Q^2}{12}\ (k_1, k_2) \quad (4.28)$$

The PSD of the sum of two processes is equal to the sum of their respective PSD. since,

$$S(e_i + e_j)(z_1, z_2) = \mathbf{Z}_2 \left[\mathcal{r}e_i(k_1, k_2) + \mathcal{r}e_j(k_1, k_2) \right]$$

$$= Se_i(z_1, z_2) + Se_j(z_1, z_2) \quad (4.29)$$

Which is,

$$(Se_i + Se_j)\ (w_1, w_2) = Se_i\ (w_1, w_2) + Se_j\ (w_1, w_2) \qquad (4.30)$$

For a digital 2-D digital filter having a transfer function $H(z_1, z_2)$ and the input and output are $x(n_1, n_2)$ and $Y(n_1, n_2)$ respectively. Then the 2-D z transforms of $rX(k_1, k_2)$ and $rY(k_1, k_2)$ are related by,

$$S_Y\ (z_1, z_2) = H(z_1, z_2)\ H(z_1^{-1}, z_2^{-1})\ S_X\ (z_1, z_2) \quad \text{Or}$$

$$S_Y\ (e^{jw_1t_1}, e^{jw_2t_2}) = |H(e^{jw_1t_1}, e^{jw_2t_2})|^2\ Sx\ (e^{jw_1t_1}, e^{jw_2t_2}) \qquad (4.31)$$

The output noise spectrum is expressed as the relative power spectral density (RPSD) is given by,

$$RPSD = 10.0\ \text{Log}_{10}\ \{S_o\ (w_1, w_2)/S_i\ (w_1, w_2)\} \qquad (4.32)$$

Where,

$S_o\ (w_1, w_2)$ = Output noise power spectral density (PSD).

$S_i\ (w_1, w_2)$ = Power spectral density of single noise sourse.

$S_i\ (w_1, w_2) = Q^2/12$

Fig. 4.13 to 4.20 snows 2-D RPSD (in db) contours vs. frequency w_1 & w_2 in radians.

Comparing relative power spectral density (RPSD) contours VS. frequency w_1 and w_2 in radians, it is concluded that RPSD contours shape in case of C D I is the same as that of its magnitude response contoures shown in previous chapters. In the case of N C I, the RPSD varies between 5 to -5 db. In the realizations, R_I or R_{II}, RPSD is constant for every frequency. Thus from the product quantization error point of view, the proposed realizations appear to be better.

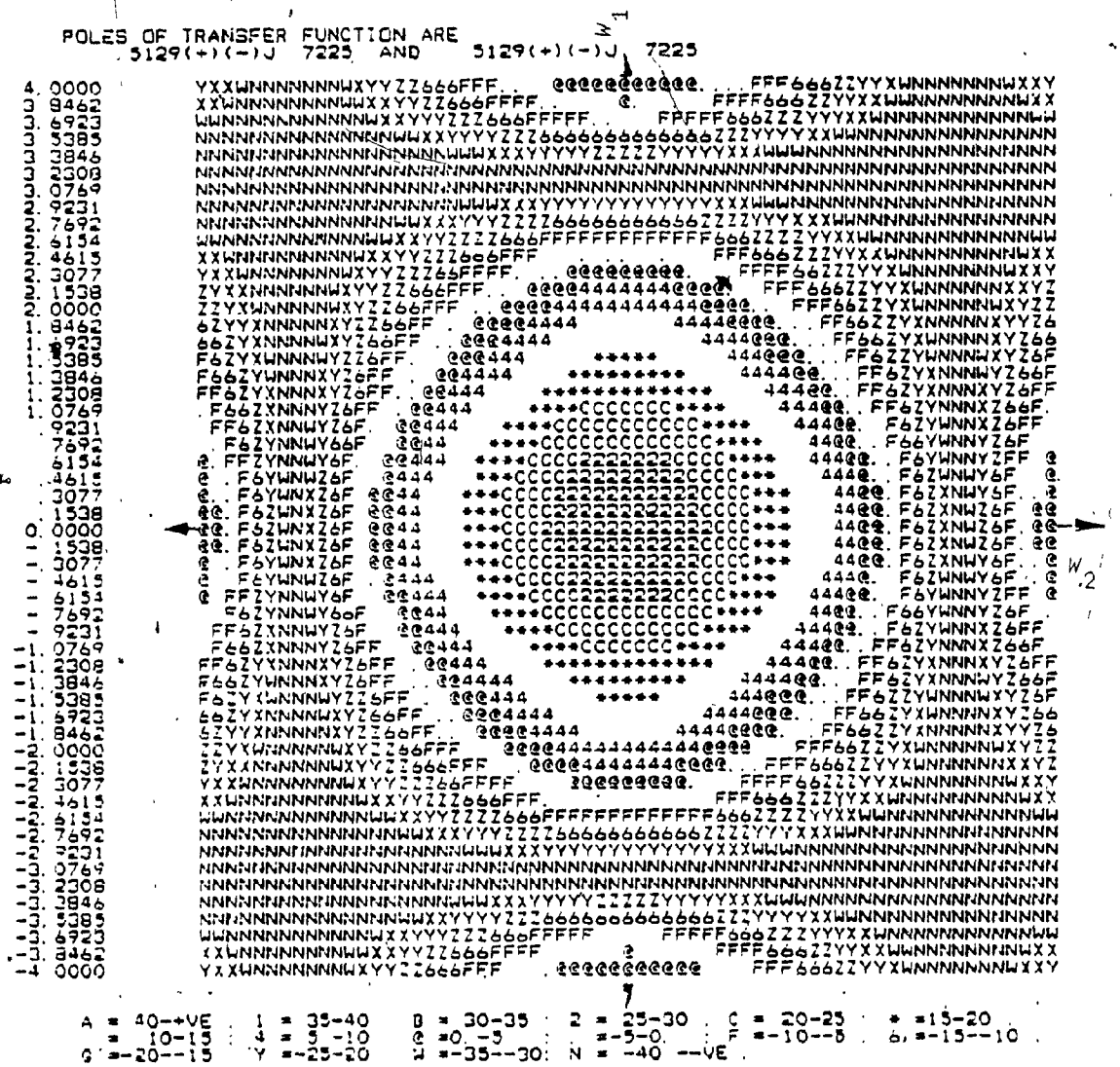

Fig. 4.13

RSPD (in db.) contours vs. (w_1, w_2) for C D I,

corresponding to Eqn.(3.3)

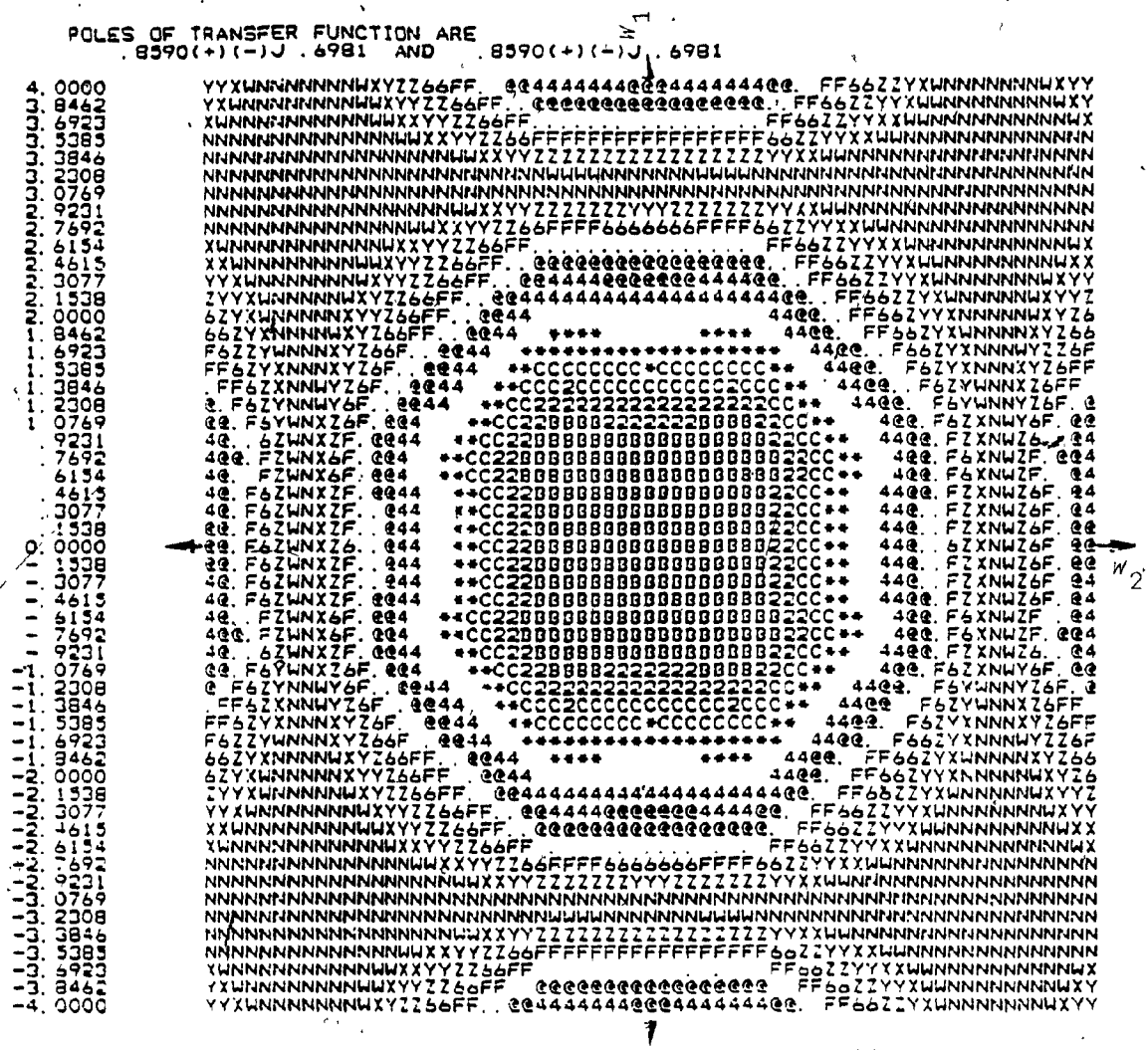

Fig. 4.14

RSPD (in db.) contours vs. (w_1, w_2) for C D I,

corresponding to Eqn.(3.4)

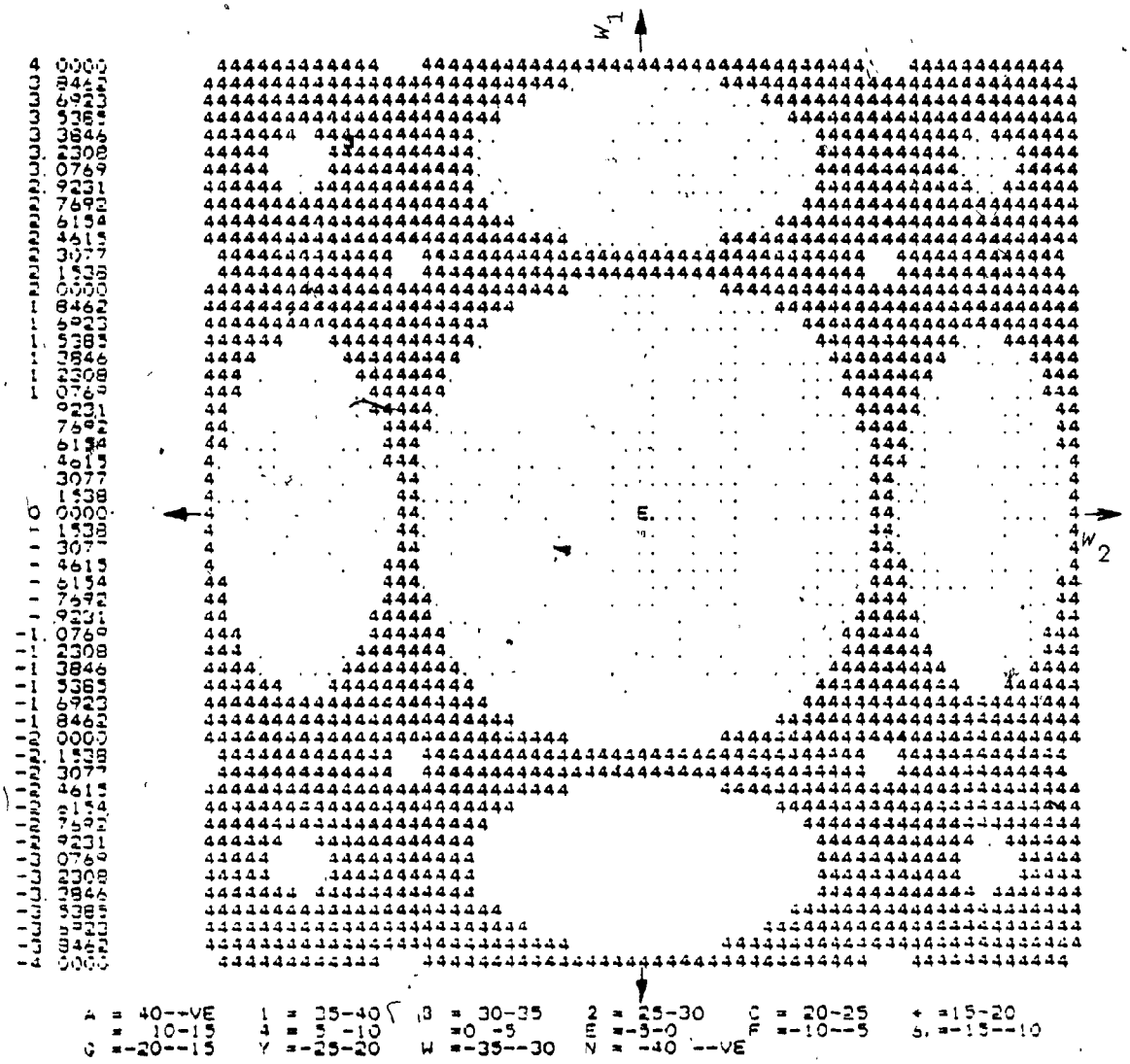

Fig. 4.15

RSPD (in db.) contours vs. (w_1, w_2) for W C I, corresponding to Eqn. (3.2)

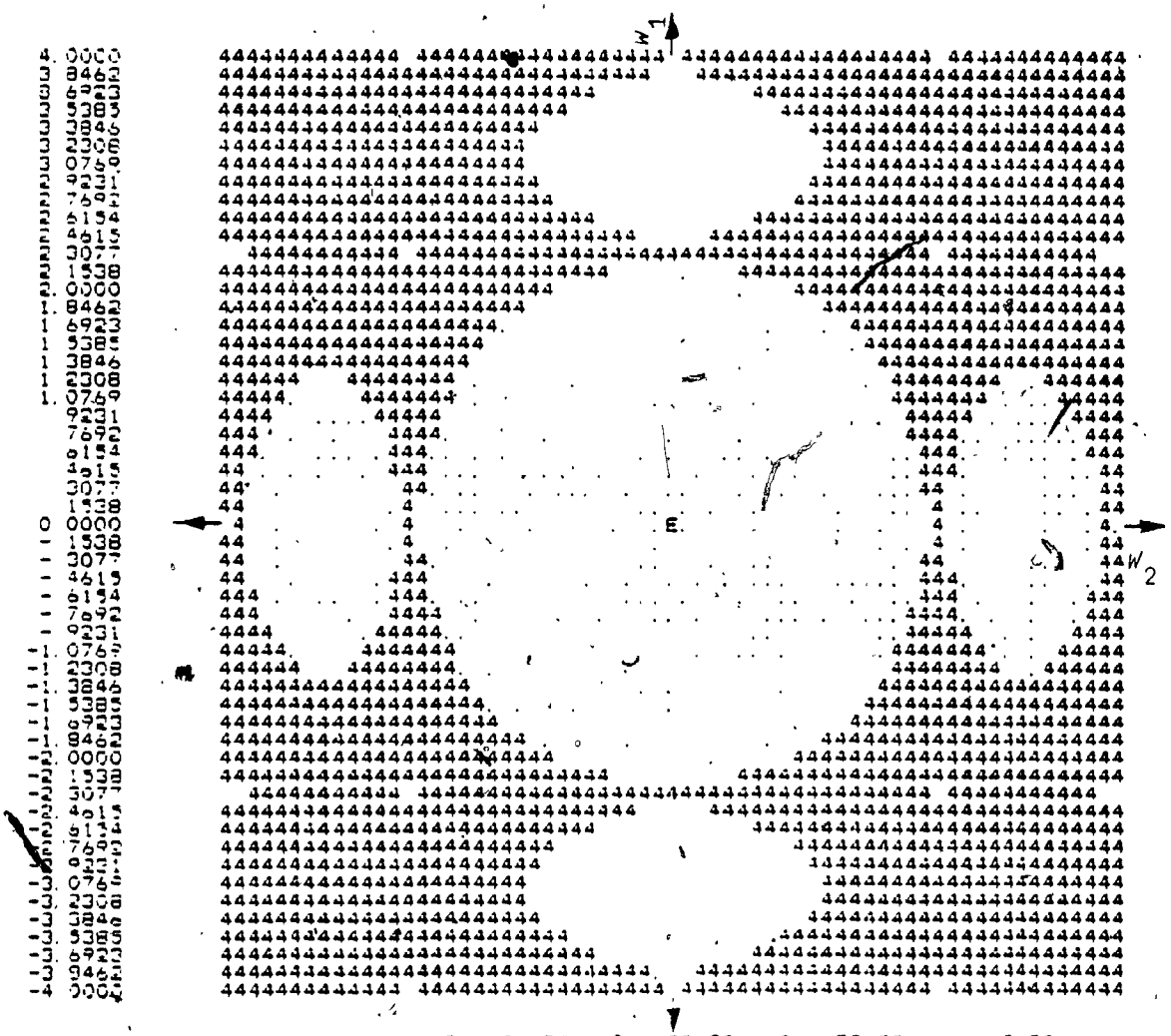

Fig. 4.16

RSPD (in db.) contours vs. (w_1, w_2) for W C I

corresponding to Eqn. (3.3)

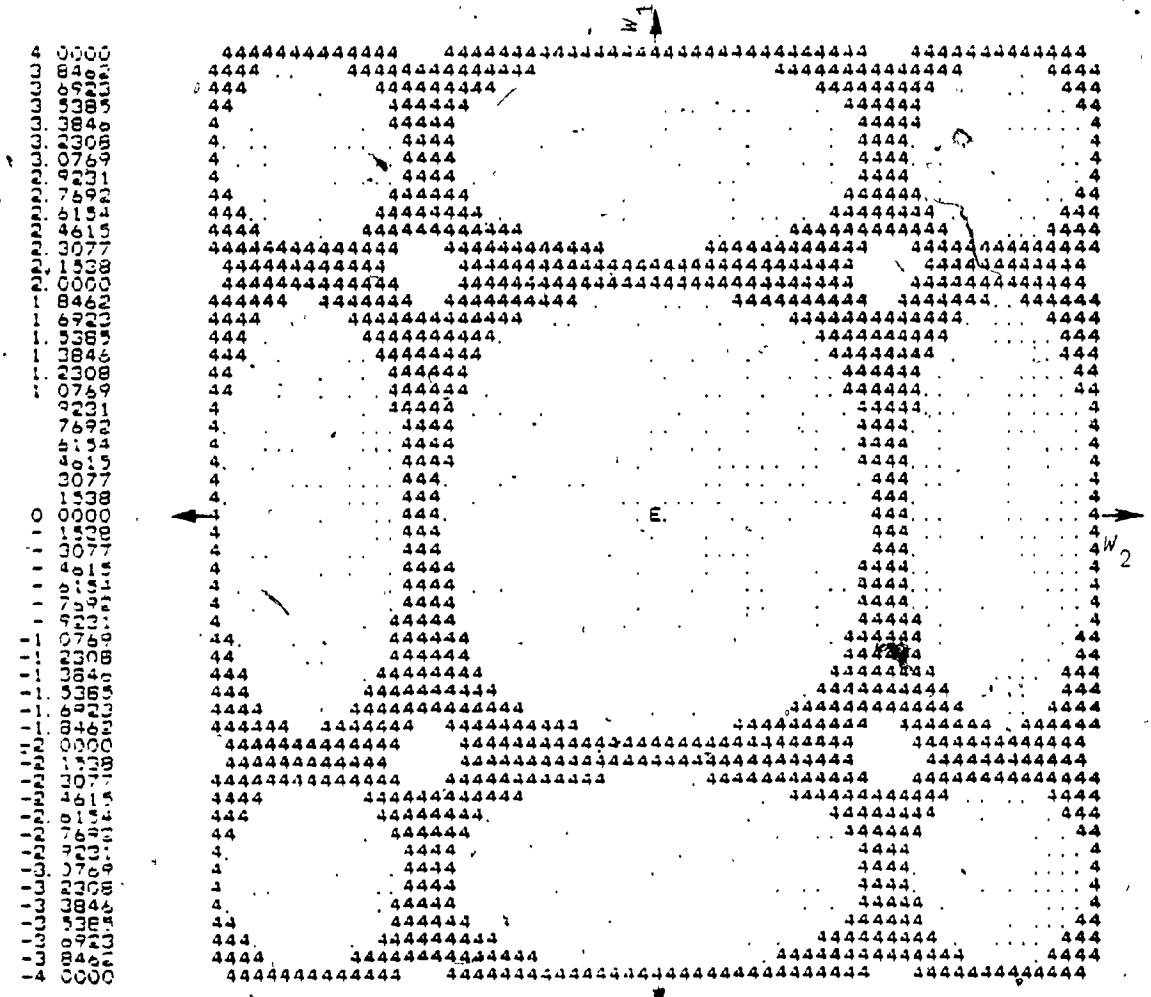

Fig. 4.17

RSPD (in db.) contours vs. (w_1, w_2) for W C I, corresponding to Eqn.(3.4)

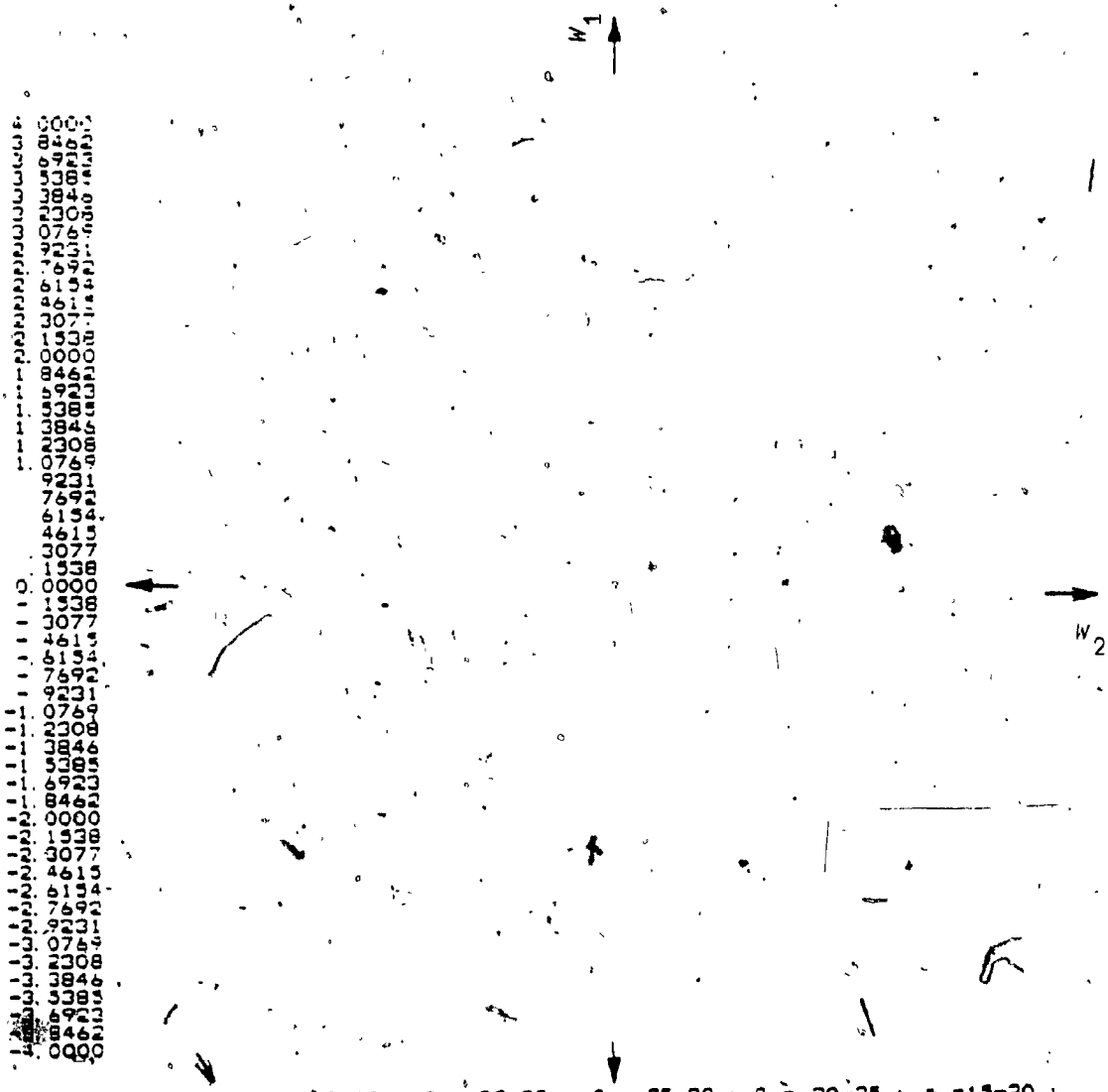

Fig. 4.18

RSPD (in db.) contours vs. (w_1, w_2) for R_{II}

corresponding to Eqn. (3.2)

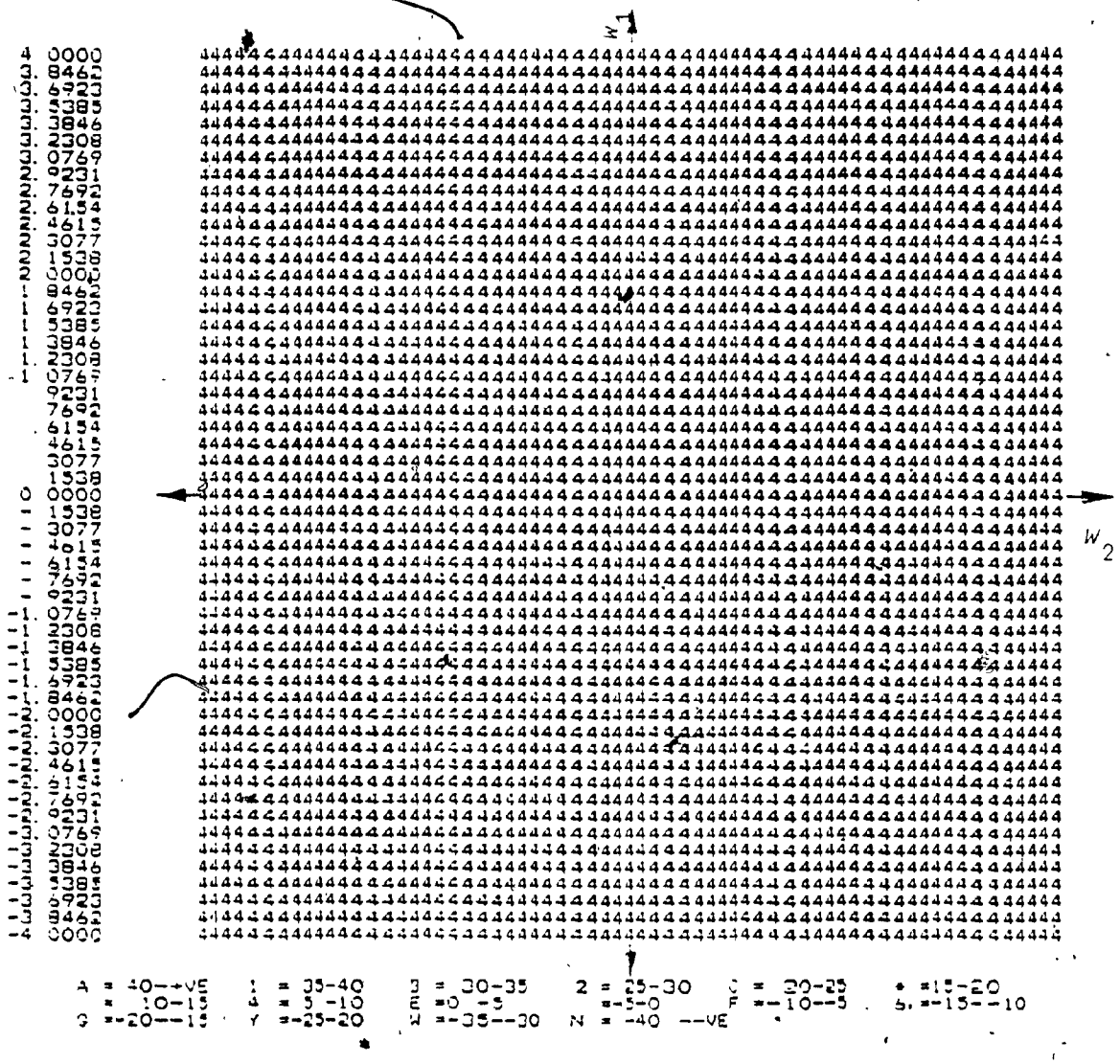

Fig. 4.19

RSPD (in db.) contours vs. (W_1, W_2) for R_{II}

corresponding to Eqn.(3.4)

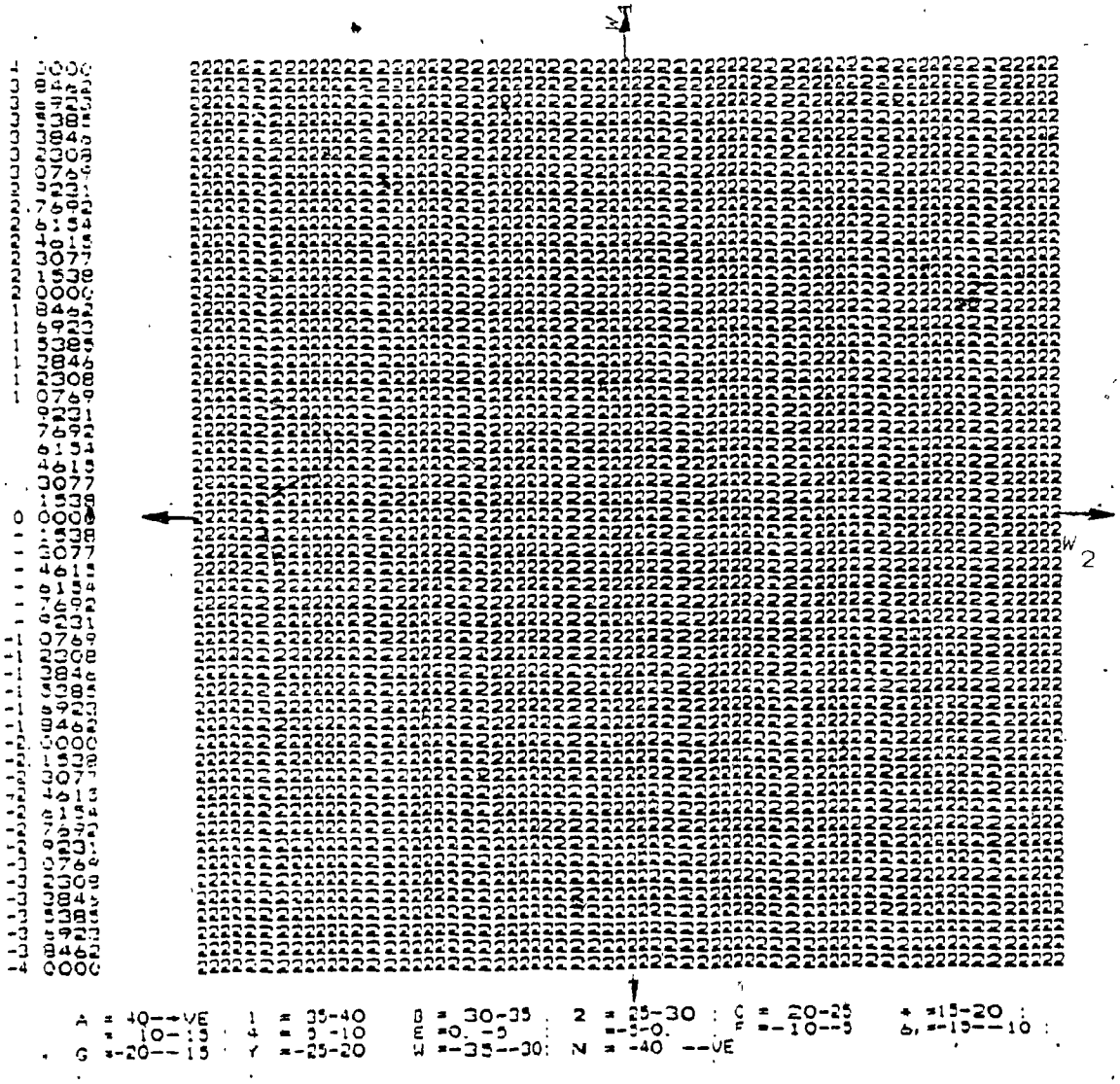

Fig. 4.20

RSPD (in db) contours vs. (w_1, w_2) for R_{II}

Corresponding to Eqns. (3.3), (3.5) and (3.6)

4.4 Summary and Discussion:

In order to assess the suitability of a digital realization, one has to determine the coefficient sensitivity, and the product quantization error. In this chapter we have determined the fixed-point sensitivity and the product quantization error of three different structures.

From the sensitivity point of view, it is observed that the realization proposed in chapter 2 is inferior compared to C D I and W C I. However, from the point of view of product quantization error, it is found that the realizations R_I and R_{II} appear better compared to C D I and W C I. In fact, they are constant at all frequencies.

Proposed structures required more arithmatic operations compared with cascade wave structure and cascade canonic structures for implementation.

Chapter 5

CONCLUSIONS

5.1 Conclusions

A new digital structure which realizes exactly 2-D product separable transfer function is discussed in this thesis. The realization consists of a cascade connection of the wave-digital realization of a doubly-terminated 2-variable analog cascade-decomposable network and a suitable 2-variable digital parallel realization. This also requires two-port wave digital realizations of different combinations of resistive and reactive elements in the series arm or the shunt arm of the analog network.

The fixed-point coefficient quantization error and product quantization error of proposed exact realization of PSTF has been studied.

For coefficient quantization error analysis, the error RMS value defined in [12] has been used to measure the deviation of the actual frequency response from the ideal one, when the multiplier coefficients are rounded off for implementation. For minimum wordlength analysis, the statistical approach given in [24] has been used with confidence factor Y = 0.95. It is found that the sensitivity and hence coefficient quantization error for the proposed realization structure is higher than that of cascade-direct and cascade-wave realizations.

Product quantization error has been studied using transpose network approach [9] and simulating second order low-pass filters having different pole locations, on digital computer. It is found that the proposed exact

realization of PSTF gives constant quantization error in its magnitude response. Therefore, this structure can be used whenever product quantization error is the criterion.

Since a large number of realizations of PSTFs are possible, it is suggested that investigations shall be carried out to determine the optimum structure (or structures) which may give better overall performance. Suitable frequency transformations shall be found to design other types of filters.

APPENDIX - I

DATA FOR FIG. - 2. 24(a)

R1(OHM)	R2(OHM)	L1(HEN)	L2(HEN)	C1(F)	C2(F)
1 0000 0					
	1.0000	.7071	.7071	1.4142	1.4142

2-D PSTF IS,

$$H(S1,S2)= \frac{K}{(S1^{**}2+A1S1+A0)(S2^{**}2+B1S2+B0)}$$

WHERE,
K=.999961 5403679
A1=1.4142
A0=.99998082
B1=1.4142
B0= 99998082

POLES OF GIVEN TRANSFER FUNCTION ARE,

REAL1= .70710000
IMAG1=+(-) .70710000

REAL2= .70710000
IMAG2=+(-) 70710000

PORT RESISTANCES OF FIG. 2.26 ARE,

RL	RA	RB	RC	RD
.000000	1.707114	.499997	.291391	1.000005

CASCADE SECTION MULTIPLIER COEFFICINTS FOR FIG. - 2.26 ARE,

THETA1	THETA2	ALFA1	ALFA2	BETA1	BETA2
.00000	0. 00000	.29239	.58578	.58579	.29239

PARALLEL SECTION REALIZATION COEFFICIANTS FOR FIG. 2.27 ARE,

DEL3= .58578411
DEL2= .41421589
DEL1= .17156822
THETA(P)= .585736441

APPENDIX - II

DATA FOR FIG. 2.24(a)

R1(OHM)	R2(OHM)	L1(HEN)	L2(HEN)	C1 F)	C2(F)
1.0000	1.0000	.9748	.9748	1.3066	1.3066

2 D PSTF IS,

$$H(S1\ S2) = \frac{K}{(S1^{**}2+A1S1+A0)(S2^{**}2+B1S2+B0)}$$

WHERE,
K=.61333390814795
A1=1.0258
A0=.78507266
B1=1.0258
B0=.78507266

POLES OF GIVEN TRANSFER FUNCTION ARE,

REAL1= .51290000
IMAG1=+(-) .72250000

REAL2= .51290000
IMAG2=+(-) .72250000

PORT RESISTANCES OF FIG. 2.26 ARE,

RL	RA	RB	RC	RD
1.000000	1.974849	.551572	.320551	1.295400

CASCADE SECTION MULTIPLIER COEFFICIENTS FOR FIG. - 2.26 ARE,

THETA1	THETA2	ALFA1	ALFA2	BETA1	BETA2
.12869	0.00000	.24745	.50637	.58116	.27930

PARALLEL SECTION REALIZATION COEFFICIANTS FOR FIG. - 2.27 ARE,

DEL3= .50636735
DEL2= .49363215
DEL1= .01273571
THETA(P)= .81466768.

APPENDIX - III

DATA FOR FIG. 2.24(a)

R1(OHM)	R2(OHM)	L1(HEN)	L2(HEN)	C1(F)	C2(F)
1.0000	1.0000	.4533	.4533	1.3599	1.3599

2-D. PSTF IS,

$$H(S1,S2)= \frac{K}{(S1^{**}2+A1S1+A0)(S2^{**}2+B1S2+B0)}$$

WHERE,
K=2.631233805748
A1=2.206
A0=1.62212324
B1=2.206
B0=1.62212324

POLES OF GIVEN TRANSFER FUNCTION ARE,

REAL1=1.10300000
IMAG1=+(-.63680000

REAL2=1.10300000
IMAG2=+(-.63680000

PORT RESISTANCES OF FIG. 2.26 ARE,

RL	RA	RB	RC	RD
1.000000	1.453309	.488274	.293429	.746733

CASCADE SECTION MULTIPLIER COEFFICIENTS FOR FIG. - 2.26 ARE,

THETA1	THETA2	ALFA1	ALFA2	BETA1	BETA2
-.14499	0.00000	.39295	.63809	.60095	.33597

PARALLEL SECTION REALIZATION COEFFICIANTS FOR FIG. - 2.27 ARE,

DEL3= .58303484
DEL2= .81191515
DEL1= .37515963
THETA(P.= .39073743I

APPENDIX - IV

DATA FOR FIG. - 2.24(a)

R1(OHM)	R2(OHM)	L1(HEN)	L2(HEN)	C1(F)	C2(F)
1.0000	1.0000	.9743	.7071	1.3066	1.4142

2-D PSTF IS,

$$H(S1,S2) = \frac{K}{(S1^{**}2+A1S1+A0)(S2^{**}2+B1S2+B0)}$$

WHERE,
K=.7850576023064
A1=1.0258
A0= 73507255
B1=1.4142
B0=.99998082

POLES OF GIVEN TRANSFER FUNCTION ARE,

REAL1= .51290000
IMAG1=+(-) .72250000

REAL2= .70710000
IMAG2=+(-) .70710000

PORT RESISTANCES OF FIG. 2.26 ARE;

RL	RA	RB	RC	RD
1.000000	1.707114	.499997	.302422	1.277271

CASCADE SECTION MULTIPLIER COEFFICIENTS FOR FIG. 2.26 ARE

THETA1	THETA2	ALFA1	ALFA2	BETA1	BETA2
.12176	0.00000	.23677	.58573	.50485	.29239

PARALLEL SECTION REALIZATION COEFFICIANTS FOR FIG. - 2.27 ARE,

DEL3= .50536735
DEL2= .49363215
DEL1= .01273571
THETA(P)= .314657681 .

APPENDIX - V

DATA FOR FIG. - 2.24(a)

R1(OHM)	R2(OHM)	L1(HEN)	L2(HEN)	C1(F)	C2(F)
1.0000	1.0000	.9748	.4533	1.3066	1.3599

2-D PSTF IS,

$$H(S1\ S2) = \frac{K}{(S1^{**}2+A1S1+A0)(S2^{**}2+B1S2+B0)}$$

WHERE,
K=1.273484606875
A1=1.0258
A0=.78507266
B1=2.206
B0=1.62212324

POLES OF GIVEN TRANSFER FUNCTION ARE,

REAL1= .51290000
IMAG1=+(-) .72250000

REAL2=1.10300000
IMAG2=+(-) .63680000

PORT RESISTANCES OF FIG. 2.25 ARE,

RL	RA	RB	RC	RD
1.000000	1.463309	.438274	.298093	1.272942

CASCADE SECTION MULTIPLIER COEFFICIENTS FOR FIG. - 2.25 ARE,

THETA1	THETA2	ALFA1	ALFA2	BETA1	BETA2
.12008	0.00000	.23413	.63803	.61050	.33597

PARALLEL SECTION REALIZATION COEFFICIANTS FOR FIG. - 2.27 ARE,

DEL3= .50336735
DEL2= .49363215
DEL1= .01273571
THETA(P)= .31466768

REFERENCES

1. Rabiner, R.L. and Gold, B. "Theory and Application of Digital Signal Processing." Prentice Hall, 1975.
2. Huang, T.S. "Topics in Applied Physics, Two-Dimensional Digital Signal Processing." Springsh - verlag co., New York, 1981.
3. Corrington, M.S. "Two-Dimensional Recursive Digital Filters for Background Removal in Pictures". Cicruit and System Newsletter, Vol. 7, No. 6, December, 1973.
4. Goodman, D. "Some Difficulties with Double Bilinear Transformation in 2-D Digital Filter Design." Proc. IEEE. Vol. 66, July, 1978.
5. Rajan, P.K., Reddy, H.C., Swamy, N.M.S. and Ramachandran, V. "Generation of Two-Dimensional Digital Functions without Non-Essential Singularities of the Second Kind". IEEE International Conference on Accoustics speech and signal processing, April, 1979.
6. Rajan, P.K. and Swamy, N.M.S. "Quadrantal Symmetry Associated with Two-Dimensional Digital Transfer Functions". IEEE Transactions on Circuits and Systems, Vol. cas - 25, No. 6, June, 1978.
7. _____. "Some Results on the Nature of a 2-Dimensional Filter Functions Possessing Certain Symmetry in its Magnitude Response". Electronics Circuits and System, Vol. 2, No. 5, September, 1978.
8. _____. "Symmetry Constraints on Two-Dimensional Half-Plane Digital Transfer Functions". IEEE Transactions on Accoustics, speech and signal processing, April, 1979.
9. Antoniou, A. "Digital Filters Analysis and Design". McGraw-Hill, 1978.

10. Agarwal, R.C. and Burrus, S. "New Recursive Digital Filter Structures Having Very Low Sensitivity and Round-Off Noise". IEEE Transaction on Circuit and System. Vol. cas-22, No. 12, 1975.

11. Crochier, R.E. "A Computational Methods for Sensitivity Analysis of Digital Filters". M.I.T. QPR., No. 109.

12. Walter H. Ku and Sui-Srig Ng. "Floating-Point Coefficient Sensitivity and Round-Off Noise of Recursive Digital Filters Realize in Ladder Structure". IEEE Transaction on circuit and Systems , Vol. cas-22, No. 12, December, 1975.

13. Terrell, T.J. "Introduction to Digital Filters." The Macmillan Press Ltd., London, 1980.

14. Thyagrajan, K.S. "One and Two-Dimensional Wave Digital Filters with Low Coefficient Sensitivity". Ph.D. Thesis, Concordia University, 1977.

15. Shanks, J.L., Tretel, S. and Justice, J.M. "Stability of Two-Dimensional Recursive Filters". IEEE Transaction Audio-Accoustic, Vol. Au-20, June, 1972.

16. Mitra, S.K., Sagar, A.D. and Pendergrass, N.A. "Realization of Two-Dimensional Recursive Digital Filters". IEEE Transactions on Circuits and Systems, Vol. cas-22, No. 3, 1975.

17. Swamy, N.M.S., Thyagrajan, K.S. and Ramachandran, V. "Two-Dimensional Wave Digital Filters Using Doubly Terminated Two-Variable LC Ladder Configuration." Journal of the Franklin Institute, Vol. 304, No. 415, 1978.

18. Ramman, B. "Approximation and Realization of a Class of Multivariable Analog and Digital Transfer Functions". Ph.D. Thesis, Concordia University, 1981.

19. Vanvalkenburg. " Introduction to Modern Network Synthesis". John Wiley & Sons, Inc., 1960.

20. Hazony, D. "Elements of Network Synthesis." Rainhold, 1963.

21. Balabanian, N. "Network Synthesis". Prentice Hall, 1958.

22. Rezk, M.G. "Digital Filter Structures Based on Generalized Immittance Converters, and Comparison with other Structures". Ph.D. Thesis, Concordia University, 1978.

23. Antoniou, A., Rezk, M.G. "A Comparison of Cascade and Wave Fixed-Point Digital Filter Structures". IEEE Transaction of Circuit and System. Vol. cas-27, December, 1980.

24. Crochiere, R.E."A New Statistical Approach to the Coefficient Wordlength Problem for Digital Filters". IEEE Transaction on Circuit and System, Vol. cas-22, 1975.